Aus der III. Medizinischen Klinik und Poliklinik

der Universitätsmedizin der Johannes Gutenberg-Universität Mainz

Evaluation of T-cell receptor reprogrammed natural killer cells as an "off the shelf" adoptive cellular immunotherapy against acute myeloid leukemia

Evaluation T-Zell-Rezeptor reprogrammierter Natürlicher Killerzellen für eine adoptive zelluläre ’off the shelf’ Immuntherapie bei akuter myeloischer Leukämie

Inauguraldissertation

zur Erlangung des Doktorgrades der Medizin

der Universitätsmedizin

der Johannes Gutenberg-Universität Mainz

Vorgelegt von

Jan Wernersbach

aus Worms

Mainz, 2023

Wissenschaftlicher Vorstand: [redacted]

1. Gutachter: [redacted]

2. Gutachter: [redacted]

3. Gutachter: [redacted]

Tag der Promotion: 24. Oktober 2023

1 Table of contents

2 List of abbreviations

°C	Degree Celsius
µg	Microgram
µl	Microliter
ABC	Avidin-biotin complex
ACT	Adoptive cellular therapy
AEC	3-Amino-9-ethylcarbazole
ALL	Acute lymphoid leukemia
AML	Acute myeloid leukemia
APC	Antigen presenting cell
B-LCL	B-lymphoblastoid cell line
bp	Base pair
BSA	Bovine serum albumine
CAR	Chimeric antigen receptor
CD	Cluster of differentiation
cDNA	Complementary DNA
CLL	Chronic lymphocytic leukemia
CML	Chronic myeloid leukemia
CRS	Cytokine release syndrome
CTL	Cytotoxic T lymphocytes
DC	Dendritic cell
dH_2O	Distilled Water
DLBCL	Diffuse large B cell lymphoma
DMSO	Dimethyl sulfoxide
DNA	Deoxyribonucleic acid
dNTP	Deoxynucleotide triphosphate
E. coli	Escherichia coli
E:T	Effector to target ratio
EBV	Epstein-Barr virus
EDTA	Ethylendiamintetraacetat
ELISA	Enzyme-linked immunosorbent assay
ELISpot	Enzyme-linked immune spot assay
env	Envelope
FACS	Fluorescence-activated cell sorting
FCS	Fetal calf serum
FDA	Food and Drug Administration (USA)

FLuc	Firefly luciferase
GALV	Gibbon ape leukemia virus
gDNA	Genomic DNA
GFP	Green fluorescence protein
GvHD	Graft-versus-host disease
GvL	Graft-versus-leukemia
h	Hour
H_2O	Water
HIV	Human immunodeficiency virus
HLA	Human leukocyte antigen
HSCT	Hematopoietic stem cell transplantation
IFN	Interferone
IFN-γ	Interferon gamma
Ig	Immunoglobulin
IL	Interleukin
IL-2	Interleukin-2
IRES	Internal ribosomal entry site
ITAM	Immunoreceptor tyrosine-based activation motif
kb	Kilo base
l	Liter
LB	Lysogeny broth
LTR	Long terminal repeats
M	Molar
mAB	Monoclonal antibody
MDM2	Murine double minute 2 homolog oncoprotein
MHC	Major histocompatibility complex
min	Minutes
ml	Milliliter
mM	Millimolar
MMLV	Moloney murine leukemia virus
mRNA	Messenger RNA
NCR	Natural cytotoxicity receptor
NEB	New England Biolabs
ng	Nanogram
NK cell	Natural killer cell
P/S	Penicillin/Streptomycin
PBMC	Peripheral blood mononuclear cells

PCR	Polymerase chain reaction
PD-1	Programmed cell death protein 1
RNA	Ribonucleic acid
RS	Restriction Site
RT	Room temperature
scFv	Single chain variable fragment
SDS	Sodium Dodecyl Sulfate
sec/s	Second
SV40	Simian virus 40
T_A	Annealing temperature
TAE	Tris-acetate-EDTA
TCR	T-cell receptor
VSV	Vesicular stomatitis virus
α	Alpha
β	Beta
γ	Gamma
δ	Delta
ε	Epsilon
ζ	Zeta

3 List of tables

4 List of Figures

5 Introduction

The 5-year mortality rate of AML patients remained consistent over the last 30 years, while great success in terms of mortality and prognosis could be achieved for other tumor entities, especially within the field of hematological malignancies. (1, 2) Despite continuous improvements in treatment strategies and implementation of new therapeutic approaches, AML patients, in particular the elderly and unfit, still face poor prognosis. (3, 4)

Within the last decade, the introduction of CAR-T cells resulted in a great leap in treatment prospects for patients with acute lymphoblastic/lymphocytic leukemia (ALL) or diffuse large B-cell lymphoma (DLBCL). (5, 6) However, despite great efforts, these improvements could not be transferred to AML, yet. This might be due to the fact that AML resembles a tumor entity of characteristic low immunogenicity as a relatively low number of leukemia associated antigens (LAA) are present on AML blasts. (7, 8) Therefore, development of effective immunotherapy appears to be more challenging. While chimeric antigen receptors recognizing CD33 or CD123 represent the most advanced approaches in adoptive cellular therapy to AML, they face the limitation of on-target/off-tumor reactivity, as both markers are also expressed by hematopoietic stem cells, resulting in severe and dose-limiting side effects. As most of the AML characteristic, surface-expressed antigens are also present on healthy tissues, the aforementioned problem will also occur for other classical CARs due to their limitation of surface antigen recognition. (9) Consequently, alternative tools of immune cell redirection need to be explored in order to generate more specific adoptive cellular therapy for the treatment of AML.

In contrast to CARs, T cell receptors (TCRs) are capable of recognizing processed oligopeptides in the context of a major histocompatibility complex (MHC) also known as human leukocyte antigen (HLA). Importantly, these processed oligopeptides derive from virtually any protein from within or of the surrounding of the presenting cell. Therefore, TCR-recognition is not limited to surface expressed antigens, but covers the whole proteome. (10) Thus, TCRs represent an attractive redirection agent especially with respect of the scarcity of LAAs in AML.

As the earliest approach of ACT with genetically modified immune cells, much experience could be gained on TCR-redirected T cell therapy. However, over the years, certain methodological limitations became apparent. Whereas initial problems, such as TCR-mispairing between the transgenic and endogenous receptor could be solved entirely, for example by modifying the TCR-sequence or CRISPR/Cas mediated knockout of the inherent TCR, others remained despite every effort. (11, 12) Today, clinically practiced T cell-ACT relies on autologous T lymphocytes in order to avoid severe graft-versus-host-disease (GvHD) caused by the infusion of allogeneic T cell preparations. (13, 14) Therefore, this therapeutic approach is entirely dependent on the fitness of the patient´s immune cells and due to its

individuality time consuming, expensive and logistically cumbersome. (15) In the context of leukemia, particularly AML, most patients present with impaired immune cell function in their course of disease. (16, 17) As a result, an ACT-source relying on the patient himself does not appear to be the most suitable immune cell platform for effective immunotherapy against AML.

In contrast to T cells, transfer of allogeneic NK cells is feasible with minimal risk of GvHD and, due to the resulting killer cell immunoglobulin-like receptor (KIR)-mismatch, even beneficial to its treatment efficacy. (18, 19) As a consequence, NK cells offer the potential for an off-the-shelf cellular platform for ACT. (1) Moreover, in the context of hematological malignancies, adoptive transfer of NK cells bears the potential to compensate endogenous NK cell impairment which is characteristic and of prognostic value for patients with leukemia. (16, 17) While wild-type allogeneic NK cells were already proven to be efficient as a stand-alone treatment to hematological malignancies, multiple approaches of genetic modification (GM) enhancing therapeutic efficacy are currently under investigation. (19, 20) However, despite early clinical successes of GM-NK cell-ACT, so far genetic modification of NK cells is mainly restricted to CAR-redirection and therefore prone to methodological-unavoidable on-target/off-leukemia toxicities. (9)

Consequently, we addressed this problem by implementing TCR-redirection to the spectrum of genetic modification of NK cells to AML in order to generate a new promising candidate for ACT. Therefore, inspired by early preclinical studies, we genetically modified NK92 cells, a FDA-approved natural killer cell line with high cytolytic potential, to express AML-reactive TCRs and human CD3 resulting in an unlimited source of potent AML-specific immune cells for ACT. (10, 21) Due to the scarcity of LAAs in AML, we further genetically modified the TCR-positive NK cells to express the CD8-coreceptor. As a result we were able to break the previous bottleneck of CD8-independency for applicable TCRs increasing the likelihood of finding TCRs recognizing AML-specific LAAs suitable for this new therapeutic approach. Therefore, we hereby present a proof of concept for an off-the-shelf cellular platform for TCR-redirected NK cell-based ACT tailored to the specific challenges of AML-immunotherapy.

6 Discussion of literature

6.1 Hematological malignancies

6.1.1 Leukemia

The term “leukemia” represents a multitude of conditions caused by the malignant transformation of hematopoietic stem cells (HSCs) and their descendants resulting in uncontrolled proliferation and accumulation of dysfunctional tumor cells, called blasts, in the blood, bone marrow and/or lymphatic tissues. (1) As a result of the limited space within the bone marrow, physiological hematopoiesis is suppressed in the course of disease by continuous proliferation of leukemic blasts leading to a shortage of healthy and functional erythrocytes, thrombocytes and leukocytes. In the majority of cases the lack of blood cells, called cytopenia, occurs primarily affecting the erythrocytes and thrombocytes. Therefore, this so-called bicytopenia is the most important criterion for the detection of potential leukemia patients from ordinary blood count diagnostic. As in leukemic conditions the malignant transformation predominantly involves a member of the white blood cells and ordinary cell counting does not distinguish between healthy and malignant cells, the number of leukocytes typically varies between too many (leukocytosis), too little (leukopenia) or normal with some tendencies for special types of leukemia. Respectively, the common symptoms of leukemia result from cytopenia. Patients typically present with fatigue and shortness of breath due to anemia resulting from impaired erythropoiesis. Moreover, increased bleeding and bruising are a consequence of thrombopenia, whereas an enhanced susceptibility to infections is caused by the reduced amount of functional immune cells. (22)

Currently, on the basis of risk factors identified to correlate with the probability of its occurrence, leukemia is assumed to be caused by a variety of genetic and environmental factors. (23)

In general, four main types can be differentiated by the percentage of blasts in the bone marrow (acute vs chronic) and the lineage the leukemic stem cells derive from (myeloid vs lymphoblastic/lymphocytic) resulting in acute myeloid (AML), acute lymphoblastic/-cytic (ALL), chronic myeloid (CML), and chronic lymphoblastic/-cytic leukemia (CLL). (23) Acute leukemia presents more severe, due to its sudden onset resulting from the rapid proliferation of malignant cells suppressing the physiological hematopoiesis. In contrast, chronic leukemia typically progresses much slower, and therefore characteristic symptoms become apparent much later in the course of disease.

In detail, leukemia is currently classified based on a variety of clinical, morphologic, immunophenotypic, and genetic features according to the 2016 revision of the World Health Organization (WHO) classification of tumors of hematopoietic and lymphoid tissues. (24)

Interestingly, acute leukemia is, due to its high proliferation rate, more susceptible to conventional chemotherapy and radiation as both modalities target rapidly dividing cells. Therefore, curative treatment options are currently more accessible for patients with acute hematologic malignancies than for patients suffering from chronic leukemia.

6.1.1.1 ALL

The acute lymphoblastic/lymphocytic leukemia (ALL) being the most common leukemia-type in children is caused by an excess cell division of members of the lymphoid lineage resulting from chromosomal alterations such as translocations, insertions or deletions. (25) It can be subcategorized according to the presence of certain chromosomal or genetic mutations as well as by the affiliation to B- or T-lymphocytes. (1) The present standard of care for pediatric ALL comprises combination chemotherapy. Rarely, hematopoietic stem cell transplantation (HSCT) is performed, in the case a patient does not respond properly to conventional treatment. In order to increase therapeutic efficacy, clinical trials combining chemotherapy with blinatumomab, a bispecific monoclonal antibody, are underway. (26) Fortunately, the 5-year survival rate for childhood ALL patients is currently about 87%. However, it deteriorates dramatically upon relapse. Therefore, the implementation of an effective immunosurveillance preventing relapse is a major goal in the ongoing development of new therapeutic approaches. (27) Within the last years, B cell ALL received a pioneering role as one of the first malignancies to be treated with CAR-T cell therapy in clinical routine stating the immense potential of immunotherapy and resulting in a drastic improvement of relapse-patient´s prognosis. (28)

6.1.1.2 CLL

Chronic lymphocytic leukemia represents the most frequent leukemia in adults resulting in proliferation of abnormal cells that, under normal circumstances, would differentiate into B cells, due to alterations in genes responsible for hematopoiesis. (29) As a consequence of the disease-characteristic B cell deficiency, CLL patients are more susceptible to bacterial infections. The established treatment options include chemotherapy in combination with targeted therapies, such as monoclonal antibodies. (30) As not every patient responds effectively to the state-of-the-art therapy, new treatment options are continuously explored. Interestingly, impressive results could be achieved by the use of allogeneic natural killer cells as adoptive cellular therapy (ACT) to CLL suggesting a potential new option in its treatment repertoire. (31, 32)

6.1.1.3 CML

In the US, chronic myeloid leukemia accounts for approximately 15% of leukemia patients and primarily affects the elderly with a median age of 64 at diagnosis. (33) CML occupies an exceptional position in the portfolio of leukemia as it is caused by a specific somatic mutation resulting in an abnormal continuously active state of a receptor tyrosine kinase that leads to

uncontrolled proliferation. In detail, the somatic mutation occurs in form of a reciprocal translocation between chromosomes 9 and 22. The resulting shortened chromosome 22, also referred to as “Philadelphia chromosome”, conveys the fused genes of its own breakpoint cluster region (BCR) and the ABL-1 tyrosine kinase, originally located on chromosome 9. As a consequence, the BCR-ABL fusion-gene induces, due to continuous activity of the tyrosine kinase, disinhibited cell division and blockage of apoptosis resulting in the pathological accumulation of abnormal cells deriving from HSCs, called CML.

Fortunately, CML is, due to its mutational uniformity, prone to treatment with targeted therapies. In the majority of cases, CML can be effectively treated with tyrosine kinase inhibitors (TKIs) specifically targeting the pathological gene-fusion-product BCR-ABL.

6.1.2 AML

Acute myeloid leukemia (AML) represents an aggressive neoplasia of the myelopoiesis resulting from a pathological clonal proliferation of a member of the myeloid cell lineages at any stage of differentiation. (34)

Prior to the discovery of effective treatment options, only 50% of the patients survived the first 5 months after symptoms caused by anemia, neutropenia and thrombocytopenia due to spatial suppression of hematopoiesis by AML blasts had become apparent. At the time, the natural course of disease resulted in a one year mortality-rate of 100%. (35)

Complete remissions and long-term success could be achieved for the first time after the implementation of daunorubicin and cytarabine in 1970. (36) Since then, the prognosis of patients with AML improved continuously. Thereby, particularly the young patients profited from advanced treatment options whereas prognosis remained poor for patients older than 70 to 75 years of age. (3, 4) Despite constant improvements of therapeutic modalities, 5-year mortality rates of AML-patients remained consistent over the last 30 years.(1, 2)

Recently, great success could be achieved for the treatment of acute B cell lymphoblastic leukemia (B-ALL) and diffuse large B cell-lymphoma (DLBCL) by the implementation of state-of-the-art immunotherapeutic approaches, namely CAR-T cell-therapy. For AML however, to date allogeneic hematopoietic stem cell transplantation (allo-HSCT) and donor lymphocyte infusion (DLI) represent the only clinically established options of immunotherapy for high-risk AML patients pretreated with intensive chemotherapy. (37) To the present day, patients that are not eligible for or fail induction chemotherapy regimens face palliative treatment options only. (38) Therefore, great efforts are undertaken in order to broaden the spectrum of clinically available curative therapies and to tie up with the story of success of anti-CD19 CAR T cell-therapies in B-ALL and DLBCL. (5)

6.1.2.1 Epidemiology

The occurrence of AML rises with increased age resulting in an age-specific incidence of greater than 100 cases per 100.000 people older than 70. According to a Swedish register the median of adult AML-patients amounts 72 years of age. (39)

6.1.2.2 Etiology and risk factors

The uncontrolled proliferation of immature myeloblasts in AML is usually caused by the acquisition of multiple chromosomal aberrations or mutations resulting in uncontrolled activation of proliferation. In average 5 recurrent genetic alterations can be detected in every AML patient while the most common mutations to occur affect one of the following genes: FLT3, NPM1, DNMT3A, IDH1 and IDH2. (1, 34) Interestingly, within approximately 50% of AML-patients, leukemic blasts with different mutational profiles can be detected indicating an oligoclonal, instead of the historically assumed clonal, origin of the AML-pathogenesis. Today, this clonal heterogeneity is thought to be accountable for the occurrence of relapse and differences in responses to therapeutic measures. (40)

As AML occurs due to genetic alterations, risk factors mainly comprise chemical or physical agents resulting in DNA-damage upon exposition. Therefore, radioactive radiation, benzols, products from mineral oil, paints, ethylene oxides, herbicides and pesticides represent common environmental factors associated with the development of AML. Furthermore, a significant correlation between smoking and the occurrence of AML could be detected in a large meta-analysis resulting in a 40% increased risk for active smokers compared to non-smokers ($p < 0{,}001$). (41) In addition, AML-risk is elevated iatrogenically by radiation and chemotherapy, especially by alkylating agents and topoisomerase-II inhibitors. Therefore, cancer patients receiving conventional treatment have an increased probability of developing so-called secondary AML due to therapy-related DNA-damage in HSCs. (42)

Moreover, increasing age and family burden represent the most common risk factors that are not influencable.

6.1.2.3 Prognosis

Being genetically heterogeneous, chromosomal and genetic analyses are relevant for the prognosis in AML. (43) Moreover, as natural killer cell dysfunction is related to disease progression in leukemia, the patient´s immune status is also assumed to be predictive for the individual outcome. (16, 17) Referring to data from the US, currently the general 5-year survival rate amounts 28% while patients not eligible to or having failed intensive chemotherapy face no curative treatment options. (38, 44)

6.1.2.4 Treatment

In general, AML patients (except for acute promyelocytic leukemia [APL]) are allocated to two different treatment regimens depending on the biological age and fitness of each individual patient. Thus, patients with a biological age younger than 75 and no severe comorbidities are treated with curative intentions, whereas patients that don´t match the aforementioned criteria are admitted to palliative care due to low chances of long-term remission upon intensive treatment. (45)

6.1.2.4.1 Palliative therapeutic intentions to “unfit” patients

As with increasing age the probability of achieving CR as well as long-term remission deteriorates and risks for therapy-associated complications rise simultaneously, so-called “unfit” patients are preferentially treated with palliatively intended cytoreductive chemotherapy or best supportive care (BSC). (35, 39, 46) According to the medical guideline for AML of the German society of hematology and oncology (DGHO), patients are categorized as “unfit”, when they meet the following criteria: (34)

I. Biological age > 75 years;
II. Comorbidities such as advanced diabetic syndrome; severe liver, renal or heart failure (EF < 30%)
III. ECOG ≥ 3
IV. Low chances of recovery, high risk for premature death in the course of induction therapy

In this special subpopulation of AML-patients, the complications expected to occur in the course of curative treatment would exceed its potential benefits. (44) Therefore, prolonging survival while maintaining maximum quality of life (QoL) becomes the main therapeutic objective for “unfit” patients. (34, 46) Recently, the new standard-of-care for this subgroup of patients, venetoclax, a BCL2-inhibitor, in combination with a hypomethylating agent, namely azacitidine or decitabine, has markedly improved both QoL and survival rates compared to previously established treatment protocols and therefore changed the perspectives of therapeutic goals in AML-treatment not only for unfit patients substantially. (34, 38)

6.1.2.4.2 Curative therapeutic intentions to “fit” patients

As previously mentioned, AML-patients categorized as “fit” comprise no severe comorbidities and a biological age under 75. Therefore, the probability of achieving long-term remission is high enough to outnumber the therapy-associated risk and temporary reduction of quality of life. (34) The course of treatment is generally divided into induction chemotherapy aiming to achieve complete remission (CR), followed by post-remission therapy to maintain CR. (1) While treatment protocols are continuously updated to the most recent findings of clinical research, the standard induction therapy scheme “7 + 3” consists of combination

chemotherapy with cytarabine and anthracycline (e.g. daunorubicine) or anthracenedione. However, in addition to this general regimen, depending on the results of preliminary genetic, phenotypic and morphologic diagnostics, specific treatment protocols tailored to the risk profile and expected treatment response of each individual AML-patient can already be offered.(34)

Fortunately, the majority of patients achieve complete remission upon intensive induction chemotherapy. Nevertheless, without further treatment, a high number of these patients experiences relapse. (37) Therefore, post-remission therapy is performed in order to consolidate the therapeutic success of the previous treatment. In turn, AML-patients are categorized according to their prognosis, in favorable, intermediate and unfavorable. In short, allogeneic hematopoietic stem cell transplantation (allo-HSCT) is recommended for patients with intermediate and unfavorable prognosis, whereas patients with a favorable prognosis typically face chemotherapy-based (commonly cytarabine) high-dose consolidation and subsequent maintenance therapy. (34)

Despite the performance of post-remission therapy, relapse of AML, even in patients receiving allo-HSCT, is common. (47) As patients with relapsed leukemia often present with chemoresistance and a significantly impaired immune system, additional treatment options are desperately needed to effectively increase their prognosis and reduce mortality rates. (48, 49) Results of recent clinical trials testing targeted therapy treatment options in a post-transplant setting revealed that isocytrate dehydrogenase (for IDH-mutated AML), Ivosidenib (for IDH1 mutated AML), Enasidenib (for IDH2 mutated AML) and Venetoclax (selective BCL2 inhibitor) were all capable to effectively improve the clinical outcome of AML patients. (50-52) Furthermore, induction of the immune system appears to be a promising approach in relapse prevention. As allo-HSCT and donor lymphocyte infusions (DLIs) are already standard immunotherapies, further adoptive cellular therapy-options are currently explored having the potential to improve antitumoral immune responses without damaging off-target tissues. (37, 53) Therefore, numerous immunotherapeutic approaches for AML-treatment are under investigation including bispecific antibodies, CAR-T and NK cell therapy. (54) In the rising field of NK cell-immunotherapies, adoptive transfer and blocking of immune checkpoint inhibitors (ICIs) have proven to be promising treatment candidates for primary and relapsed leukemia already. (55-57) More recently, the introduction of CAR-redirected NK cell therapy has revolutionized treatment not only of leukemia, but also of lymphoma and solid cancers. (19, 58-60)

6.2 Immune evasion in Leukemia

In respect of the continuous progress in the understanding of cancer, in 2011 Hannahan and Weinberg proclaimed the capability of immune evasion of malignant transformed cells as an emerging hallmark of cancer attesting the high relevance of the interaction between cancer cells and the immune system for tumorigenesis and -perisistence. (61) Physiologically, cells that underwent mutational transformation are recognized by special members of the innate (NK cells) and adaptive (cytotoxic T-lymphocytes) immune system. Subsequently, apoptosis is induced resulting in an effective clearance of potential cancer-progenitors. However, in the course of tumorigenesis the increasing mutational burden of cancer cells eventually results in their potential to evade this immunosurveillance. The mechanisms underlying this important step in carcinogenesis are numerous and diverse with antigenic modulation, imitation of healthy tissues or the establishment of an immunosuppressive tumor microenvironment being only examples for the many ways of immune escape. (62, 63)

Leukemia, compared to other, especially solid malignancies, is characterized by a particularly low rate of mutations per kb DNA resulting in comparatively low quantities of tumor/leukemia associated antigens (LAA). As a result hematological malignancies are considered to be less immunogenic as tumors with high mutational burden such as melanoma or non-small cellular lung cancer (NSCLC). (8) This is due to the reduced repertoire of LAAs potentially to be recognized by cytotoxic T lymphocytes upon their presentation in the context of major histocompatibility class (MHC) I complex. Therefore, leukemia is exceptionally prone to immune evasion as it results in minimal T cell activation inherently. (7) In addition, this special property can further aggravate, when shedding of MHC by leukemic blasts occurs resulting in impaired T cell recognition. (64)

6.2.1 NK cell impairment in leukemia

Besides evading the adaptive immune system by reduced T cell function due to low immunogenicity, the leukemic microenvironment seems to induce a decrease in innate immune system functions as NK cell-encroachment is observed not only in one, but in all major categories of leukemia (AML, ALL, CML and CLL). (65-67) In detail, leukemia patients typically present with reduced numbers of active NK cells possessing impaired degranulation and cytotoxic capabilities. In addition to observational studies, the high potential of NK cell impairment by the leukemic environment could be confirmed experimentally as coinjection of NK cells with leukemic blasts resulted in reduced effector function and proliferation of NK cells compared to the control group in a RAG CC KO mouse model. (68) In a clinical setting, this special property of leukemic conditions has great influence on patient´s individual prognosis

and therefore can be used for its determination. (17) Consequently, understanding the mechanisms underlying the reduction of innate immunosurveillance by NK cell impairment bears great potential for the development of new therapeutic approaches to leukemia.

Leukemic blasts typically escape NK cell recognition by manipulation of the expression pattern of activating and inhibitory NK cell-ligands on their surface resulting in reduced activation of effector cell properties such as cytokine degranulation or cytotoxicity of interacting NK cells. (69) In detail, upregulation of inhibitory receptor-ligands such as NKRP1A as well as downregulation of activating NKG2D-receptor-ligands MICA/MICB have been described to occur in the context of leukemia and, resulting in NK cell impairment, to be indicative of poor prognosis. (70-72) In this context, NKp44, a member of the natural cytotoxicity receptor (NCR) family, plays a special role. Being an activating NK cell receptor, binding of NKp44-ligands normally results in NK cell activation. However, NKp44 also mediates inhibitory signaling upon binding of the proliferating cell nuclear antigen (PCNA) or HLA I. In leukemia, blasts modulate their NKp44-interaction via upregulation of PCNA and HLA I in order to escape NK cell-surveillance. (73, 74)

Leukemic blasts bear the potential to effectively escape NK cell recognition by other mechanisms as well. By secreting transforming growth factor-β (TGF-β), for example, tumor cells are capable to establish an immunosuppressive microenvironment which inhibits NK cell function and survival. (75, 76) Moreover, blasts can shed activating receptors on their surface by releasing specific enzymes such as matrix metalloproteinases (MMPs), disintegrin or metalloproteinase (ADAM) resulting in reduced recognition by immune cells without the necessity of gene-expression downregulation. (77)

As NK cell impairment is a characteristic property of leukemia, restoration of NK cell effector function appears to be a promising approach to overcome leukemic immune evasion and enable effective treatment. (1)

6.3 Immunotherapy – the new era of antitumor treatment

Despite continuous improvements in clinical care and rapidly multiplying treatment options for cancer patients, the status quo of current oncological therapy remains unsatisfactory for many tumor entities. With a present 5-year survival rate of 28% AML is one of their representatives. (38, 44) As conventional therapy, comprising chemotherapy and irradiation, aims to kill rapidly proliferating cells, by these means, besides tumor cells, also healthy tissues with high proliferative properties are affected resulting in dose-limiting adverse effects. (1) Moreover, conventional treatment modalities destroying malignant cells by introducing DNA-damage to

rapidly dividing cells bear the risk of inducing so-called secondary leukemia by off-target DNA-alterations within HSCs.

In response to a more comprehensive understanding of the interactions between cancer and the immune system, immunotherapy gained attention as a treatment option that enables the inherent, physiologically effective, antitumoral immune system to regain dominance and push back tumor propagation. In contrast to conventional treatment options, immunotherapy possesses the potential of specific antigen-recognition which, in the context of cancer therapy, results in unmatched targeting accuracy. Therefore, an immense variety of immunotherapeutic approaches has evolved and is currently under investigation for implementation into clinical practice, of which several proved to be highly promising candidates to combat cancer cells with superior specificity. (5, 6)

6.3.1 Antibody-based immunotherapy

In general, immunotherapy can be subdivided based on the nature of the therapeutic agent into cellular and (largely) antibody-based immunotherapy. Monoclonal antibodies such as Rituximab (directed against CD20 on leukemia and lymphoma cells) and Herceptin (anti-HER2-mAb for the treatment of breast cancer) represent effective tools to target and eliminate tumor cells upon administration. Additionally, a variety of different methodological strategies, including vaccines, have been explored to augment immune responses to tumor antigens such as MAGE-3 and NY-ESO-1. Moreover, the development of so called checkpoint inhibitors focuses on blocking receptors or ligands of physiological regulatory circuits of the immune system, like e.g. PD-1, PDL-1, Lag-3, regulatory T cells or CTLA-4, that are frequently co-expressed on cancer cells leading to cancer-induced immunosuppression. (78) Therapeutic efficiency and clinical applicability have been proven for many antibody-based immunotherapeutic approaches. However, they all have in common that they depend on the fitness of the patient´s immune system. As elaborated previously, in some tumor entities, especially leukemia, cancer-induced immunosuppression occurs bearing low potential for stimulation of the patient´s inherent immune system. In this scenario, providing immunosuppressed cancer-patients with highly functional antitumoral immune cells – cellular immunotherapy – appears to be the more effective treatment option. (79)

6.3.2 Cellular immunotherapy

Cellular immunotherapy, also known as adoptive cellular therapy (ACT), describes the application of cytotoxic immune cells (T lymphocytes or NK cells) to cancer patients in order to eliminate tumor cells. Over time, many different approaches have been established varying in the cell type used and the extent of the cellular therapeutics´ preprocessing. While early ACT was, for example, based on in vitro expansion and stimulation of autologous tumor-infiltrating lymphocytes (TILs), current approaches focus mainly on the application of

genetically modified T or NK cells due to great advances in gene editing possibilities (e.g. CRISPR-Cas). (80) Thus, redirecting agents – receptors that result in activation of effector functions upon binding of a defined antigen – can be conveniently integrated into the genome of the cytotoxic immune cells retargeting their killing activity towards cancerous cells. (81) Within the last years, the immense therapeutic potential of ACT in combination with genetic engineering became apparent as the first chimeric antigen receptor (CAR)-redirected T cell-product to be approved by the FDA achieved great clinical success for the treatment of patients with acute lymphoblastic/lymphocytic leukemia (ALL) or diffuse large B-cell lymphoma (DLBCL). (5, 6) As a consequence, numerous new CAR-constructs have been established aiming to transfer these impressive results to other tumor entities by targeting different antigen-structures. However, as clinical experience in CAR-T cell therapy grows, treatment-specific side effects and challenges become apparent. (82) Therefore, current research is increasingly focusing on alternative redirecting agents and cellular platforms to broaden the spectrum of effective ACT available.

6.3.2.1 Redirecting immune effector cells for ACT

As depicted in Fig. 6.3.1, the main redirecting cellular structures to be transgenically expressed in immune cells in the context of ACT comprise T cell receptors (TCRs) and chimeric antigen receptors (CARs). Historically, TCRs were the first receptors to be successfully used for ACT in order to change targeting abilities of autologous T cells by gene editing to tumor-associated antigens (TAAs). (83-85) In addition, as elaborated previously, within the last decades *in silico*-designed, synthetic receptors that are specialized on immune cell-activation upon specific antigen-recognition – CARs – evolved as an alternative option and were recently approved for clinical application. (28)

While TCRs and CARs both are capable of effective activation of cytokine degranulation and cytotoxicity in immune cells, they profoundly differ in their mechanisms of antigen recognition. As in original CAR-constructs the fragment antigen-binding (Fab) region of an antibody confers its targeting-specificity, the properties of CAR-mediated antigen recognition are comparable to the ones of antibodies. Therefore, original CARs are capable to bind not only to epitopes of fully cell surface expressed protein antigens, but also to gangliosides and carbohydrates, as long as they are expressed on the cell surface. (86)

On the contrary, TCR-recognition is limited to processed oligopeptides in the context of an MHC complex. Nevertheless, as these peptide-antigens derive from the whole protein-repertoire from within and the surroundings of the presenting cell, TCRs possess the potential to recognize the whole proteome and, in the context of cancer, the tumor´s mutagenome. (10, 86) Since such cancer-specific mutations and their corresponding TAAs can´t be found in normal tissues, TCRs bear the potential of unmatched therapeutic specificity. However, due to

MHC-restriction, TCR-redirection is prone to HLA-downregulation frequently occurring in cancer patients. (87)

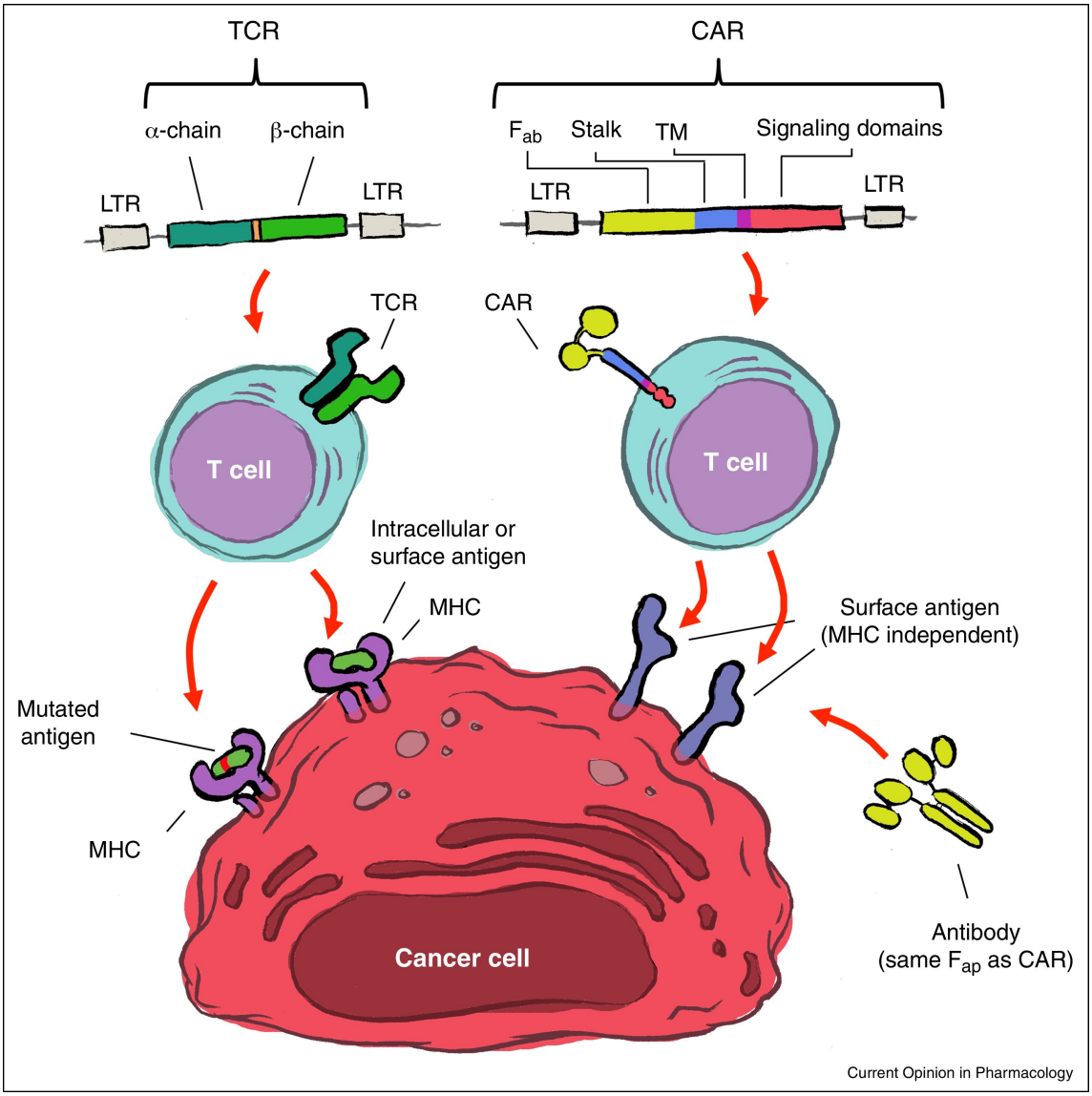

Figure 6.3.1 Juxtaposition of TCR- and CAR-antigen-recognition. Illustration from Stauss H. J. et al. 2015. (86)

6.3.2.2 Cellular platforms for ACT

Despite the different advantages and disadvantages of redirecting T cells by transgenic TCRs or CARs, both approaches were shown to be highly effective against various malignancies in a clinical setting. (5, 6, 88-91) As a result some CAR-T cell-products, e.g. redirected against CD19, were FDA-approved and implemented into everyday clinical practice. (5, 6, 28) Thereby, in the upscaling-process to guarantee the availability of these state-of-the-art therapeutics to applicable patients, methodological limitations of T cell-based CAR-therapy became apparent. Due to the great risk of induction of graft-versus-host-disease (GvHD) by allogeneic T cells, all approaches in CAR-T cell-therapy currently rely on autologous T lymphocytes as their cellular platform. (13, 14) As a consequence, the quality of the therapeutic product relies on the fitness of each patient´s individual T cells, which depends e.g. on age,

and pretreatment of the patient. Therefore, better standardization of T lymphocyte quality in terms of viability, potential effector functions and state of activation is extremely challenging and only to a certain point feasible. From a physician´s perspective, due to aforementioned variations, fluctuations in effectiveness between individual CAR-T cell-preparations must be considered and likely result in less predictable treatment responses. In addition, the limitation to autologous T cell preparations leads to high logistical effort to be undertaken in the course of T cell-product-manufacturing, resulting in high treatment costs. (15) Thus, alternative cellular platforms are continuously reviewed in order to establish a better available and more standardized treatment option.

In this context NK cells have been gaining great interest as adoptive transfer of allogeneic NK cells was already proven to be effective in patients with hematological and solid malignancies. (20, 92-96). In this line, CAR-redirected NK cells resulted in effective antitumoral responses in numerous clinical trials with only minimal risk of GvHD and without CAR-T-associated toxicities such as cytokine release syndrome (CRS). (19, 97, 98) Moreover, focusing on the long-term effects of CAR-NK cell transfusion, persistence and proliferation of effector cells for up to 12 months could be detected *in vivo* and in a clinical trial using HLA-mismatched NK cells redirected with an anti-CD19-CAR in patients with relapsed and refractory CLL and lymphoma. (99, 100). Thus, NK cells bear the potential of a non-individualized application across histocompatibility barriers as an off-the-shelf cellular therapeutic resulting in reduced costs and an increased access to treatment. (1) In contrast to T cell-ACT, several sources of NK cells have been established for clinical application and serve as platforms for genetic modification in ACT. Next to *ex vivo* expansion of NK cells from donor-derived peripheral or cord blood, NK cells can also be differentiated from already CAR-engineered induced pluripotent stem cells (iPSCs). (99-102) In addition, “NK92”, an NK cell line with high cytolytic potential is already approved for ACT by the FDA and represents an attractive, unlimited multiplying cellular source receptive to gene editing. (103-105)

In the field of NK cell-based ACT all ongoing and already performed clinical trials were and are utilizing CARs, when additional receptor-based redirection was or is desired. This circumstance is mainly due to the fact that CARs are capable of potent NK cell stimulation without further genetic modification. TCRs on the contrary, are dependent on concomitant transgenic expression of the human CD3 complex to successfully redirect NK cells as they do not endogenously express all components necessary for the formation of a functional TCR-complex. (10, 21, 106) In preclinical studies, the NK cell line NK92 as well as *ex vivo* expanded NK cells from peripheral blood were shown to elicit effective antitumoral reactivity upon expression of therapeutic TCRs together with the transgenic CD3-complex *in vitro* and *in vivo*. (10, 21, 107) As a result, these early studies, paving the way for further development of TCR-

based NK cell-ACT, suggest great therapeutic potential deriving from the combination of the benefits of NK cells as a cellular platform and the broad antigen-recognition spectrum of TCRs to be explored in detail in prospective studies.

6.3.2.3 NK-ACT against AML

As previously elaborated, leukemia and in particular AML frequently result in impaired immune cell functions, especially of the NK cell population. (65-67) Therefore, adoptive transfer restoring the physiological NK cell effector function appears to be a promising approach for immunotherapy against AML. (1) As listed in table 9.3.1, the majority of currently ongoing clinical trials on NK cell-ACT to treat AML is based on genetically unmodified HLA-mismatched NK cell preparations with NCT05247957 being the only one examining the efficacy of genetically modified NKG2D CAR-NK cells in patients with relapsed or refractory AML. (108) Therefore, the development of gene edited NK cell-ACT appears to lack behind in the treatment of AML compared to other tumor entities, such as ALL and CLL. (1) This fact might be due to the complexity of CAR-design in the context of the low immunogenicity of AML blasts. Interestingly, despite the scarcity of LAAs in AML and the, compared to CARs, superior potential of their recognition by TCRs no clinical trial utilizing TCR-redirected NK cells for the treatment of AML has been performed yet. (8, 10, 86)

Identifier	Phase	Conditions	NK cells' source	Other interventions
Hematopoietic Stem Cell Transplant (HSCT) setting				
NCT05247957	I	AML	CAR-NK cell	–
NCT05272293	I/II	AML	Expanded haploidentical NK cells	K562-mbIL21-41BBL
NCT05256277	I	AML	Cytokine-induced memory-like NK cells	CT101a
NCT04632316	I/II	AML	PBMC-derived NK cell	Cyclophosphamide-Fludarabine (Cy/Flu)
NCT01904136	I/II	AML, MDS, CML	PBMC-derived NK cell	Cyclophosphamide, Fludarabine, Melphalan, Mycophenolate Mofetil, Tacrolimus
NCT01823198	I/II	High-risk AML or MDS	PBMC-derived NK cell	IL-2, Busulfan, Fludarabine Phosphate
NCT04166929	II	AML, MDS	PBMC-derived NK cell	–
NCT03300492	I/II	AML, MDS	PBMC-derived NK cell	NK-DLI
NCT02809092	I/II	R/R AML	PBMC-derived NK cell	IL-21
NCT04836390	II	AML	PBMC-derived NK cell	IL-21
NCT01619761	I	AML, MDS, et al	UCB-derived HSPC-NK cell	Cyclophosphamide, Fludarabine Phosphate, Lenalidomide, Melphalan, Mycophenolate Mofetil, Tacrolimus
NCT02727803	II	AML, MDS, et al	UCB-derived HSPC-NK cell	Busulfan, Clofarabine, Cyclophosphamide, Fludarabine Phosphate, Melphalan, Rituximab
NCT04024761	I	Relapsed AML, MDS, or MPN	Cytokine Induced Memory-like NK Cell	IL-2, Fludarabine, Cyclophosphamide
NCT03068819	I/II	Relapsed AML	Cytokine Induced Memory-like NK Cell	CD3 + T Cell Product Infusion
NCT02782546	II	R/R AML	Cytokine Induced Memory-like NK Cell	ALT-803, Tacrolimus, Mycophenolate mofetil, G-CSF

NCT04209712	Early Phase I	AML with MRD	PBMC-derived NK cell	IL-2
Non-Hematopoietic Stem Cell Transplant (non-HSCT) setting				
NCT02890758	I	AML, MDS, et al	PBMC-derived NK cell	ALT-803
NCT04221971	I	R/R AML	PBMC-derived NK cell	Chemotherapy
NCT03955848	N/A	AML in Remission	PBMC-derived NK cell	IL-2
NCT04220684	I	R/R AML or MDS	PBMC-derived NK cell	IL-21, Cytarabine Hydrochloride, Fludarabine
NCT04327037	I	AML	PBMC-derived NK cell	IL-2
NCT04347616	I/II	R/R AML	UCB-derived HSPC-NK cell	IL-2
NCT04310592	I	AML	Placental-derived HSPC-NK cell	CYNK-001
NCT01898793	I/II	R/R AML or MDS	Cytokine Induced Memory-like NK Cell	ALT-803, IL-2, Fludarabine, Cyclophosphamide,
NCT04354025	II	R/R AML	Cytokine Induced Memory-like NK Cell	IL-2, Fludarabine, Ara-C, G-CSF

Table 6.3.1 Ongoing clinical trials of adoptive NK cell therapy in AML. Modified table from Rahmani et al.2022. (108)

6.4 Current challenges in ACT

Being the first FDA-approved genetically modified therapeutic to express a CAR redirected against hematological neoplasia, most clinical experience could be gained on anti-CD19-CAR-T cell therapy to relapsed B-ALL and DLBCL patients. (5, 6) Strikingly, despite outstanding clinical effectiveness documented in early clinical trials, severe adverse effects accompanying CAR-T cell treatment are increasingly being reported. For example, in a study investigating anti-CD19-CAR-T therapy for relapsed B-ALL patients over half of the participants developed GvHD and/or CRS in the course of treatment, while two patients died from infection and one from cardiac arrest. (109) Unfortunately, this study was not an exception but rather a representative for the severe acute toxicities observed in the course of CAR-T therapy in general. (82) Thus, the aforementioned cytokine release syndrome (CRS) commonly occurs throughout CAR-T treatment resulting in severe, up to grade IV, toxicities with the necessity to apply tocilizumab, an anti-IL-6 antibody, as a rescue therapy. (110, 111) In addition, patients undergoing CAR-T ACT are prone to develop neurologic toxicities such as brain edema and the treatment-specific CAR-T cell-related encephalopathy syndrome. (82) Besides adverse events specifically related to CAR-T therapy, also common side effects like tumor lysis syndrome occur as a result of overwhelming tumor cell destruction. Depending on the antigen targeted by the CAR, especially in the treatment of hematological neoplasia, prolonged neutropenia can be observed caused by CAR-T cell-induced myeloablation due to on-target/off-tumor-reactivity. In this case HSCT can become necessary in order to restore the patient´s immune system. (112)

The last side effect mentioned can be bypassed by the selection of a more specific antigen to be targeted by the adoptive cellular therapeutic. In the context of hematological neoplasia and AML in detail, this appears to be very challenging as AML blasts are generally considered to

be less immunogenic due to low mutational rates resulting in less TAAs to be potentially targeted compared to solid malignancies. (8) As most antigens highly expressed on the surface of leukemic cells – therefore accessible to CAR-recognition – are also to some extent present on physiological myeloid progenitors and stem cells, CAR-T therapy is prone to result in severe and irreversible neutropenia due to aforementioned on-target/off-leukemia reactivity. (9) Thus, developing retargeting structures agents recognizing the mutagenome of AML blasts seems to be a promising approach to overcome this methodological limitation. As TCRs are capable of intracellular peptide-recognition, they bear the potential to specifically bind to fragments of mutated proteins and consequently represent a promising candidate for leukemia-specific redirection of immune cells.

6.5 A new approach for adoptive cellular therapy to AML

While TCR-based redirection appears to be a favorable approach for ACT to AML, certain challenges occur upon expression of transgenic TCRs in T cells, which represents the current standard of care. As wild-type T lymphocytes possess an endogenous TCR, redirection with a therapeutic TCR bears the risk of so-called TCR-mispairing. (11, 12) Thereby, the α- and β-chains of both, the transgenic and endogenous TCR do not associate with their designated counterpart, but instead form new, chimeric receptors consisting of transgenic and endogenous subunits. As a result, these mispaired TCRs convey an unknown antigen-specificity and a significant risk for off-target reactivity with the potential to cause severe adverse events. (113) Consequently, measures were taken to avoid the possibility of TCR-mispairing. For the expression in genetically unmodified T cells, the DNA-sequence of the transgenic TCR was optimized by murinization of its constant domains or the introduction of a disulfide bond between the α- and β-chain constant regions. (86) In addition, due to new gene editing possibilities such as CRISPR/Cas, specific knockout of the endogenous TCR is performed in state-of-the-art TCR-based T cell-ACT in order to eliminate the potential of TCR-mispairing and off-target reactivity deriving from the innate TCR. (114) Therefore, the caveat of TCR-mispairing in T cell-based ACT can be minimized.

However, conferring new antigen-recognition capacities to immune cells via therapeutic TCRs results in a strict dependence of its efficiency on the expression of corresponding peptide-MHC-complexes on target cells. Hence, TCR-based ACT is prone to MHC-class I downregulation, which is a common mechanism of immune escape in cancer cells. (78, 115) When applied on T lymphocytes as a cellular platform, loss of HLA-class I inevitably results in failure of TCR-ACT.

In contrast, MHC-class I downregulation represents an activating stimulus on NK cells mediated by the endogenous receptor repertoire regulating NK cell reactivity to malignant transformed or virally infected cells. (116) Therefore, NK cells represent a promising cellular source for TCR-based ACT capable of maintaining its therapeutic efficiency even upon HLA-class I downregulation of cancer cells. (107) Moreover, as NK cells bear the potential of allogeneic transfer without causing GvHD, which is commonly observed in T cell therapy, they qualify for the establishment of an off-the-shelf cellular therapeutic resulting in reduced costs, simplified manufacturing processes and therefore in increased accessibility to patients. (10) These economic benefits of NK cells towards T lymphocytes can be further increased, when the continuously growing and highly cytotoxic NK cell line “NK92” is used as a cellular platform for adoptive therapy. As safety of infusion, especially without occurrence of GvHD or CRS, of irradiated NK92 cells into cancer patients has been proven in numerous clinical trials, this cell line was approved by the FDA for adoptive transfer purposes. (117-119) While the current standard of care, autologous T cells are expensive and logistically challenging, from an economical perspective NK92 represents the most favorable alternative of cellular sources currently available for ACT. (15)

In 2019, Mensali et al. were the first to describe a new approach for adoptive cellular therapy, depicted in Fig. 6.5.1, as they were able to present the proof-of-concept for redirection of NK cells with therapeutic T cell receptors. Utilizing NK92 cells they retrovirally transduced the human CD3 complex in addition to a transgenic TCR-construct resulting in functional expression of the TCR-CD3-complex in NK92. As a result, the genetically modified NK cells mediated TCR-specific effector functions *in vitro* and *in vivo*. (10) In the same year, these observations were confirmed by Parlar et al. who also transduced NK92 cells in order to express CD3 together with different TCRs. (21) Since then, TCR-based ACT was no more limited to T lymphocytes but also applicable to NK cells consequently bearing the potential to combine the benefits of TCR-recognition properties with the advantages of NK cell-transfer such as minimal GvHD and CRS.

Searching for an approach in the field of ACT that carries the potential to effectively treat AML, we found that redirection of NK cells with AML-reactive TCRs resulted in a promising symbiosis addressing the special challenges in AML-treatment with the potential of mutagenome-recognition conferred by TCRs and the restoration of NK cell impairment by economically beneficial NK92. In addition, as TCR-signaling in T lymphocytes usually occurs in the presence of CD8 or CD4 as TCR-coreceptors, in this study we intended to examine the effect of concomitant coreceptor-expression, exemplified by CD8, on the effector functions of TCR-redirected NK92 cells. Due to natural variations in the affinity of TCRs to their corresponding antigen, the ones with high-affinity are capable to induce efficient downstream signaling

resulting in activation of effector cell functions even without the support of their coreceptor. As in previous studies the NK92 cells were neither equipped with CD4 nor CD8, the TCRs utilized were of high-affinity as they were able to induce efficient antitumoral reactivity together with CD3 only. (10, 21) However, as TCR-antigen-recognition represents a very delicate mechanism highly supervised in the course of T cell maturation, an increased affinity of a TCR bears the risk of increased crossreactivity-associated toxicities. (120) Furthermore, high-affinity TCRs only represent a subpopulation of tumor-reactive TCRs as potential ACT-redirection-agents. In consideration of the scarcity of LAAs in AML, we therefore intended to broaden the spectrum of TCRs applicable, with simultaneously reduced risk of on-target toxicities, for this therapeutic approach by implementing CD8-coreceptor expression to NK92 cells. In the following, each component of the therapeutic approach underlying this study is introduced in further detail.

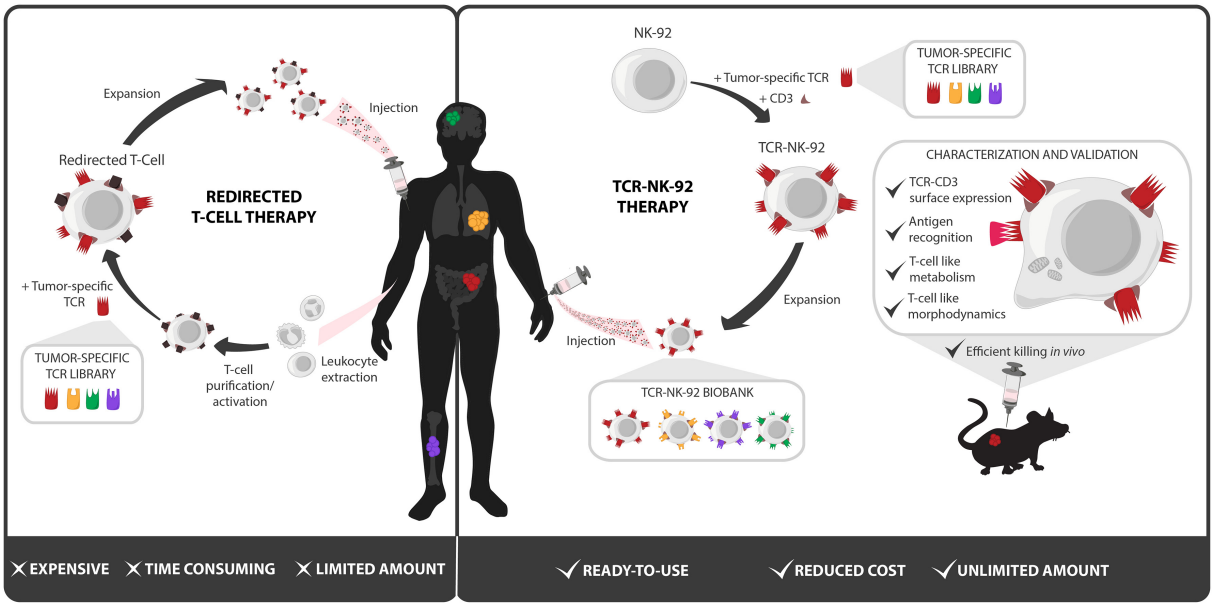

Figure 6.5.1 Comparison between the current standard in TCR-redirected immunotherapy and the new approach of NK92 TCR-based off-the-shelf ACT. Illustration obtained from Mensali et al. 2019. (10)

6.5.1 NK cells

Next to T and B cells, NK cells are a member of the lymphoid cell lineage originating from HSCs and represent around 10% of the lymphocytes circulating within the human body. (121) As a first line of defense, NK cells take part in eradication of cancerous or virally infected cells. Unlike T cells, they are not dependent on multiple stimuli prior to efficient cell lysis. On the contrary, NK cells, as part of the innate immune system, are equipped with an extensive repertoire of germline-encoded activating and inhibiting receptors allowing immediate exertion of effector cell functions upon first contact to a suitable target.

NK cells are typically characterized by the absence of CD3- and presence of CD56-expression ($CD3^-$ $CD56^+$). Moreover, depending on the amount of CD56 expressed on the cell surface as well as the presence of CD16, NK cells are subdivided into two fractions, namely: $CD3^-$ $CD56^{dim}$ $CD16^+$ and $CD3^-$ $CD56^{bright}$ $CD16^-$ NK cells. (121, 122) The $CD3^-$ $CD56^{bright}$ $CD16^-$ NK cell-fraction is typically located in lymph nodes characterized by extensive cytokine production in the course of stimulation, e.g. viral infection or tumor cells.(122, 123) $CD3^-$ $CD56^{dim}$ $CD16^+$ NK cells on the other hand, predominantly occupy the peripheral blood and exert perforin and granzyme mediated cytolytic activity upon stimulation. (122) Interestingly, NK cells are capable to switch their subpopulation as stimulation with peripheral tissue fibroblasts results in differentiation of $CD56^{bright}$ into $CD56^{dim}$ NK cells. (124) Moreover, NK cells seem to develop memory properties contributing to cancer cell surveillance. (125)

6.5.1.1 It´s all about the balance – mechanisms underlying NK cell activation

As depicted in Fig. 6.5.2, NK cells interact with the cells they encounter in the course of circulation through the human body. As a key role player in immunosurveillance, NK cells are able to distinguish between healthy and malignant or virally transformed tissues, and exert similar effector functions as T lymphocytes including degranulation of inflammatory cytokines and cytotoxicity mediated by perforine and granzymes. In detail, NK cells release IFN-γ, TNF-α, Granulocyte-Macrophage Colony-Stimulating Factor (GM-CSF), and IL-33 along with IL-4, -7, and -12 in order to stimulate immune responses. (126) However, unlike T cells, activation of NK cells does not depend on specific antigen-recognition, but relies on a balance of activating and inhibitory signals from an assortment of germline-encoded receptors. (127, 128) Without any interaction, NK cells are in a latent state, neither activated nor inhibited. (1) As illustrated in Fig. 6.5.2 A, upon contact with healthy host tissues, predominantly inhibitory receptor-ligand interactions occur preventing NK cell-cytotoxicity, due to the subsequent shift of the NK cell-balance to inhibition. (129) On the contrary, NK cells encountering virally infected or cancerous cells can be stimulated to elicit effector functions as a consequence of upregulation of activating NK-receptor-ligands on damaged cells. (Fig. 6.5.2. C) In general, NK cell activation or inhibition is always the result of multiple receptor-ligand interactions. (130) Interestingly, due to the balance of activating and inhibiting stimuli determining the action of NK cells, the absence of inhibiting signals can also result in induction of NK cell-reactivity towards the cell encountered. (Fig. 6.5.2 B) This mechanism is especially relevant in the context of MHC class I downregulation often occurring in the course of cancer immune evasion. The lack of MHC I, which under normal conditions induces NK cell inhibition, activates NK cells to induce target-cell-apoptosis due to missing inhibitory signals representing an important feature to specifically target malignant cells, which by this mean already escaped T cell-recognition. (1, 131, 132) However, as NK cells do not react against erythrocytes

physiologically missing MHC class I expression, lack of MHC I solely is not sufficient for induction of NK cell killing.

Depicted in Fig. 6.5.2 D, antibody-dependent cellular cytotoxicity (ADCC) represents another mechanism of NK cell-activation serving as an interface between the adaptive and innate immune system. In detail, antibodies secreted by plasma cells bind to pathological antigens expressed on the surface of a damaged cell. Subsequently, circulating NK cells recognize via CD16 the Fc part of the antibody resulting in stimulation of effector functions towards the opsonized target cell. (133)

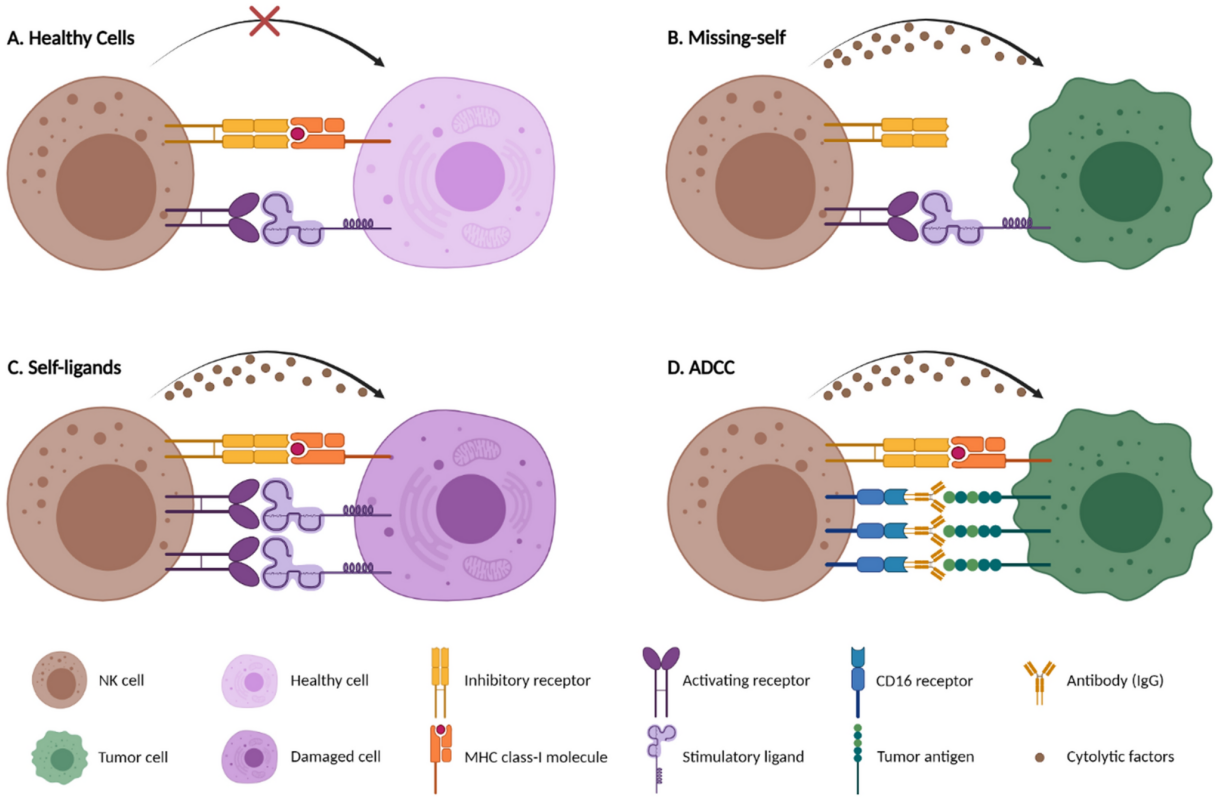

Figure 6.5.2 Inherent mechanisms underlying NK cell´s activation resulting in effective antitumoral responses. Illustration obtained from Rahmani et al. 2022. (108)

6.5.1.2 NK cell receptors

Focusing on the receptors responsible for the delicately coordinated threshold of NK cell reactivity, numerous molecules are found to play a noteworthy role in the orchestration of NK cell responses, and are depicted along with their corresponding ligands in Fig. 6.5.3. All NK cell receptors have in common, that, unlike TCRs, they are germ-line encoded and do not undergo further maturation processes.

NKG2D is an activating receptor present on all NK cell subsets specialized on the recognition of malignant or stressed cells as by these its ligands, the MHC class I polypeptide related

sequence A and B (MICA; MICB) and UL16 binding protein 1 (ULBP1-6) are typically upregulated resulting in NK cell mediated cytotoxicity. (134, 135) In addition, natural cytotoxicity receptors (NCR), a family consisting of NKp30, NKp44 and NKp46, also result in activating signaling upon binding to their corresponding antigen. Exceptionally, NKp44 is the only NCR capable of NK cell inhibition induced by its interaction with the proliferating cell nuclear antigen (PCNA). (136, 137) Likewise, the killer cell immunoglobulin-like receptors (KIRs) bear the potential to activate and inhibit NK cell effector functions. Whereas KIR2DS1 and KIR2DL4 activate NK cells, with special relevance in cancer elimination, KIR2DL1, KIR2DL2/3, KIR3DL1 and KIR3DL2 contain intracellular immunoreceptor tyrosine-based inhibitory motives (ITIMs) resulting in inhibitory signaling in response to ligand-binding. (138) All KIRs recognize HLA/MHC class I and therefore, the lack of inhibitory signaling mediated by KIRs is predominantly responsible for aforementioned NK cell-stimulation by MHC I-downregulation. (139) Furthermore, in the context of ACT, KIRs appear to play an important role in adoptive transfer of NK cells as due to haploidentical HSCT KIR-mismatched NK cells have been shown to be therapeutically beneficial. (18)

CD155 and CD112 represent special ligands to NK cells as they have the potential of their activation or inhibition depending on the NK receptor binding. While the DNAX accessory molecule (DNAM-1) results in activation, TIGIT, the T cell immunoreceptor with immunoglobulin and ITIM domain, leads to inhibition of NK cell cytotoxicity. (140) Interestingly, TIGIT serves as a target for immune checkpoint inhibition (ICI) as blocking of TIGIT resulted in improved antitumor effects of NK and T cells. (141) Another inhibitory receptor already commonly used for ICI and relevant for NK cell regulation is the programmed cell death protein 1 (PD-1). Upon binding to its ligand PD-L1 NK cell effector functions are efficiently inhibited. Thus, in line to already established clinical applications, blocking the PD-1/PD-L1-interaction appears to be beneficial for NK cell-based ACT. (142, 143) Additionally, NKG2A, already early expressed in the maturation process of NK cells, results in inhibitory signaling upon binding of its ligand HLA-E, a member of the HLA/MHC class I-complexes. (144)

Furthermore, NK cells are equipped with a multitude of cytokine receptors enabling their crosstalk with other members of the immune system. Binding of the corresponding cytokines can potentially result , in stimulation of prolonged functional abilities and therefore long-lived NK cells. (1, 145)

Thanks to the profound understanding of the complex biology underlying NK cell-interactions, new approaches are continuously established to enhance NK-effector functions such as overall efficacy, persistence and homing to consequently improve NK cell-immunotherapy. (15, 146-148)

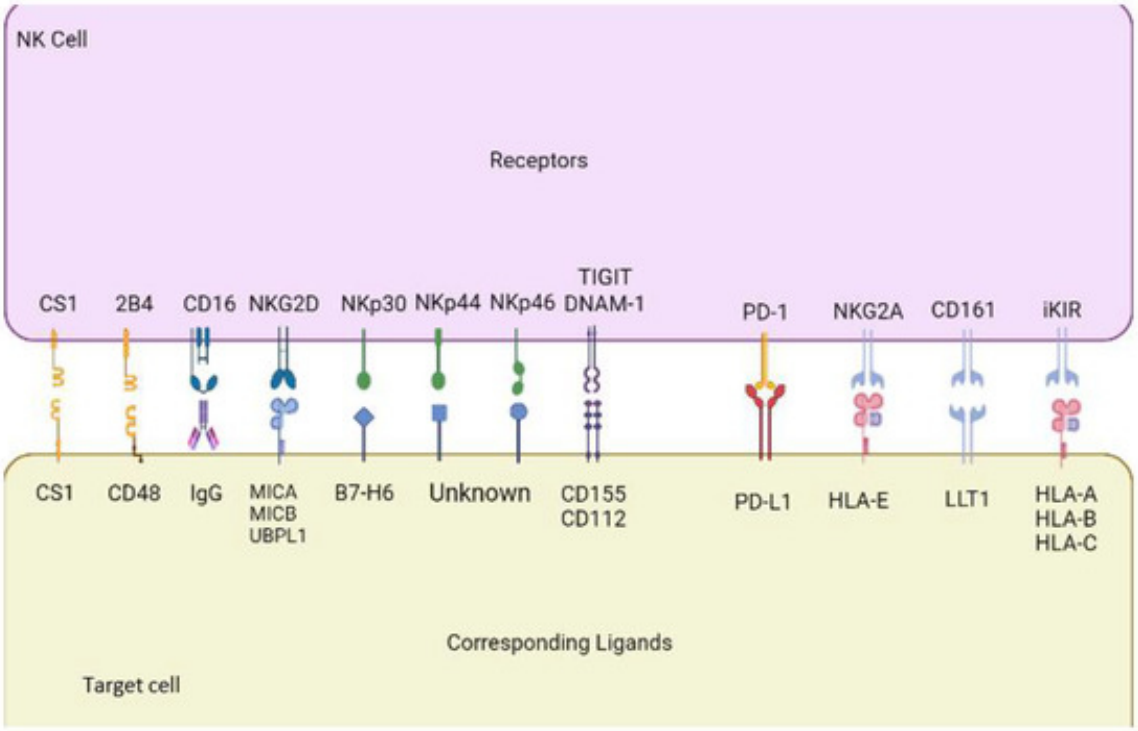

Figure 6.5.3 Overview of the key NK cell receptors and their corresponding ligands responsible for eradication of malignant transformed cells. Illustration obtained from Allison et al. 2022. (1)

6.5.1.3 NK92 – an indefinite cell-source approved for clinical application

Over the years, several NK cell-sources have been established for clinical application. Today, NK cells specifically expanded from peripheral or cord blood as well as differentiated from induced pluripotent stem cells represent common resources for NK cell therapeutics. (99-102) Together, they all require costly and time-consuming manufacturing processes while the half-life of the generated effector cells is limited.

In contrast, NK92 is an IL-2 dependent, continuously growing natural killer cell line established from a non-Hodgkin lymphoma patient. (103, 149) As safe infusion of irradiated NK92 cells in cancer patients with advanced disease could be demonstrated in various clinical trials, the cell line was approved by the FDA for clinical application and represents an attractive alternative to previously mentioned NK cell-sources that by now has been used in the clinic for at least two decades. (117-119, 150, 151)

Throughout this time, certain limitations of NK92 as a cellular source for ACT have become apparent. Due to the necessity of irradiation prior to the application of NK92 cells into patients, this approach results in reduced NK cell-persistence compared to alternative cellular sources. (152) In addition, the NK cell clone NK92 is negative for the expression of CD16. Consequently, NK92-mediated tumor cell recognition can´t be augmented by ADCC, unless further genetic engineering is performed. (1)

However, the cell line NK92 possesses more convincing characteristics making it an attractive option for ACT. Since NK92 cells lack the majority of inhibitory KIRs, the line bears high cytotoxic potential and therefore unmodified NK92 cells already show therapeutic effects in patients with refractory hematological malignancies as well as melanoma. (153, 154) Moreover, gene editing procedures to further stimulate the antitumoral reactivity of NK92 are due to its continuous expansion not time-sensitive and thus can be more complex resulting in ready-to-use genetically modified cell lines. Due to these advantages and especially its robust anti-tumor reactivity, the cell line NK92 receives increasing attention in the context of NK cell-ACT. (150, 151, 155-157)

6.5.2 Therapeutic TCRs

The T cell receptor (TCR) is a heterodimer mainly composed of an α- and β-protein chain responsible for the recognition of processed protein fragments (antigens) presented in the context of MHC complexes. In this study, TCRs, subsequently described in detail, are used to redirect NK cells to mediate specific, T cell like antitumoral responses. (158)

6.5.2.1 AML-reactive TCRs

The TCRs used in this study to redirect NK92 cells against AML were manufactured in our laboratory (AG Hartwig, III. Department of Medicine – Hematology and Medical Oncology, University Medical Center of the Johannes Gutenberg-University Mainz) by the previous PhD student Anita Bhatti according to the protocol for fast and robust TCR cloning from Birkholz et al. (159) In detail, the $CD8^+$ cytotoxic T lymphocyte (CTL) clones 25F2, 5B2 and 5H11, previously generated in donor-patient MHC-matched or single locus mismatched mixed lymphocyte leukemia cultures and shown to exert effector functions against AML *in vitro* and *in vivo* in a patient tailored NOD/scid $IL2Rcg^{null}$ xenograft AML model, served as a template for PCR-cloning of eponymous TCRs responsible for the CTL clone´s AML-recognition. (160) Subsequently, the DNA-sequence of every TCR was codon-optimized in order to enhance expression. Furthermore, the constant domains of the TCRs were murinized to reduce the risk of mispairing with the endogenous TCR upon transgenic expression in T cells. Murinization also increases association of the CD3 subunits with the TCR, forming a more stable TCR-complex. (86)

The resulting TCRs obtained were HLA-restricted to HLA-B*58:01 (25F2-TCR), HLA-Cw*07:01 (5B2-TCR) and HLA-B*57:01 5H11-TCR. (160)

As determination of the exact antigens recognized by the three AML-reactive TCRs used in this study is still part of ongoing research, TCR-recognition properties can currently only be estimated by the reactivity of the corresponding CTL clones to various tissue samples of their

designated patients. Whereas CTLs 5B2 and 25F2 were shown to react specifically to patient-derived AML blasts, CTL 5H11 exerted reactivity to AML and EBV-transformed B cells (B-LCL) but not to fibroblasts indicating that its corresponding TCR might recognize a hematopoiesis-specific minor-histocompatibility antigen while 5B2- and 25F2-TCRs presumably recognize AML-associated or AML-specific antigens.

6.5.2.2 MDM2-reactive TCR

Tumor associated antigens (TAAs) universally expressed across a variety of tumor entities represent attractive targets for immunotherapy but they are only rarely identified. (161-163) Typically, these ubiquitous TAAs derive from proteins involved in malignant transformation and are predominantly the result of endogenous processing of intracellular self-proteins. (164) As a consequence, these peptides are presented in the context of a MHC allel, and are therefore mainly accessible to TCR-recognition. (164)

The human homolog of the murine double-minute 2 (MDM2) oncoprotein is a representative of the aforementioned universal targets against which Stanislawski et al. were able to generate a highly efficient TCR reactive to a multitude of solid and hematological malignancies. (164) Therefore, we incorporated this TCR into our study in order to establish an ACT-drug which is not only approved for universal transfer across HLA-barriers but also capable to recognize a broad-spectrum of malignancies. In the following, detailed background information on MDM2 and the TCR-manufacturing process is provided.

6.5.2.2.1 MDM2

The ubiquitin-protein ligase MDM2 is an oncoprotein physiologically inactivating the tumor suppressor p53. As depicted in Fig. 6.5.4, in the context of a negative feed-back loop, upon activation p53 induces transcription of the MDM2-gene subsequently resulting in its ubiquitination and degradation by newly produced MDM2. Consequently, overexpression of MDM2 leads to an increased inactivation of the tumor suppressor p53 and therefore results in reduced inhibition of cancer formation. Due to the ubiquitous expression of MDM2, its pathological upregulation bears the potential of cancer-development in virtually any human tissue. Therefore, overexpression of MDM2 can be detected in a multitude of malignancies, comprising leukemia, lymphoma, gliomas, neuroblastoma, sarcomas, testicular germ cell tumors, breast and urothelial cancer. (165-167)

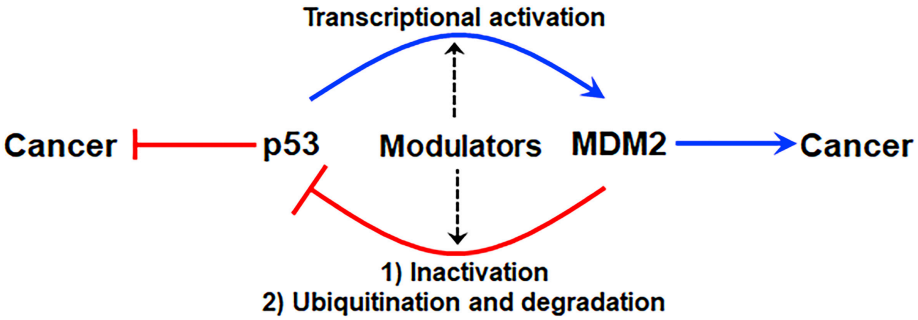

Figure 6.5.4 Autoregulatory feed-back loop between MDM2 and the tumor suppressor p53. Illustration obtained from Qin et al. 2018. (168)

6.5.2.2.2 Generation of the MDM2-reactive TCR

Transgenic mice expressing a human-mouse chimeric MHC class I protein composed of the human HLA-A2.1 joined to the mouse H2-K^b were immunized with the MDM2 peptide fragment 81-88 (amino acids) resulting in the generation of HLA-A2.1 restricted mouse T cells reactive to the $MDM2_{81-88}$ epitope. In addition, as the transgenic mice were concomitantly genetically modified to express human CD8, all T lymphocytes reactive to MDM2 were also dependent on the human CD8-coreceptor. Next, clonal CTL cell lines were generated and tested for their effector potential. From the most efficient clone´s cDNA mouse TCR α- and β-chains were isolated and cloned into expression vectors for retroviral transduction. (164) Finally, common optimization steps were performed, e.g. codon-optimization, in order to increase expression upon transduction to human immune cells. Extensive studies on the resulting MDM2-reactive TCR (MDM2-TCR) revealed its sensitive dependency on the coexpression of human CD8 for mediation of efficient effector functions by human T cells. (169)

6.5.3 TCR-coreceptors

TCR-recognition in T lymphocytes does not only involve the TCR-complex, consisting of the highly individual TCR and the γ-, δ-, ε- and ζ-subunits of CD3, but rather a battery of additional surface molecules fine-tuning the interaction with target cells. The most important of these "supplementary" receptors confer the so-called "coreceptors", CD8 and CD4. Mature T cells characteristically only express one of the two coreceptors and are therefore classified as $CD8^+$ or $CD4^+$ T lymphocytes. As illustrated in Fig. 6.5.5, CD8 binds to MHC class I whereas CD4 binds to MHC class II. Due to tissue-specific expression patterns of both MHC classes, a T cell´s coreceptor-expression determines the fate of its function. While MHC class II is only expressed on antigen-presenting cells, such as dendritic cells and macrophages, MHC class I is present on every cell of the human body that is capable of multiplication. As a result, $CD4^+$ T cells are primarily involved in orchestrating complex immune reactions via cytokine secretion. In contrast, $CD8^+$ T lymphocytes comprise the immunosurveillance of the adaptive immune system checking every cell for cancerous or virally transformation. Upon recognition, $CD8^+$ T lymphocytes, also called "cytotoxic T cells", kill the damaged cell by inducing apoptosis via

degranulation of perforin and granzymes. Therefore, in adoptive cellular therapy aiming to eliminate cancer cells, mainly TCRs deriving from $CD8^+$ T cells are used as redirecting agents, as this cell subset is specialized on the recognition of malignant transformed cells. (158)

On a molecular level, CD8 is a heterodimer physiologically consisting of an α- and β-chain. (170) Thereby, the α-subunit associates intracellularly with the lymphocyte-specific protein tyrosine kinase (Lck), which is responsible for the initiation of the TCR signaling cascade. (171) While the CD8β-chain´s exact mechanism of action has not yet been decoded completely, there is evidence that due to its characteristic palmitoylation it enhances the assembly of its counterpart, CD8α, and Lck. (172) Taken together, association of a TCR and the CD8αβ-heterodimer results in more effective intracellular signaling by the CD8-mediated recruitment of the cascade initiating Lck. In addition, binding to the α_3-domain of MHC class I the CD8-coreceptor adds stability to the interaction between the TCR and its corresponding peptide-MHC-complex. (173) Consequently, the antigen-independent association between CD8 and MHC I promotes prolonged TCR-interaction. Therefore, CD8 enables TCRs with lower affinity to its designated target resulting in appropriate stimulation of effector functions with additionally reinforced capacities for the initiation of signaling cascades. Respectively, in the context of TCR-redirection of NK cells for ACT, CD8 appears to be a promising tool to augment TCR-mediated effector functions.

In contrast to CD8, CD4 binds with an exceptionally low affinity to its designated MHC molecule (MHC class II) resulting in a negligible contribution to the TCR´s interaction with its corresponding peptide-MHC complex. Nevertheless, the CD4-coreceptor also promotes intracellular TCR signaling upon antigen-recognition by Lck-recruitment. (174)

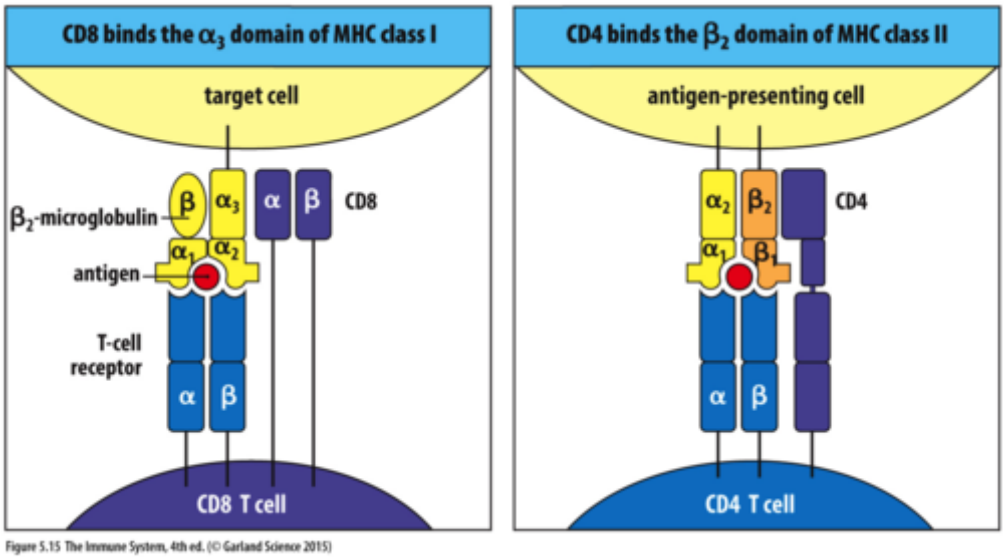

Figure 6.5.5 Interactions of CD4 and CD8 with their corresponding MHC complex augmenting TCR-mediated T cell stimulation. Illustration obtained from the second edition of "The Immune System" published by Garland Science, NY ©2005. (175)

7 Material and methods

7.1 Material

7.1.1 Instruments and Equipment

Equipment	Type	Manufacturer
Autoclave	Varioklave 40-60	H+P, Oberschleißheim
Centrifuge	Heraus Mega Fuge 16R	Thermo Scientific, Waltham, USA
CO_2 Incubator	Heracell 150i	Thermo Scientific, Waltham, USA
Counting chamber	Fuchs-Rosenthal	Marienfeld Superior, Lauda-Königshofen
Electrophoresis chamber	Mini Horizontal	neoLab, Heidelberg
Flow cytometer	BD FACS Canto II	BD Biosciences, Heidelberg
Freezer -80°C	Hera Freeze, HFU 686	Thermo Fisher, Dreieich
Freezing Container	Mr. Frosty	Nalgene, Rochester, UK
Gel documentation system	iBright	Thermo Fisher, Dreieich
Heating block	Thermomixer 5436	Eppendorf, Hambung
High-precision scale	EW 150-3M	Kern, Balingen-Frommern
Ice machine	UBE 50/35	Ziegra, Isernhagen
Laboratory balance	MD BA 100	Sartorius, Göttingen
Laminar Flow Hood	HERAsafe	Thermo Fisher, Dreieich
Luminescence Microplate Reader	FluostarOmega-Reader	BMG LABTECH, Offenburg
Magnetic stirrer, heatable	Variomag	Monotherm, München
Microscope	Axiovert 25	Carl Zeiss AG, Jena
Microwave		Bosch, Stuttgart
Nitrogen Tank	Taylor-Wharton XL-180	Tec Lab, Königstein
pH meter	HI2210 und pH211	Hanna, Vöhringen
Pipettes	Research plus	Eppendorf, Hamburg
Pipetting aid	Pipetus	Hirschmann, Eberstadt
Refrigator-Freezer Combo		Liebherr, Ochsenhausen
Scintillation Counter		Perkin Elmer, Hamburg
Shaker/Incubator Hood	TH30	Edmund Bühler, Hechingen

Spectrophotometer	NanoDrop-1000	Thermo Scientific, Waltham, USA
Table Centrifuge	Biofuge Fresco	Heraeus, Buckinghamshire, UK
Thermocycler	Tpersonal	Biometra, Göttingen
Vortexer	Vortex Genie 2	Bohemia, NY, USA
Waterbath	SW22	Julabo, Seelbach

Table 7.1.1 Instruments and Equipment

7.1.2 Consumables

Name	Manufacturer
Beakers	Schott, Mainz
Cell culture dishes	Greiner, Frickenhausen
Cell culture flasks	Greiner, Frickenhausen
Cell culture plates	Greiner, Frickenhausen
Centrifugal Filters, Macrosep Advance, 10K	Pall Laboratory, Bad Kreuznach
Disposable Glass Pasteur Pipettes	Poulten & Graf, Wertheim
Disposable gloves	Semperit, Wien, AT
Eppendorf tubes	Eppendorf, Hamburg
Erlenmeyer flasks	Corning, Fogostraat, NL
FACS tubes	BD Biosciences, Heidelberg
Falcon tubes 15 and 50 mL	BD Biosciences, Heidelberg
Freezing vials	Nunc, Wiesbaden
Pipette tips	Starlab, Ahrensburg
Polypropylene centrifuge tubes	Greiner, Frickenhausen
Serological pipettes 1-50 mL	Greiner, Nürtingen
Syringes 1, 2, 5, 10 mL	Braun, Melsungen
Sterile filters	Millipore, Eschborn

Table 7.1.2 Consumables

7.1.3 Chemicals and additives

Name	Synonym	Manufacturer
Acetic acid (100%)		Applichem, Darmstadt
Agarose		Starlab, Ahrensburg
Bovine serum albumine	BSA	Sigma-Aldrich, Steinheim
^{51}Chromium		
Dimethyl sulfoxide	DMSO	Applichem, Darmstadt
Ethanol	EtOH	Carl Roth, Karlsruhe

Ethylenediaminetetraacetic acid	EDTA	Applichem, Darmstadt
Glycerol		Sigma-Aldrich, Steinheim
Glycin		Merck, Darmstadt
Hydrochloric acid 37%	HCl	Carl Roth, Karlsruhe
Isoropyl alcohol	2-Propanol	Carl Roth, Karlsruhe
LB-agar		Sigma-Aldrich, Steinheim
LB-medium		Sigma-Aldrich, Steinheim
(D-)Luciferin		Thermo Fisher Scientific, Dreieich
Methanol	MeOH	Carl Roth, Karlsruhe
Phosphate buffered saline	PBS	Biochrom, Berlin
Polyethylenimine	PEI	Polysciences, Warrington, PA
Potassium acetate	KoAc	Applichem, Darmstadt
Rubidium chloride	RbCl	Carl Roth, Karlsruhe
Sodium azide		Carl Roth, Karlsruhe
Sodium deoxycholate		Applichem, Darmstadt
Sodium fluoride	NaF	Applichem, Darmstadt
Sodium hydroxide	NaOH	Applichem, Darmstadt
Sodium lauryl sulfate	SDS	Carl Roth, Karlsruhe
Sodium orthovanadate	Na3VO	Carl Roth, Karlsruhe
Tergitol-NP40	NP40	Carl Roth, Karlsruhe
Tetramethylethylenediamine	TEMED	Sigma-Aldrich, Steinheim
Trichloroacetic acid	TCA	Applichem, Darmstadt
Tris(hydroxymethyl)-aminomethane	TRIS	Applichem, Darmstadt
Trypan Blue (0,4%)		Merck, Darmstadt
Triton X 100		Applichem, Darmstadt
Tween-20		Bio-Rad, München
2-Mercaptoethanol	ß-MeOH	Sigma-Aldrich, Steinheim
3-(N-morpholino)propanesulfonic acid	MOPS	Applichem, Darmstadt

Table 7.1.3 Chemicals and additives

7.1.4 Enzymes, Kits and Reagents for Molecular Biology

Name	Manufacturer
DNA Gel Loading Dye 6x	Life Technologies, Darmstadt
dNTPs	New England Biolabs, Frankfurt am Main
GelRed Nucleic Acid Stain	Thermo Fisher Scientific, Dreieich

NEBuilder	New England Biolabs, Frankfurt am Main
NucleoBond Plasmid Isolation Kit	Macherey Nagel, Düren
NucleoSpin Gel and PCR Clean up Kit	Macherey Nagel, Düren
One Taq® DNA Polymerase 2x MM	New England Biolabs, Frankfurt am Main
Primers	Sigma-Aldrich, Steinheim
Q5 High-Fidelity Polymerase + buffer	New England Biolabs, Frankfurt am Main
Restriction endonucleases + buffers	New England Biolabs, Frankfurt am Main
RNeasy Mini Kit	Qiagen, Hilden
SuperScript III reverse transcription kit	Thermo Fisher Scientific, Dreieich
T4 Ligase + buffer	New England Biolabs, Frankfurt am Main

Table 7.1.4 1.1.1 Enzymes, Kits and Reagents for Molecular Biology

7.1.5 Size Standards

Name	Manufacturer
GeneRuler 1 kb Plus DNA Ladder	Life Technologies, Darmstadt
GeneRuler 1 kb DNA Ladder	Life Technologies, Darmstadt

Table 7.1.5 Size Standards

7.1.6 Oligonucleotides

Name	Sequence 5'-3'	Description	RS
UH360	GCATCGCAGCTTGGATACAC	5´ sequencing primer binding upstream to MCS of pMXs_IRES-constructs	-
UH361	AAGCGGCTTCGGCCAGTAAC	3´ sequencing primer binding downstream to MCS of pMXs_IRES-constructs	-
UH488	GCCGGATCTAGCTAGTTAATTAAGCCACCATGGCCTTACCAGTG	5´ primer of CD8α chains for NEBuilder® DNA assembly	
UH493	CTCGAGGCCTGCAGGAATTCCTATGTTTTCAGGATCCATGGGTTAAGCAGC	3´ primer of CD8β2 chain for NEBuilder® DNA assembly	
UH494	CTCGAGGCCTGCAGGAATTCTCATTTGTAAAATTGTTTCATGAAACGAAGCCGGG	3´ primer of CD8β3 or 5 chains for NEBuilder® DNA assembly	

UH495	CTCGAGGCCTGCAGGAATTC TCAGGATCCATGGGTTAAGC AGC	3´ primer of CD8β6 chain for NEBuilder® DNA assembly	
UH496	AGCGTCTACGTAAATTCCGC CCCTCTCCCT	5´ primer for cloning of pMXs_IRES_Neo	SnaBI
UH497	ACTGCTGTCGACTCAGAAGA ACTCGTCAAG	3´ primer for cloning of pMXs_IRES_Neo	SalI
UH504	ACCTGCTTGCTTTAGCAGAG AGAAGTTTGTGGCGCCGCTG CCGACGTATCTCGCCGAAAG GC	3´ primer of CD8α chains with overlap including P2A sequence for NEBuilder® DNA assembly	
UH505	CTGCTAAAGCAAGCAGGTGA TGTTGAAGAAAACCCCGGGC CTCTCCAGCAGACCCCTGCA TA	5´ primer of CD8β chains with overlap including P2A sequence for NEBuilder® DNA assembly	

Table 7.1.6 Oligonucleotides

7.1.7 Plasmids

Name	Description	Resistance
pMXs_IRES_Puro	MMLV-based retroviral transfer vector (Cell Biolabs, San Diego, USA) featuring ψ-package signal, MCS, MMLV-LTRS and IRES-linked puromycin resistance for expression of exogenous genes in mammalian cells	Ampicillin Puromycin
pMXs_IRES_Neo	Retroviral transfer vector generated by exchanging the IRES-Puro cassette from pMXs_IRES_Puro with an IRES-Neo sequence	Ampicillin Neomycin
pMXs_IRES_Hygro	Retroviral transfer vector generated by exchanging the Puro cassette from pMXs_IRES_Puro with a sequence encoding Hygromycin resistance	Ampicillin Hygromycin
pMXs_hCD3complex_IRES_Puro	Retroviral transfer vector encoding the δ-, γ-, ε-, ζ-subunits of the human CD3 complex each linked by 2A “self-cleaving” peptide sequences generated by Gateway®; parental vector: pMXs_IRES_Puro	Ampicillin Puromycin

pMXs_TCR-5H11_IRES_Puro	Retroviral transfer vector encoding the murinized and codon optimized α- and β-chain of TCR-5H11 linked via P2A “self-cleaving” peptide sequence; parental vector: pMXs_IRES_Puro	Ampicillin Puromycin
pMXs_TCR-25F2_IRES_Puro	Retroviral transfer vector encoding the murinized and codon optimized α- and β-chain of 25F2 linked via P2A “self-cleaving” peptide sequence; parental vector: pMXs_IRES_Puro	Ampicillin Puromycin
pMXs_TCR-5B2_IRES_Puro	Retroviral transfer vector encoding the murinized and codon optimized α- and β-chain of 5B2 linked via P2A “self-cleaving” peptide sequence; parental vector: pMXs_IRES_Puro	Ampicillin Puromycin
pMXs_TCR-MDM2_opt_IRES_Neo	Retroviral transfer vector encoding the optimized murine α- and β-chains linked via P2A “self-cleaving” peptide sequence of a TCR reactive to the MDM2 oncoprotein	Ampicillin Neomycin
pMXs_CD8α1β2_IRES_Neo	Retroviral transfer vector encoding the α1- and β2-subunit of human CD8 linked via P2A “self-cleaving” peptide sequence generated by NEBuilder® DNA assembly; parental vector: pMXs_IRES_Neo	Ampicillin Neomycin
pMXs_CD8α1β5_IRES_Neo	Retroviral transfer vector encoding the α1- and β5-subunit of human CD8 linked via P2A “self-cleaving” peptide sequence generated by NEBuilder® DNA assembly; parental vector: pMXs_IRES_Neo	Ampicillin Neomycin
pMXs_CD8α2β3_IRES_Neo	Retroviral transfer vector encoding the α2- and β3-subunit of human CD8 linked via P2A “self-cleaving” peptide sequence generated by NEBuilder® DNA assembly; parental vector: pMXs_IRES_Neo	Ampicillin Neomycin
pLenti_EF1a_Pac_2A_GFP/FLuc	Lentiviral vector based on human immunodeficiency virus-1 (HIV-1) for gene transfer to mammalian cells encoding GFP and Firefly Luciferase linked via T2A “self-cleaving” peptide sequence; GFP- and FLuc-expression is driven by EF1α promoter upstream of the MCS	Ampicillin Puromycin

psPAX2	Lentiviral packaging plasmid containing Gag, Pol, Rev and Tat	Ampicillin
pMD2.G	Lentiviral, amphotropic, vesicular stomatitis virus envelope G (VSV-G) expressing plasmid	Ampicillin
pHIT60	Retroviral packaging plasmid encoding MMLV Gag and Pol, human CMV IE promoter and SV40 ori	Ampicillin
pCOLT-GALV	Retroviral, amphotropic plasmid containing the gibbon ape leukemia virus envelope, human CMV IE promoter and SV40 ori	Ampicillin
pBulneo-Luc+	Destination vector for Gateway Cloning serving as template for the IRES_Neomycin sequence for pMXs_IRES_Neo cloning	Ampicillin Neomycin

Table 7.1.7 Plasmids

7.1.8 Bacteria

7.1.8.1 Stbl3™ Chemically Competent E. coli

One Shot® Stbl3™ Chemically Competent *E. coli* deriving from the HB101 *E. coli* strain were originally obtained from ThermoFisher Scientific (Darmstadt, Germany) and repeatedly used for propagation of retroviral vectors after regeneration of chemical competence by rubidium-chloride method. As in these cells the frequency of homologous recombination of LTRs, as found in pMXs vectors, is significantly reduced, Stbl3 are well suited for reliable replication of lenti- and retroviral plasmid DNA.

Genotype: *F$^-$mrcB mrrhsdS20(r_B^-, m_B^-) recA13 supE44ara-14galK2 lacY1 proA2rpsL20(StrR) xyl-5 λ-leumtl-1*.

7.1.9 Cells

7.1.9.1 AML blasts

AML blasts were isolated either from peripheral blood, bone marrow biopsies, or therapeutic leukapheresis products of patients MZ580, MZ653, MZ667 as well as MZ921 by standard Ficoll separation and cryopreserved until use. As confirmed by flow cytometry, all leukemia samples contained >95% leukemia blasts. Leukemia patients participated in the study after informed consent in accordance with the Helsinki protocol. High-resolution genomic HLA typing of the AML samples was performed according to standard procedures. AML blasts served as targets for functional analysis of NK92 redirected with corresponding TCRs.

7.1.9.2 B-LCL

EBV-transformed B-lymphoblastoid cell lines (B-LCL) were generated from peripheral blood mononuclear cells (PBMC) of patient MZ580 and MZ667 according to standard procedures. Due to EBV-transformation continuously expanding B-LCLs were able to be transduced with lentiviral supernatant to express Firefly Luciferase (FLuc) and thus suited to serve as targets in bioluminescence-based cytotoxicity assays.

7.1.9.3 IM-9

IM-9 is an EBV-transformed B-lymphoblastoid cell line (B-LCL) generated from the peripheral blood of a female patient with multiple myeloma endogenously expressing the MDM2 oncoprotein.

7.1.9.4 Jurkat 76

The T-cell leukemia cell line Jurkat 76 (J76) lacks expression of the TCR α- and β-chain and is very receptive for gene transfer. Therefore, J76 were used as expression control for therapeutic TCRs.

7.1.9.5 K562

Derived from a patient with chronical myelogenous leukemia (CML), the erythroleukemia cell line K562 (ATCC® CCL-243™) is characterized by a very low expression of major histocompatibility complex (MHC) class I and II. Thus, K562 cells served as targets in functional assays to examine the cytotoxicity mediated by innate natural killer cell activity of genetically modified NK92.

7.1.9.6 Phoenix-AMPHO

Phoenix-AMPHO (ATCC® CRL-3213™) is a second-generation retrovirus producer cell line that is highly transfectable with lipid-based transfection protocols. The adherent cells were established by adenoviral transduction of HEK293T/17 cells to stably express gag-pol and the amphotropic envelope protein GALV encoded by the helper plasmids pHIT60 and pCOLT-GALV, respectively. Phoenix cells were used for generation of supernatants containing GALV-pseudotyped retroviral particles in the course of gentical modification of effector cells.

7.1.9.7 293T

Containing the SV40 T-antigen the 293T cell line (ATCC® CRL-3216™), a highly transfectable derivate of human embryonic kidney 293 cells, originally referred to as 293tsA1609neo, is competent to propagate vectors carrying the SV40 region of replication. 293T served as producer cell line for the generation of amphotropic lentiviral supernatants.

7.1.9.8 Cytotoxic T lymphocyte clones 5H11 and 25F2

AML-reactive cytotoxic T lymphocyte clones 5H11 and 25F2 (CTL 5H11 and CTL 25F2) were previously manufactured in our laboratory (AG Hartwig, III. department of medicine – hematology and medical oncology, university medical center of the Johannes Gutenberg-University Mainz) in a allogeneic donor-patient specific humanized NOD/scidIL2Rcg^{null} mouse model by Jana Albrecht. (160)

7.1.9.9 PBMCs transduced to stably express the MDM2-TCR

PBMCs transduced to stably express the MDM2-TCR were kindly provided by Dr. Hakim Echchannaoui (III. Dept. of Medicine – Hematology and Medical Oncology, University Medical Center of the Johannes Gutenberg-University Mainz).

7.1.9.10 NK92

NK92 (ATCC® CRL-2407™) is a cytotoxic and interleukin-2 (IL-2) dependent natural killer cell line that was established from peripheral blood mononuclear cells of a patient with rapidly progressive non-Hodgkin´s lymphoma. As the only NK cell line established, NK92 have consistently shown high antitumor cytotoxicity and no toxic side effects in clinical trials leading to an FDA-approval for cellular therapy. NK92 are highly receptive for genetic redirection to tumor antigens and therefore represent an attractive effector cell source for adoptive cellular therapy.

7.1.10 Receptors for NK92-redirection

7.1.10.1 AML-reactive TCRs

The AML-reactive TCRs 25F2, 5B2 and 5H11 were cloned by Anita Bhatti according to Birkholz K. et al. (159) from eponymous cytotoxic T-lymphocyte (CTL) clones that were originally generated by the former PhD student Jana Albrecht and shown to exert anti-leukemic cytotoxicity *in vivo* and *vitro* (160). In order to enhance expression and reduce mispairing, every TCR-sequence was codon-optimized and the constant regions were murinized prior to redirection of ACT-effector cells. On the basis of the TCRs´ amino acid sequence the domains

were determined using the IMGT V-QUEST database (IMG/V-QUEST; www.imgt.org), respectively.

7.1.10.2 MDM2-TCR

The TCR reactive to the amino acids 81-88 epitope of the mouse double minute 2 homolog (MDM2) is an optimized version of the originally extracted by Stanislawski et al. from murine CTLs, generated in an MDM2-immunized human CD8 x A2.1/K^b mouse model. (164) As a consequence, this TCR is restricted to HLA-A*02:01 and dependent on CD8 to elicit potent effector functions in T cells. (169) Due to the ubiquitous expression of MDM2, this TCR reacts to a broad spectrum of solid and hematological malignancies.

7.1.10.3 Coreceptors

7.1.10.3.1 Human CD3 Complex

NK92 cells expressing a polycistronic vector encoding the δ-, ε-, γ-, ζ-subunit of the human CD3 complex cloned according to Szymczak A. L. et al. (176) were kindly provided by Dr. C. Wölfel (IIIrd. Dept. of Medicine – Hematology & Medical Oncology, University Medical Center of Johannes Gutenberg-University).

7.1.10.3.2 Human CD8αβ

Vectors expressing different variants of human CD8 α- and β-chains were generated from RNA of the AML-reactive CTLs the TCRs derive from.

7.1.11 Media and Supplements for cell culture

Name	Synonym	Manufacturer
Ampicillin (100 mg/mL)		Sigma-Aldrich, Steinheim
Dulbecco's Modified Eagle's Medium	DMEM	Life Technologies, Darmstadt
Fetal Calf Serum	FCS	Thermo Fisher Scientific, Darmstadt
Folic acid		Applichem, Darmstadt
GM-CSF (human)		R&D Systems, Wiesbaden
G418		Biochrom, Berlin
Hygromycin		
Human Serum	HS	Transfusionszentrale University Medical Center Mainz
Recombinant human (rh) IL-2		Novartis, Nürnberg
Inositol		Applichem, Darmstadt
LB-agar		Sigma-Aldrich, Steinheim

LB-medium		Sigma-Aldrich, Steinheim
2-Mercaptoethanol	ß-MeOH	Sigma-Aldrich, Steinheim
MEM alpha Medium (1x) + GlutaMAX™-I + nucleosides		
Opti-MEM, no phenol red		Life Technologies, Darmstadt
Phosphate Buffered Saline, steril	PBS	Life Technologies, Darmstadt
Penicillin (10000 IU/ mL) /Streptomycin (10 mg/ mL)	Pen/Strep	Sigma-Aldrich, Steinheim
Polybrene		Sigma-Aldrich, Steinheim
Puromycin		Applichem, Darmstadt
RPMI 1640 Medium	RPMI	Life Technologies, Darmstadt
Trypsin-EDTA (0.25%), phenol red		Pan-Biotech GmbH, Aidenbach

Table 7.1.8 1.1.1 Media and Supplements for cell culture

7.1.12 Buffers and Media

7.1.12.1 Molecular biology

7.1.12.1.1 Agarose gel electrophoresis

TAE buffer (50x)	2 M Tris base, 5.71% glacial acetic acid, 0.05 M EDTA (pH8.3)

7.1.12.1.2 Miniprep DNA-isolation

Resuspension buffer	50 mM TRIS-HCl pH 7.4, 10mM EDTA, 100 µg/mL RNAse A
Lysis buffer	200 mM NaOH, 1% SDS
Neutralization buffer	3 M KoAc pH 5.5

7.1.12.2 Flow cytometry

FACS buffer	1% BSA, 0.1% sodium azide, PBS
FACS Fixation buffer	2% PFA, PBS
Permeabilisation buffer	0.2% Saponin, PBS
Blocking buffer	0.1% Triton X 100, 3% BSA, PBS
Wash buffer	0.1% Tween-20, PBS

7.1.12.3 IFN-γ ELISpot

Acetate buffer	0.147% acetic acid, 35 mM sodium acetate

7.1.12.4 Magnetic-Activated Cell Sorting (MACS)

MACS buffer	0.5% BSA, 2 mM EDTA, PBS

7.1.12.5 Cell culture media

NK92 cell culture medium	
MEM alpha Medium (1x) + GlutaMAX™-I + nucleosides	
FCS	20% (v/v)
Pen/Strep	1% (v/v)
Inositol	0.2 mM
β-mercaptoethanol	0.1 mM
Folic acid	0.02 mM

Phoenix-AMPHO cell culture medium	
DMEM	
FCS	10% (v/v)
Pen/Strep	1% (v/v)

EBV-BLCL and Jurkat76 cell culture medium	
RPMI Medium 1640 (1x) + Glutamine	
FCS	10% (v/v)
Pen / Strep	1% (v/v)

AML blasts cell culture medium
AIM V Medium

HS	10% (v/v)
Pen/Strep	1% (v/v)

Freezing medium	
RPMI Medium 1640 (1x) + GlutaMAX™-I	
Heparin	10 IU mL^{-1}
Human albumin	8% (v/v)
DMSO (added prior to use)	10% (v/v)

7.1.13 Antibodies

Antigen	**Fluoro-chrome**	**Isotype**	**Catalog Number**	**Manufacturer**
CD11a [LFA-1]	FITC	mIgG2a,κ	BD555379	BD Biosciences, Heidelberg
CD25 [IL-2Rα]	FITC	mIgG1,κ	IC2471P	R&D Systems, Minneapolis, USA
CD27	FITC	mIgG1,κ	302806	Biolegend, San Diego, USA
CD28	FITC	mIgG1,κ	BD555728	BD Biosciences, Heidelberg
CD54 [ICAM-1]	PE	mIgG1,κ	BD555511	BD Biosciences, Heidelberg
CD62L	PE	mIgG1,κ	BD555544	BD Biosciences, Heidelberg
CD80	PE	mIgG1	IOTest IM1976U	IOTest Beckman Coulter, Krefeld
CD86	APC	mIgG1,κ	BD558065	BD Biosciences, Heidelberg
CD96	PE	mIgG1	sc-53575	Santa Cruz Biotechnology, Dallas, USA
CD152 [CTLA-4]	APC	mIgG2α,κ	BD555855	BD Biosciences, Heidelberg

CD155 [PVR]	APC	mIgG1,κ	FAB 25301A	R&D Systems, Minneapolis, USA
CD159a [NKG2A]	PE	rhIgG1	130-098-814	Miltenyi Biotec, Bergisch Gladbach
CD159c [NKG2C]	PE	rhIgG1	130-103-700	Miltenyi Biotec, Bergisch Gladbach
CD215 [IL-15R]	PE	mIgG1	IC2471P	R&D Systems, Minneapolis, USA
CD274 [PDL-1]	FITC	mIgG1,κ	BD558065	BD Biosciences, Heidelberg
CD279 [PD-1]	APC	mIgG1,κ	BD558694	BD Biosciences, Heidelberg
CD314 [NKG2D]	APC	mIgG1,κ	320808	Biolegend, San Diego, USA
CD336 [NKp44]	PE	mIgG1,κ	325108	Biolegend, San Diego, USA
CD337 [NKp30]	APC	mIgG1,κ	325210	Biolegend, San Diego, USA
CD366 [TIM-3]	PE	mIgG1,κ	12-3109-41	eBioscience Thermo Fisher Scientific, Waltham, USA
[HLA-E]	APC	mIgG1,κ	342605	Biolegend, San Diego, USA
[TIGIT]	PE	mIgG2α,κ	372705	Biolegend, San Diego, USA
TCR-Vβ8	FITC	mIgG2α	IOTest IM1233	IOTest Beckman Coulter, Krefeld
TCR-Vβ8	PE	mIgG2b,κ	348104	Biolegend, San Diego, USA
TCR-Vβ21.3	FITC	mIgG2α	IOTest IM1438	IOTest Beckman Coulter, Krefeld
CD3	V450	mIgG1,κ	BD560365	BD Biosciences, Heidelberg
CD3	APC	mIgG2α,κ	300312	Biolegend, San Diego, USA
CD8α	APC	mIgG1,κ	301014	Biolegend, San Diego, USA

Isotype control	APC	mIgG1,κ	400120	Biolegend, San Diego, USA
Isotype control	PE	mIgG1,κ	IOTest A07796	IOTest Beckman Coulter, Krefeld
Isotype control	FITC	mIgG1,κ	BD555909	BD Biosciences, Heidelberg
Isotype control	PE	mIgG2α,κ	IOTest A09142	IOTest Beckman Coulter, Krefeld

Table 7.1.9 Antibodies

7.1.14 Software

Name	Manufacturer
Prism 8	GraphPAD, La Jolla, USA
FacsDiva 6.1.3	BD Biosciences, Heidelberg
FlowJo 10.6.2	FlowJo LLC, Ashland, USA
SnapGene	GSL Biotech LLC, Chicago, USA
Office 365	Microsoft, Redmond, USA

7.2 Methods

7.2.1 Molecular Biology

7.2.1.1 RNA isolation

In order to generate expression vectors for the retroviral transfer of the human costimulator CD8 into TCR transduced NK92, RNA was extracted from from 4 x 10^6 CTLs of the clones 25F2 and 5B2 (see above) using the RNeasy Mini Kit according to the manufacturer´s instructions. The amount of isolated RNA was determined by spectrophotometry (NanoDrop™), and purity was evaluated according to the optical density measured at 260/280 nm and 260/230 nm. Samples were considered as sufficiently pure for subsequent experiments with 260/280 nm ratios of approx. 2 and 260/230 nm of greater 1.

7.2.1.2 Reverse transcription

Template DNA for the amplification of the CD8 sequences was established by reverse transcription of isolated RNA (see 11.1.1) using the SuperScript™ III Reverse Transcriptase (RT) kit. Complementary DNA (cDNA) was synthesized from 2 µg of isolated RNA filled up to 11 µl with RNAse free water and supplemented with 1 µl oligo $(dT)_{20}$ primers as well as 1 µl 10

mM deoxynucleotide triphosphates (sNTP) mix. After heating the mixture to 65°C for 5 min and subsequent incubation on ice for 1 min, 4 µl 5x First-Strand Buffer, 1µl 0.1 M 1,4-ditiothreitol, 1 µl RNaseOUT™ recombinant RNase inhibitor and 200 U of SuperSript™ III RT were added. Then, DNA synthesis was performed by incubating the reaction mixture at 50°C for 60 min following inactivation by heating at 70°C for 15 min. The cDNA was stored at -20°C until further use and its concentration was determined by NanoDrop™.

7.2.1.3 Polymerase chain reaction

The polymerase chain reaction (PCR) served as a tool for highly specific amplification as well as 5´ and 3´ modification of DNA sequences in the context of expression vector generation. Moreover, due to its sensitivity PCR was used to detect positively transformed bacteria colonies by a protocol referred to as colony-PCR.

7.2.1.3.1 DNA amplification for cloning

In order to reduce the occurrence of mutations due to misincorporation of nucleotides, the 3´-5´ exonuclease, "proofreading", activity possessing Q5® high-fidelity polymerase was used for DNA amplification in the course of cloning procedures. Depending on the strategy of DNA assembly, gene specific primers were designed containing a defined restriction site (restriction cloning) or overlapping sequence (in-fusion cloning) added as an "overhang" to the 5´end of 15-20 base pairs (bp) complementary to the gene of interest´s endings. Enzyme-specific annealing temperatures of the primers were determined using the NEB Tm Calculator online tool and potentially interfering secondary structures were ruled out by OligoAnalyzer 3.1 Tool of Integrated DNA technologies. PCRs were performed according to manufacturer´s instructions (Q5® High-Fidelity DNA Polymerase protocol) under conditions depicted in the table below.

Component	**Volume**	**Step**	**Temp.**	**Time**
5x Q5 Reaction Buffer	10 µl	Initial Denaturation	98°C	30 s
10 mM dNTPs	1 µl	30 Cycles	98°C	10 s
10 µM Forward Primer	2.5 µl		$T_{Annealing}$	30s
10 µM Reverse Primer	2.5 µl		72°C	30 s/kb
Template DNA	10 ng	Final Extension	72°C	2 min
Q5 High-Fidelity DNA Polymerase	0.5 µl	Hold	4°C	
5 x Q5 High GC Enhancer*	10 µl			
DMSO*	5 µl			

Nuclease-Free Water	to 50 µl	

Table 7.2.1 DNA amplication for cloning - protocol

Components labeled with * were added only when amplification under standard conditions failed.

7.2.1.3.2 Colony PCR

Partial amplification of plasmid DNA from a bacterial solution was performed after transformation of bacteria by the robust One*Taq*® Hot Start DNA polymerase (NEB). Screening for colonies with successful gene transfer primer pairs binding the vector backbone and within the inserted sequence were chosen. The annealing temperature was calculated as described in 7.2.1.3.1 and PCR was performed according to the NEB Protocol for OneTaq® Hot Start 2X Master Mix with Standard Buffer. In consideration of using bacteria as a template, the initial denaturation was prolonged to 5 min in order to release plasmid DNA by thermal disruption of cell membrane integrity. Detailed conditions are listed below.

Component	**Volume**	**Step**	**Temp.**	**Time**
10 µM Forward Primer	0.5 µl	Initial Denaturation	94°C	5 min
10 µM Reverse Primer	0.5 µl	30 Cycles	94°C	30 s
Bacterial suspension	3 µl		$T_{Annealing}$	60 s
One*Taq* Hot Start 2x Master Mix with Standard Buffer	12.5 µl		68°C	60 s/kb
Nuclease-Free Water	to 25 µl	Final Extension	68°C	5 min
		Hold	4°C	

Table 7.2.2 Colony PCR - protocol

7.2.1.4 Agarose gel electrophoresis

Size-dependent separation of DNA fragments was performed by means of agarose gel electrophoresis for analytical and manufacturing purposes. Therefore, 1% agarose gels were prepared mixing (1x) Tris-acetate-EDTA (TAE) buffer with the appropriate amount of agarose and 1 µlml^{-1} GelRed Nucleic Acid Stain (10.000x) which intercalates with DNA and enables the detection of the separated fragments by ultraviolet light. For loading an adequate quantity of DNA was mixed 5:1 with 6x loading dye and transferred to the gel slots. After separation at 100 volt (V) for 50 min, DNA fragments were visualized in UV-light and documented with the iBright™ imaging system. GeneRuler 1 kb (Plus) DNA Ladder was used as size standard.

7.2.1.5 Preparative digestion (incl. clean-up)

In the context of restriction cloning PCR fragments and transfer vector backbones were prepared for subsequent ligation by digestion with corresponding restriction enzymes obtained from New England Biolabs. Therefore, 50 µl reactions were generated mixing up to 5 µg of DNA with 1 µl of each restriction enzyme, 5 µl of the adequate NEB buffer and nuclease-free water. Following incubation for 3 h at 37°C agarose gel electrophoresis was performed in order to confirm successful digestion prior to gel purification of the desired DNA fragment using the NucleoSpin™ Gel and PCR Clean-up kit according to manufacturer´s protocol. The amount and purity of the DNA isolated from the agarose gel was determined by NanoDrop™.

7.2.1.6 Restriction enzyme-based cloning

The expression vectors pMXs_IRES_Neo and –Hygro as well as the plasmid pMXs_TCR-5H11_IRES_Puro were established by restriction enzyme-based cloning. Therefore, DNA sequences to be cloned were examined in silico for potential recognition sites of single cutting restriction enzymes at the location of interest. When a suitable enzyme was found, restriction digestion and clean up was performed as described in 7.2.1.5. However, in the case of absence of appropriate recognition sites, these were added to the relevant DNA sequences by Q5® PCR amplification with primers containing the enzyme-specific palindromic motif needed. Following agarose gel electrophoresis and DNA clean-up with the NucleoSpin™ Gel and PCR Clean-up kit, the whole sample volume was used for preparative digestion according to 7.2.1.5.

Having obtained the appropriate digested and purified DNA fragments ligation was performed with NEB T4 DNA Ligase according to manufacturer´s instructions. Depending on the amount of inserts a vector:insert ratio of either 3:1 (single) or 6:1 (multiple) was chosen and equivalent DNA masses were calculated using the NEBioCalculator®.

7.2.1.7 In-Fusion Cloning

In order to establish CD8 co-receptor expression vectors from cDNA of CTL clones 25F2 and 5B2, CD8 transcription variant specific primers were designed for the amplification of the α1 and -2 as well as the β2 , -3, -5 and -6 chains. As the two different α-chains share the same 3´-ending and all β-variants begin with the same 5´-sequence, universal α-chain reverse and β-chain forward primers could be applied to the corresponding subtype-specific oligonucleotides. Due to this observation, the In-Fusion Cloning was planned to create bicistronic expression vectors encoding the α-chain up- and the β-chain downstream of a P2A ribosome skipping motif. Therefore, half of the DNA sequence of P2A was added to each universal CD8 primer. In accordance to the principle of In-Fusion Cloning (Fig. 7.2.1), 15 to 20

bp of the complementary sequence up- or downstream to the DNA fragment´s prospective location were attached. Following PCR amplification (7.2.1.3) and gel purification (7.2.1.5) various combinations of CD8 α- and β-chains were cloned into the pMXs_IRES_Neo vector, linearized by the restriction enzymes Eco RI and Sal I, by the use of the NEBuilder® HiFi DNA Assembly kit according to the manufacturer´s protocol. Subsequently, 5 µl of the cloning sample were used to transduce competent Stbl3 bacteria and the success of ligation was initially evaluated by growth of ampicillin resistant colonies overnight.

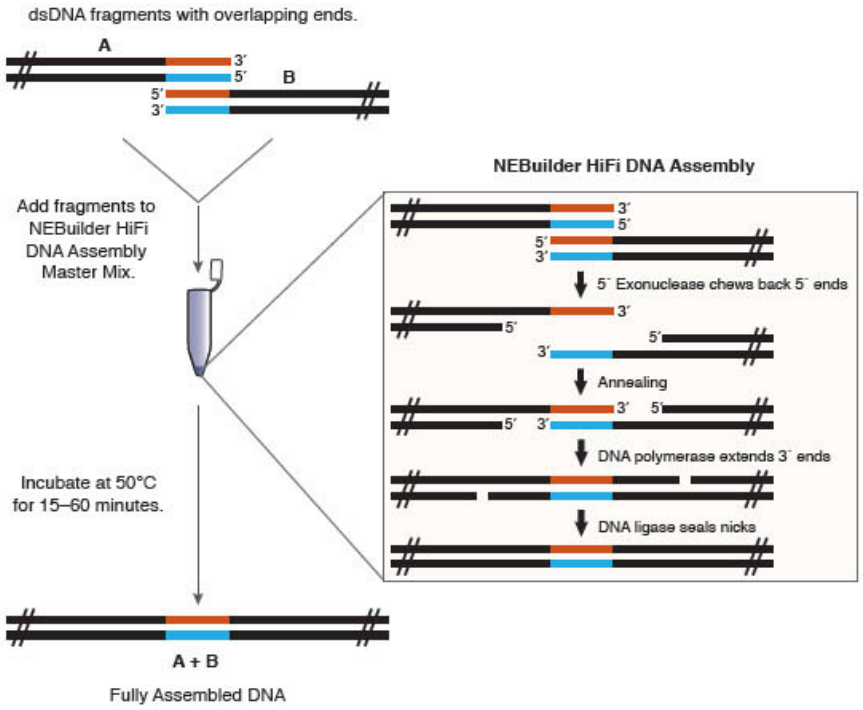

Figure 7.2.1 Principle of function of the NEBuilder HiFi DNA Assembly-method. Illustration obtained from New England BioLabs® GmbH (https://www.neb-online.de/en/cloning-synthetic-biology/dna-assembly/nebuilder-dna-assembly/) on 30th of September 2022.

7.2.1.8 Transformation

For efficient multiplication of LTR-containing vectors, such as pMXs derivatives, One Shot® Stbl3™ Chemically Competent *E. coli* were transformed. Therefore, 50 µl of competent Stbl3 bacteria were thawed on ice and mixed with up to 100 ng plasmid DNA by flicking the tube. Following incubation on ice for 30 min a heat shock was performed at 42 °C for 45 s. Immediately after, the bacteria were transferred back on ice for 2 min and then 500 µl LB-medium were added. For propagation and recovery the Stbl3 were shaken for 90 min at 37 °C and 225 rpm prior selection of positively transformed clones by plating the bacteria on a 10 cm LB agar plate containing 100 µg mL-1 ampicillin. After incubating the plates for 24 h at 37 °C, successfully transformed and therefore ampicillin-resistant colonies were picked to inoculate 3 ml of selective LB-medium. 2 ml of these starter cultures were transferred after 6 h of incubation in the bacteria shaker (see standard settings described above) into 100 ml of fresh

LB-medium containing 100 µg mL-1 ampicillin. Following 18 h of incubation under standard conditions, propagated plasmid DNA was isolated vie midiprep.

7.2.1.9 Plasmid DNA isolation via mini-/midiprep

In order to isolate plasmid DNA from successfully transformed bacteria clones mini- or midiprep was performed depending on the amount of DNA needed. For the miniprep 3 ml LB-medium supplemented with 100 µg mL-1 ampicillin were inoculated with a positive clone and incubated in the bacteria shaker at 37 °C and 225 rpm overnight. On the next day 2 ml of the culture were centrifuged at 13.000 rpm (Biofuge Fresco Heraeus, ThermoFisher Scientific) prior resuspending the bacterial pellet thoroughly in 250 µl resuspension buffer containing RNase A. Then disruption of cell membrane integrity was initiated by adding 250 µl of lysis buffer and after 5 min of incubation at room temperature, genomic DNA and proteins were precipitated applying 350 µl neutralization buffer. Following another centrifugation step at 13.000 rpm for 10 min, plasmid DNA solved in the supernatant was transferred into a new reaction tube. For further purification a DNA pellet was generated by centrifugation at 13.000 rpm for 10 min after the addition of 510 µl isopropanol. The DNA was washed with 300 µl of 70% ethanol and centrifuged again at 13.000 rpm for 10 min. Finally the pellet was air dried prior resuspension in 50 µl dH_2O.

When large quantities of plasmid DNA were needed, 100 ml bacterial cultures were generated as described in 7.2.1.8. After 18 to 20 h of incubation DNA isolation was performed using the NucleoBond Xtra plasmid Midi-preparation kit according to manufacturer´s instructions.

The yield of plasmid DNA was quantified utilizing the NanoDrop spectrophotometer and purity of the isolated DNA was determined by the optical density at 260/280 and 260/230 nm. DNA was considered as clean, when the 260/280 ratio was at 1.8 and the 260/230 ratio between 2.0 and 2.2.

Correct cloning of the different plasmids was confirmed by analytical digestion and sequencing.

7.2.1.10 Analytical digestion

Using appropriate restriction enzymes the integrity of successfully cloned plasmids was validated by analytical digestion. Therefore, 1 µl of each NEB restriction enzyme was added to 1 µg isolated DNA supplemented with 5 µl of the adequate 10x digestion buffer in a total volume of 50 µl. Incubation temperature and time was performed according to the optimal conditions of the enzymes chosen. Subsequently, the generated DNA fragments were analyzed by agarose gel electrophoresis.

7.2.1.11 DNA sequencing

In order to evaluate the integrity of newly established transfer vectors prior to expression in NK92, Sanger sequencing was performed by StarSEQ® GmbH (Mainz). Consequently, 1µg of midi-grade plasmid DNA was mixed with 3 µl of 10 µM forward and reverse primers, respectively and sent to the company. For sequencing of pMXs vectors the primers UH360 and UH361 (see 10.6) were used as they bind up- and downstream of the MCS of all pMXs plasmids. Sequence analysis was performed in silico by SnapGene® alignment tool.

7.2.2 Cell Culture

7.2.2.1 Media and growth conditions

NK92 cells were cultured in α-MEM supplemented with 20% heat-inactivated fetal calf serum (FCS), 1% Penicillin (10^5IU/ml) and Streptomycin (10mg/ml) (P/S), 0.2 mM inositol, 0.1 mM β-mercaptoethanol and 0.02 mM folic acid. Cells were stimulated with 200 IU/ml recombinant human IL-2 and seeded at 2 to 3 x 10^5 cells/ml in fresh complete medium every 2-3 days.

K562, the human Jurkat T cell line derivate Jurkat 76 and EBV-transformed B-lymphoblastoid cell lines (B-LCL) from patients MZ 580 and MZ 667 were kept in RPMI 1640 containing 10% heat-inactivated FCS and 1% P/S. The Phoenix-AMPHO and 293T cells were cultured at 60 to 70% confluency in Dulbecco´s Modified Eagle Medium supplemented with 10% FCS and 1% P/S. In order to passage adherent cells, medium was aspirated and cells were detached by incubation with Trypsin-EDTA at 37°C for 2 min after washing with PBS. The dissolved cells were resuspended in fresh medium and plated for appropriate confluency.

Primary AML samples were generated by standard Ficoll separation of leukapheresis products and cryopreserved until use. One day prior functional assays the AML blasts were thawed and cultured overnight in AIM V supplemented with 5% human serum.

The primary cells and all cell lines were kept in a CO_2-incubator at 5% CO_2, 37°C and 100% air humidity for cultivation. Growth, viability and potential contamination of all cells in culture were evaluated daily by light microscopy.

7.2.2.2 Determination of cell number

In order to determine the cell number, cells were harvested, centrifuged and resuspended in a known volume of medium. The cells´ viability was determined by diluting 20 µl of the cell suspension in a 1:1 ratio in trypan blue exclusion dye, which selectively passes the membranes of dead cells. The amount of unstained cells within 4 large squares of a Fuchs-Rosenthal counting chamber was determined under the light microscope, subsequently. The cell number was calculated according to the following formula:

$$\frac{\text{counted cells}}{\text{counted large squares}} * \frac{5000}{\text{ml}} \,(\text{counting chamber factor}) * 2\,(\text{dilution factor}) = \text{cells/mL}$$

7.2.2.3 Cryopreservation of cells

For cryopreservation cells were harvested, counted, pelleted by centrifugation at 450 g for 5 min at RT and resuspended in freezing medium (RPMI-1640 medium supplemented with 10 IU mL^{-1} heparin, 8% human albumin and 10% DMSO). 1 mL of the cell suspension was

aliquoted per cryo-tube and frozen at -80 °C using isopropanol filled freezing boxes for constant cooling while avoiding crystallization. After a one day, cells were transferred to the cryobank where they were stored in the gas phase of liquid nitrogen at -180 °C.

7.2.2.4 Thawing of cells

Cells were thawed by transferring frozen cryo-tubes into the preheated water bath at 37°C. Upon starting liquefaction culture medium was added and the cells were centrifuged at 450 g for 5 min, immediately. To remove the cytotoxic DMSO of the freezing medium the cells were washed again with fresh medium prior to cultivation in cell culture flasks.

7.2.2.5 Generation of viral particles

Viral particles containing supernatants were generated for subsequent transduction of NK92 (effectors) and Jurkat76 as well as K562 and EBV-B-LCLs (targets). For the expression of the AML-reactive TCRs, CD3- and CD8-complex on the effector cells, retrovirus was produced within 48 hours of incubation post transfection of amphotropic Phoenix cells with polyethyleneimine (PEI):DNA complexes.

In order to establish Firefly Luciferase (FLuc) expressing target cells, lentiviral particles were synthesized by 293T cells after transfection with pLenti_EF1_Pac_2A_GFP/FLuc transfer vector using the DNA transfection reagent TransIT-LT1 and pSPAX2 plus pMD2.G as helper plasmids.

7.2.2.5.1 Transfection of Phx ampho with PEI

In order to produce retroviral particle containing supernatants, 2.5 x 10^6 Phx ampho cells were plated per 100 mm culture dish one day prior to transfection. On the next day, co-transfection of the desired retroviral transfer vector as well as the packaging (pHIT60) and envelope (pCOLT-GALV) plasmids was performed after the assembly of PEI::DNA complexes by incubation of DNA in the presence of the transfection agent Polyethyleneimine (PEI) for 30 min at RT according to Table 7.2.1. After formation of the PEI::DNA complexes, the transfection mix was filled up to 4 ml with OptiMEM. Then the Phx cells were washed carefully with prewarmed PBS and the PEI::DNA mixture was applied dropwise onto the cells to avoid detachment. After 4 h of incubation at 37°C, the transfection mix was replaced by 5 ml of the medium in which the cells to be transduced are cultured in. Retroviral particles containing supernatant was harvested after 48 h post transfection.

PEI-transfection	**100 mm culture dish**
OptiMEM medium (serum free)	1200 µl

Polyethyleneimine PEI	80 µg
Transfer vector	10 µg
pHIT60 (packaging vector)	5 µg
pCOLT-GALV (envelope vector)	5 µg

Table 7.2.3 Transfection of Phx ampho with PEI

7.2.2.5.2 Transfection of 293T using TransIT-LT1

Lentiviral particle containing supernatants were generated by 293T cells which were plated at 1 x 10^6 cells per 100 mm culture dish 1 or 2 days before transfection. When 293T reached 60-70% confluency, co-transfection of the transfer vector pLenti_EF1a_Pac_2A_GFP/FLuc and its corresponding helper plasmids was performed with the transfection agent TransIT-LT1 in analogy to the PEI-protocol. On the day of transfection the reaction mixture was prepared according to Table 7.2.4 and incubated for 30 min at RT. Then, 6 ml complete DMEM per dish was added to the transfection mixture prior replacing the old medium of the 293T cells with the medium-DNA solution. The transfection reagent was removed on the next day by exchanging the medium with 2.7 ml DMEM supplemented with 30% FCS and 1% P/S per plate. Repeating the media change for 2 days lentivirus containing supernatants were collected from day 2 to 4 post transfection and pooled for transduction.

TransIT-LT1-transfection	**100 mm culture dish**
OptiMEM medium (serum free)	290 µl
TransIT-LT1	18 µg
Transfer vector	3 µg
psPAX2 (packaging vector)	1.8 µg
pMD2.G (envelope vector)	0.3 µg

Table 7.2.3 Transfection of 293T with TransIT-LT1

7.2.2.6 Retro- and lentiviral transduction

Transduction with the generated lenti- and retroviral supernatants was performed via spin infection with polybrene as transduction agent. As a cationic polymer polybrene neutralizes the charge repulsion between virions and the cell surface resulting in an increased infection efficiency.

Therefore, 1 x 10^6 cells were resuspended in 1 ml viral supernatant and plated into a 24-well-plate. Prior to transduction, the viral particle containing supernatant was filtered in order to remove cell debris. Then 5 µgmL^{-1} (retrovirus) or 8 µgmL^{-1} (lentivirus) of polybrene were added prior to centrifugation at 2000 rpm and 32°C for 90 min without deceleration (spin infection).

After 18 h of incubation at 37°C and 5% CO_2 cells were washed and cultured in the appropriate medium. The selection for positively transduced cells was started 3 days post transduction by the application of 1 µg/ml puromycin (TCR-, CD3-, GFP-FLuc-construct) or 500 µg/ml G418 (CD8-constructs). Jurkat76 cells were transduced with the TCR-supernatants to evaluate the quality of the generated viral suspensions and integrity of the TCR-expression vectors.

7.2.2.7 Enrichment of successfully transduced cells

7.2.2.7.1 Magnetic Activated Cell Sorting

Since the TCR- and CD3-plasmids both confer puromycin resistance, expression of the TCR::CD3 complex of dual transduced NK92 could not be increased by antibiotic selection. However, as the TCR and CD3 cell surface expression is highly interdependent, TCR positive NK92 cells were enriched using Magnetic-Activated Cell Sorting (MACS™) technology (Miltenyi Biotec) by direct labeling of successfully transduced NK92 with magnetic CD3 MicroBeads. The isolation was performed with MS columns according to manufacturer´s instructions and the increase in TCR as well as CD3 expression was verified by flow cytometry. Generally, more than 80% TCR positive NK92 cells could be obtained after two cycles of MACS enrichment.

7.2.2.8 Flow cytometry

FACS staining of extracellular antigens was performed according to this standard protocol. Per sample 1 x 10^5 cells were washed with 1 ml of FACS-buffer (PBS containing 3% bovine serum albumine and 1% sodium azide) prior to incubation with staining antibodies in 100 µl FACS-buffer for 15 min at room temperature in the dark. Following another washing step cells were resuspended in 200 µl of fixation buffer (PBS supplemented with 0.4% paraformaldehyde) and within 72 h data acquisition was performed recording 1 x 10^4 events per sample with FACSCanto (BD Biosciences, Heidelberg, Germany). Compensation and isotype controls were implemented for every sample.

Expression of transduced TCRs, CD3 and CD8 complex on NK92 was examined with the corresponding antibodies TCR Vβ21.3 FITC, TCR Vβ8 PE or FITC, CD3ε APC, CD8 APC.

The following antibodies were used for staining of effector and target cell surface markers: CD86 APC, CD274 FITC, CD152 APC, CD279 APC, CD28 FITC, HLA-E APC, CD27 FITC, NKG2D APC, NKp30 APC, NKp44 PE, TIGIT PE, CD80 PE, CD155 APC, CD366 PE, CD96 PE, NKG2A PE, NKG2C PE.

7.2.2.9 IFN-γ Enzyme-Linked Immunosorbent Spot assay

The IFN-γ secretion of TCR-transduced NK92 was detected and quantified by Enzyme-Linked Immunosorbent Spot assay (ELISpot). Therefore, 96-well ELISpot plates were coated with 0.5 µg of anti-human IFN-γ mAb 1-DK-1 (MABtech) per well. After blocking of the wells with RPMI containing 10% FCS, 1 x 10^5 effector and target cells were cocultured in duplicates at an effector to target ratio (E:T) of 1:1 in the presence of 200 IU/ml rh IL-2 for 24h at 37°C. In case peptide-loading of K562 A2 was needed, target cells were incubated for 1 hour at 37°C in 0.5 ml serum-free RPMI medium supplemented with 5 µg of appropriate peptide prior to seeding. When blocking antibodies were applied, per 1 x 10^5 target cells, 1 µg of antibody was added before incubation on ice for 20 min. Subsequently, target cells were treated as described above. Then the plate was washed and 0.1 µg biotinylated detection antibody (MABtech) was added. Following incubation and washing 100 µl/well of avidin/horseradish peroxidase complex (Standard Vectastain ABC Kit, Vector Laboratories, Burlingame, USA) were used to visualize the spots of IFN-γ secretion in the presence of 100 µl/well AEC-solution with 30% hydrogen peroxide. The resulting red spots were analyzed in terms of quantity and quality according to standard gating protocol using an Immunospot® Analyzer. To rule out possible background IFN-γ secretion controls containing effector or target cells only were carried out every assay.

7.2.2.10 Bioluminescence-based cytotoxicity assay

The cytolytic activity elicited by NK92 was examined in vitro by a recently implemented bioluminescence-based assay. Therefore, target cells were lentivirally transduced to express Firefly Luciferase (FLuc) serving as a reporter for target viability due to its ATP-dependent luminescence (see chemical reaction below).

$$\text{luciferin} + \text{ATP} \rightarrow \text{luciferyl adenylate} + \text{PP}_\text{i}$$

$$\text{luciferyl adenylate} + \text{O}_2 \rightarrow \text{oxyluciferin} + \text{AMP} + \text{light}$$

ATP: Adenosine triphosphate; AMP: Adenosine monophosphate; PP_i: Pyrophosphate

As the FLuc-mediated luminescence relies strictly on the presence of ATP the amount of radiated light correlates to the number of target cells with intact energy supply. Therefore, effector cell induced killing of targets can be detected with a very high sensitivity at an early state of cell death represented by the disruption of survival-essential ATP metabolism. To measure the effect of TCR redirection and CD8 coexpression on NK92 cytotoxicity, 1 x 10^4 FLuc transduced target cells were cocultured per well in triplicates with effectors at E:Ts from 40:1 to 0.625:1 in black 96-well plates in the presence of the FLuc-substrate D-Luciferin

(ThermoScientific). In case peptide-loading of K562 HLA-A*02:01 was performed, target cells were incubated for 1 hour at 37°C in 0.5 ml serum-free RPMI medium supplemented with 5 µg of appropriate peptide prior to seeding. After 18h of incubation relative luminescence units (RLU) were determined by the FluostarOmega-Reader (BMG LABTECH) with 10s integration time per well. Lysis of CD8 and or TCR positive cells was quantified by loss of FLuc signal.

When TCR-mediated cytotoxicity was studied, the reduction of luminescence was normalized to TCR negative NK92CD3$^+$ in order to offset general natural killer activity and referred to as "TCR-specific lysis":

$$\text{TCR} - \text{specific lysis } [\%] = \frac{\text{RLU of NK92CD3}^+ - \text{RLU of TCR}^+\text{NK92}}{\text{RLU of NK92CD3}^+ - \text{RLU of max. lysis control}} * 100$$

As TCR independent killing of K562 was examined to evaluate the remaining natural killer cell cytotoxicity of the redirected NK92, the loss of FLuc activity was quantified as "general lysis" in relation to target cells cultivated without effectors:

$$\text{general lysis } [\%] = \frac{\text{RLU of target cells only} - \text{RLU of TCR}^+\text{NK92}}{\text{RLU of target cells only} - \text{RLU of max. lysis control}} * 100$$

8 Results

8.1 Experimental strategy

In the following, the experimental workflow for the generation and *in*-vitro characterization of TCR-redirected NK92 cells simultaneously expressing the human CD8 coreceptor is described briefly and depicted in Fig. 8.1.1.

First, a polycistronic vector expressing the human CD3 complex was obtained from Dr. Catherine Wölfel (IIIrd. Dept. of Medicine – Hematology & Medical Oncology, University Medical Center of Johannes Gutenberg-University Mainz). Expression vectors of therapeutic TCRs were in-lab generated by Dr. J. Albrecht and Dr. A. Bhatti (5H11-, 5B2- and 25F2-TCR, together referred to as AML-reactive TCRs) or, in the case of MDM2-TCR, obtained from Dr. H. Echchannaoui (IIIrd. Dept. of Medicine). Then, to prepare retroviral expression vectors encoding different isoforms of the human CD8αβ complex, the puromycin resistance site of the pMXs_IRES_Puro vector backbone was exchanged by neomycin. This allowed subsequent enrichment of successfully CD8αβ-transduced NK92 TCR, already resistant to puromycin due to hCD3 and/or TCR expression. In order to coexpress the human CD8 complex with therapeutic TCRs in NK92 cells, DNA-sequences of the isoforms of the human CD8α- and –β-chain expressed by the CTL clones 5B2 and 25F2 were isolated from cDNA via PCR and transferred into the retroviral expression vector pMXs_IRES_Neo by In-Fusion-Cloning. Within the resulting bicistronic constructs, the CD8 α- and β-chains were linked by a P2A ribosomal skipping site.

Manufacturing of NK92 TCR was accomplished by a three-step transduction process. First hCD3 complex was brought to expression upon retroviral transduction and puromycin selection. Then NK92 CD3 were cotransduced with therapeutic TCRs. Finally, NK92 TCR were superinfected with hCD8αβ-heterodimers in three different αβ-isoform combinations. Expression of surface molecules resulting from genetic modification was validated by flow cytometric analysis. Effector functions of the NK92 TCR subsets newly generated were examined with regard to cytotoxicity and IFN-γ degranulation *in-vitro*. The findings observed for the lab-manufactured AML-reactive TCRs were validated by supplementarily testing of NK92 cells expressing a therapeutic TCR recognizing the $_{81\text{-}88}$-epitope (amino acids 81-88) of the MDM2-peptide in context with HLA-A*02:01.

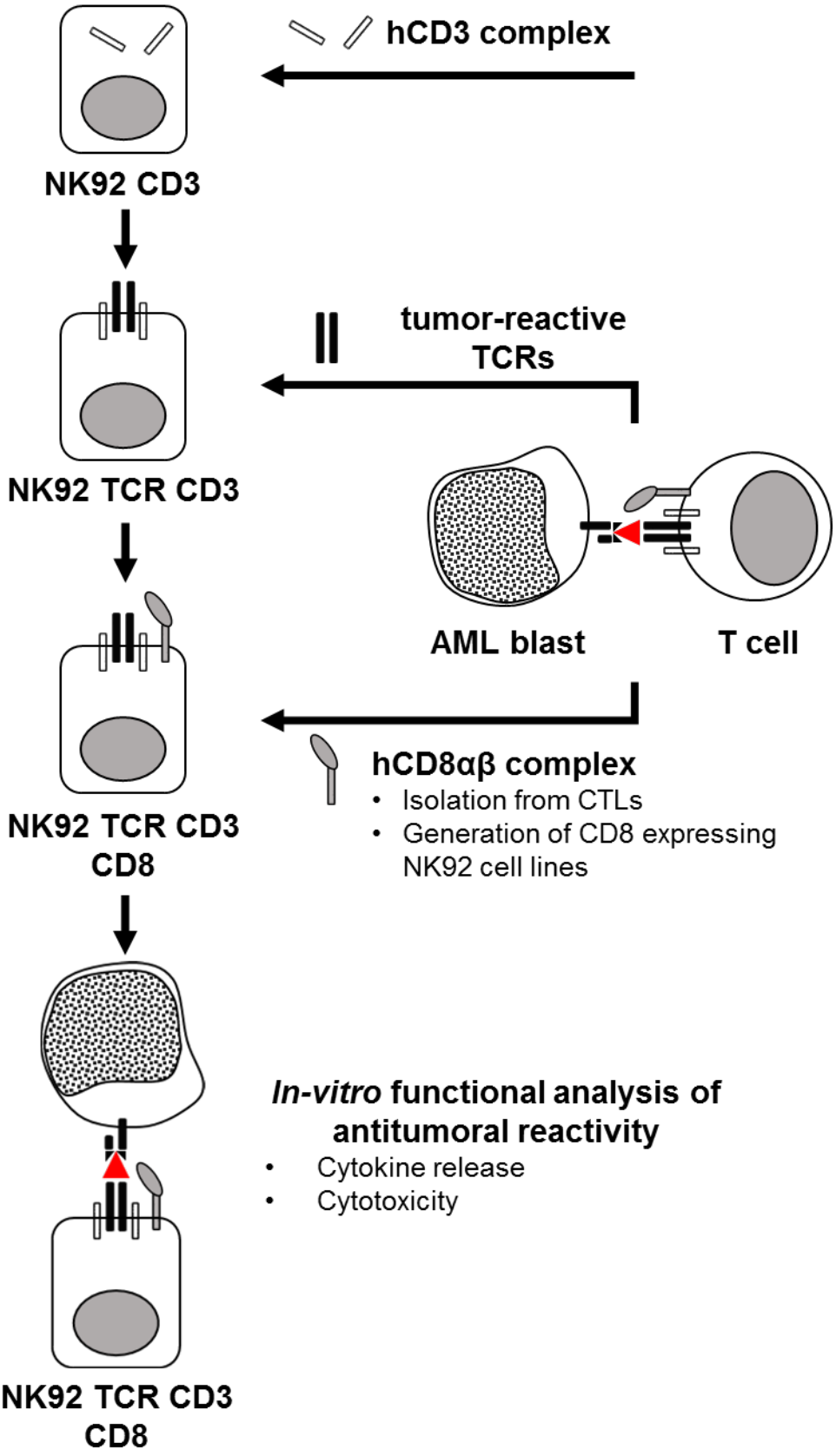

Figure 8.1.1 Synopsis of the project´s experimental workflow. Three-step generation process of NK92 stably expressing the human CD3-TCR complex and different variants of CD8αβ coreceptors. Horizontally oriented black arrows represent retroviral transduction and enrichment of the depicted cell subsets with the DNA-construct labeled.

8.2 Generation of retroviral transfer vectors expressing the human CD8 complex

8.2.1 Establishing a retroviral pMXs_IRES expression vector encoding neomycin resistance.

In order to enable side-by-side expression of the TCR-CD3 complex and human CD8 via retroviral gene transfer in NK92 cells, next to puromycin, a new antibiotic resistance needed to be established for the pMXs expression vector system to allow gene specific enrichment of successfully transduced NK cells. Thus, as depicted in Fig. 8.2.1, a new pMXs_IRES_Neo-construct was generated by enzyme-based cloning conferring neomycin resistance upon gene transfer.

Therefore, the “pBulneo-Luc+” vector, kindly provided by the Dr. C. Wölfel, was utilized as a template to amplify the DNA-sequences of the internal ribosomal entry site (IRES) and neomycin resistance in toto by polymerase chain reaction (PCR). The forward UH 496 and reverse UH497 primers were both equipped with a non-binding surplus of nucleotides attaching restriction enzyme cutting sites to the end of each tail of the amplified sequence. As UH 496 was designed to introduce a SnaBI cutting site to the 5´ end and UH 497 to integrate a SalI site to the 3´ end of the IRES-neomycin sequence, correct orientation of the insert within the pMXs vector backbone was ensured for downstream cloning procedures. Successful amplification of the IRES-neomycin DNA-fragment was validated by agarose gel electrophoresis (data not shown). Next, the IRES-neomycin DNA fragment as well as the original pMXs_IRES_Puro vector were both incubated separately with the SnaBI and SalI restriction digestion enzymes generating compatible sticky 5´ and 3´ ends on both DNA constructs. By incubating the retroviral pMXs_IRES_Puro expression vector with SnaBI and SalI the original IRES-puromycin sequence was withdrawn and the vector backbone was linearized. Finally, the two digested DNA fragments were ligated generating the new pMXs_IRES_Neo expression vector. The ligation-product was transformed into Stbl3™ chemically competent E. coli bacteria and colonies that successfully internalized the plasmid-DNA were determined by colony PCR as well as analytical digestion of DNA-minipreps. Vast amounts of pMXs_IRES_Neo plasmid-DNA could be produced by midiprep of previously positive tested bacteria colonies. Integrity of the IRES-neomycin insert was validated by Sanger-sequencing (data not shown).

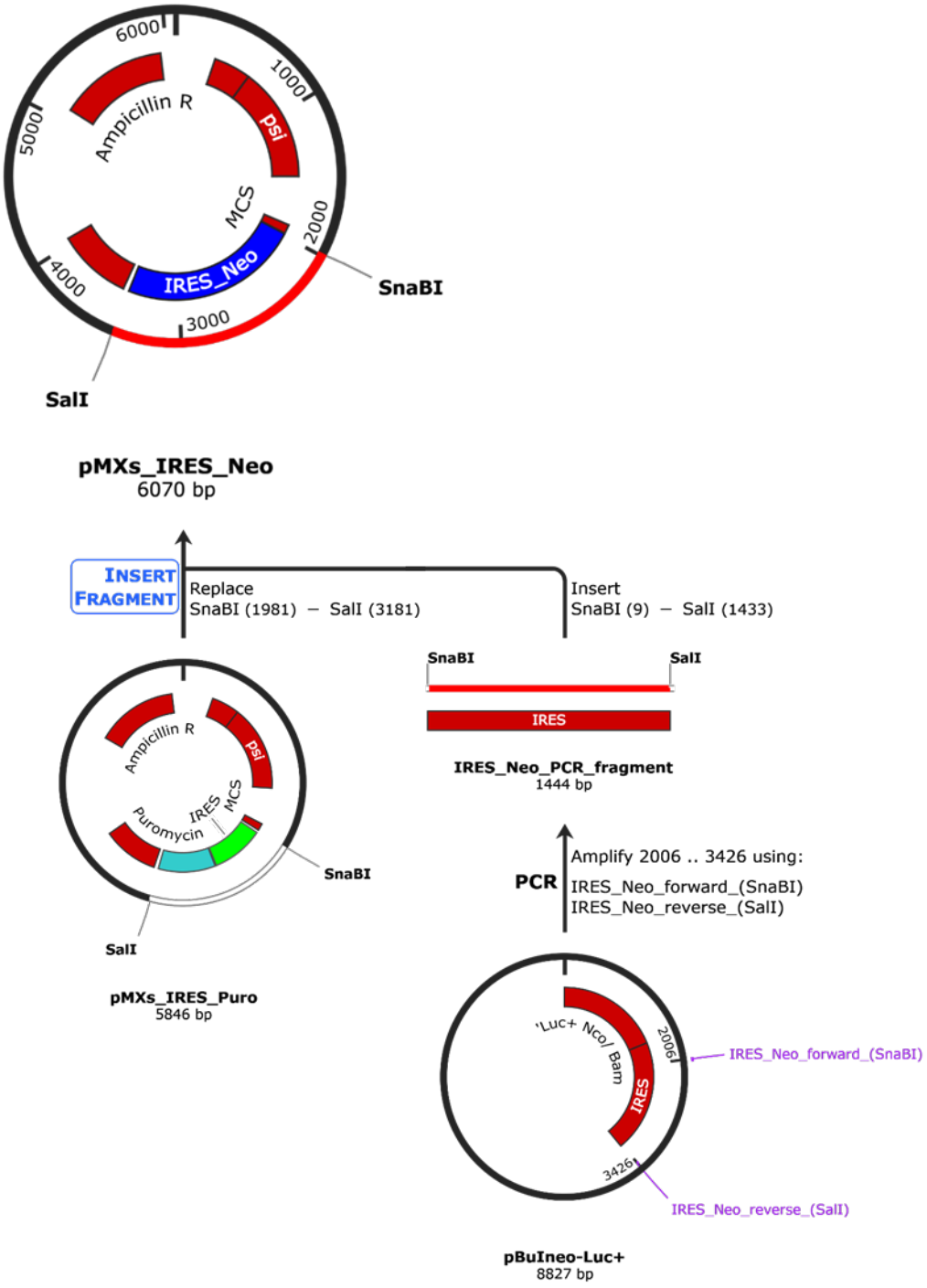

Figure 8.2.1 Cloning strategy for the generation of pMXs_IRES_Neo. The sequence encoding IRES and puromycin resistance of pMXs_IRES_Puro was replaced with IRES and neomycin resistance of pBuIneo-Luc+ by restriction enzyme-based cloning, in order to facilitate subsequent genetic modifications of NK92 cells. Restriction enzyme binding sites are labeled black. Primers are depicted in pink.

8.2.2 Analysis of the human CD8 gene.

In the process of gene expression, many variations, due to e.g. alternative splicing, can occur resulting in a magnitude of protein-"versions", all relating to the same parental gene. Due to this, a structured analysis of the multitude of transcript variants arising from the human CD8α- and β-gene was conducted, prior to the isolation of the CD8 coreceptor from cDNA of CTLs.

Therefore, “RefSeq”, the NCBI Reference Sequence Database, was searched for published protein-coding transcript variants of the α- and β-chain of the human CD8 gene. As shown in Fig. 8.2.2a, gene assembly revealed, that the transcript variants (TV) 1, 2, 3 and 5 represent the mRNA sequences resulting in protein expression of the human CD8α-chain. Interestingly, only two isoforms of the CD8α-chain are currently described at protein level. Therefore, the TVs 1, 3 and 5 all result in the same protein, the CD8α1-isoform. The transcript variant 2, however, encodes its own protein isoform, named CD8α2. In analogy, expression analysis of the CD8β-gene (Fig. 8.2.2b) resulted in a total of 6 protein-coding TVs, all encoding their own CD8β-protein-isoform. It is noteworthy, that TV 1 of the CD8β-gene represents a predicted transcript variant. In contrast, to our knowledge all other TVs have been isolated previously.

Primer design for the isolation of the CD8-isoforms expressed by the original CTL clones 5B2 and 25F2 was performed according to the result of the gene expression analysis and manufacturer´s instructions of NEBuilder® HiFi DNA Assembly. As the CD8α-isoforms only differ in the expression of one exon within the coding sequence, transcript variants 1 and 2 could both be amplified by the combination of the forward (UH 488) and reverse (UH 504) primers designed for CD8α-isolation. Whether TV 1 or 2 of the CD8α-chain was integrated into the coreceptor expression vectors, could only be determined by downstream sequencing analysis. The gene expression analysis of CD8β revealed, that all transcript variants share the same 5´ sequence. Thus, an universal forward primer (UH 505) was designed. Specific amplification of the different CD8β transcript variants was enabled by the generation of compatible reverse primers, characteristic for each TV, namely UH 493 for TV 2 and UH 495 for TV 6. In analogy to the CD8α-gene, the CD8β transcript variants 3 and 5 could not be specifically isolated, since they have common sequences at their 5´ and 3´ ends. Therefore, allocation between TV 3 and 5 could only be performed by subsequent sequencing analysis. Isolation of the transcript variant 1 was ommitted, as it is only predicted. In addition, integration of TV 4 into the expression vectors was waived, as it lacks the transmembrane region of the CD8β-chain and is therefore secreted. Thus, TV4 does not lead to a functional CD8 coreceptor expressed in NK cells.

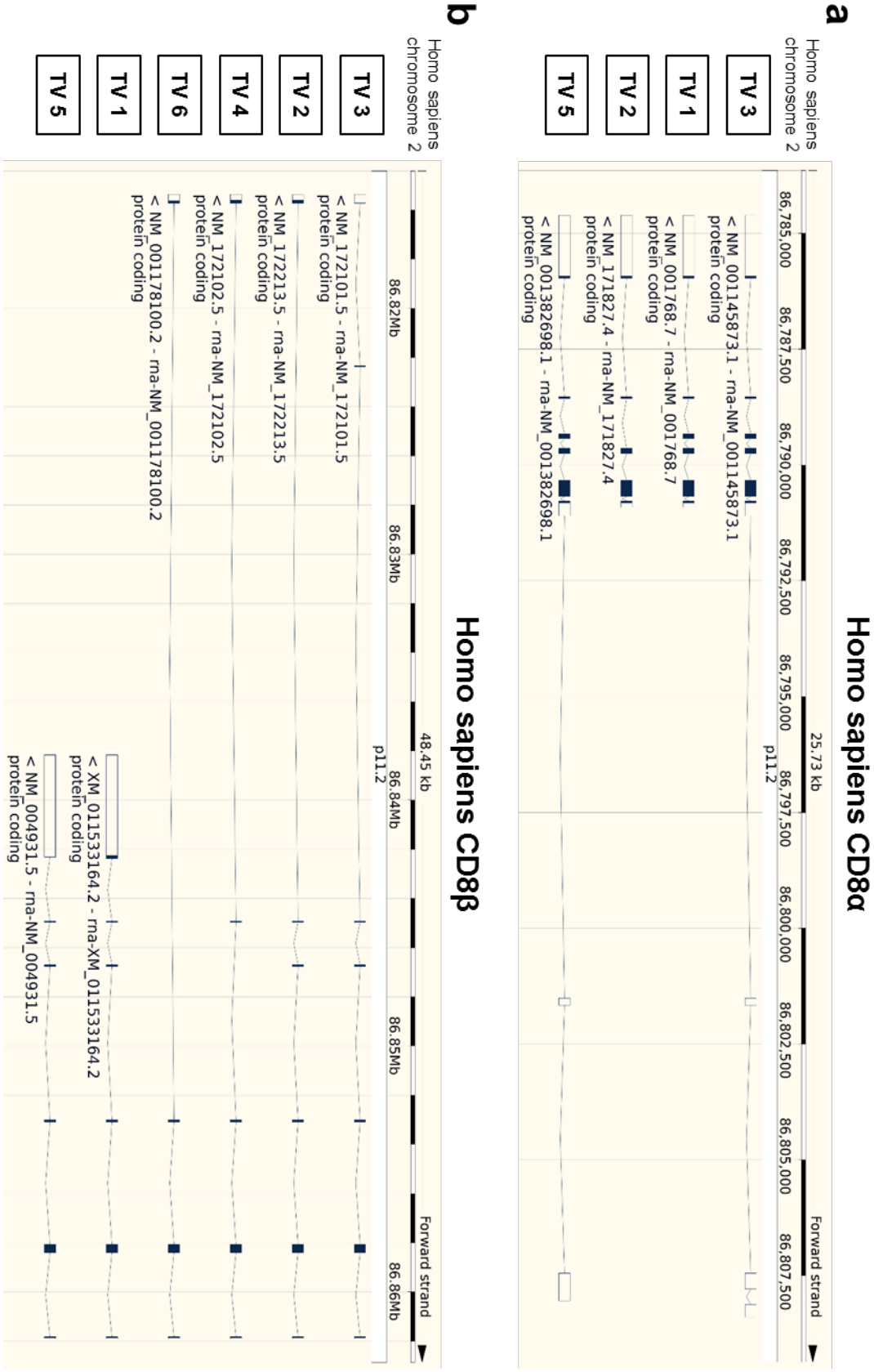

Figure 8.2.2 Transcript variants of the human CD8 gene. Gene assembly of protein coding transcript variants (TV) of the human CD8α- and CD8β-gene on chromosome 2 p11.2 as published in the NCBI Reference Sequence Database (RefSeq). (**a**) TV 1, 3 and 5 encode the human CD8α1-isoform. TV 2 expresses the CD8α2-isoform. (**b**) In contrast to CD8α, all TV of the human CD8β-gene encode for an eponymous isoform. Worthy of note is that the TV1 only represents a predicted transcription variant unlike the other TVs depicted. Genome assembly was performed with the latest release (107) of Ensembl.

8.2.3 Generation of expression vectors encoding variants of the human CD8αβ complex.

As different transcript variants, and therefore protein isoforms, exist for both CD8 chains, a variety of CD8αβ coreceptor combinations was available for transgenic expression of human CD8 in NK cells. Furthermore, differences in the enhancement of TCR-signaling between CD8 coreceptor-isoforms and changes in the CD8-isoform expression profile in accordance to T cell activation have been described.(177) Due to this reason, isolation of CD8-isoforms was conducted using a cDNA library of CTL clones 5B2 and 25F2 as a template, in order to extract versions of the CD8 coreceptor endogenously expressed by T lymphocytes the TCRs 5B2 and 25F2 derived from.

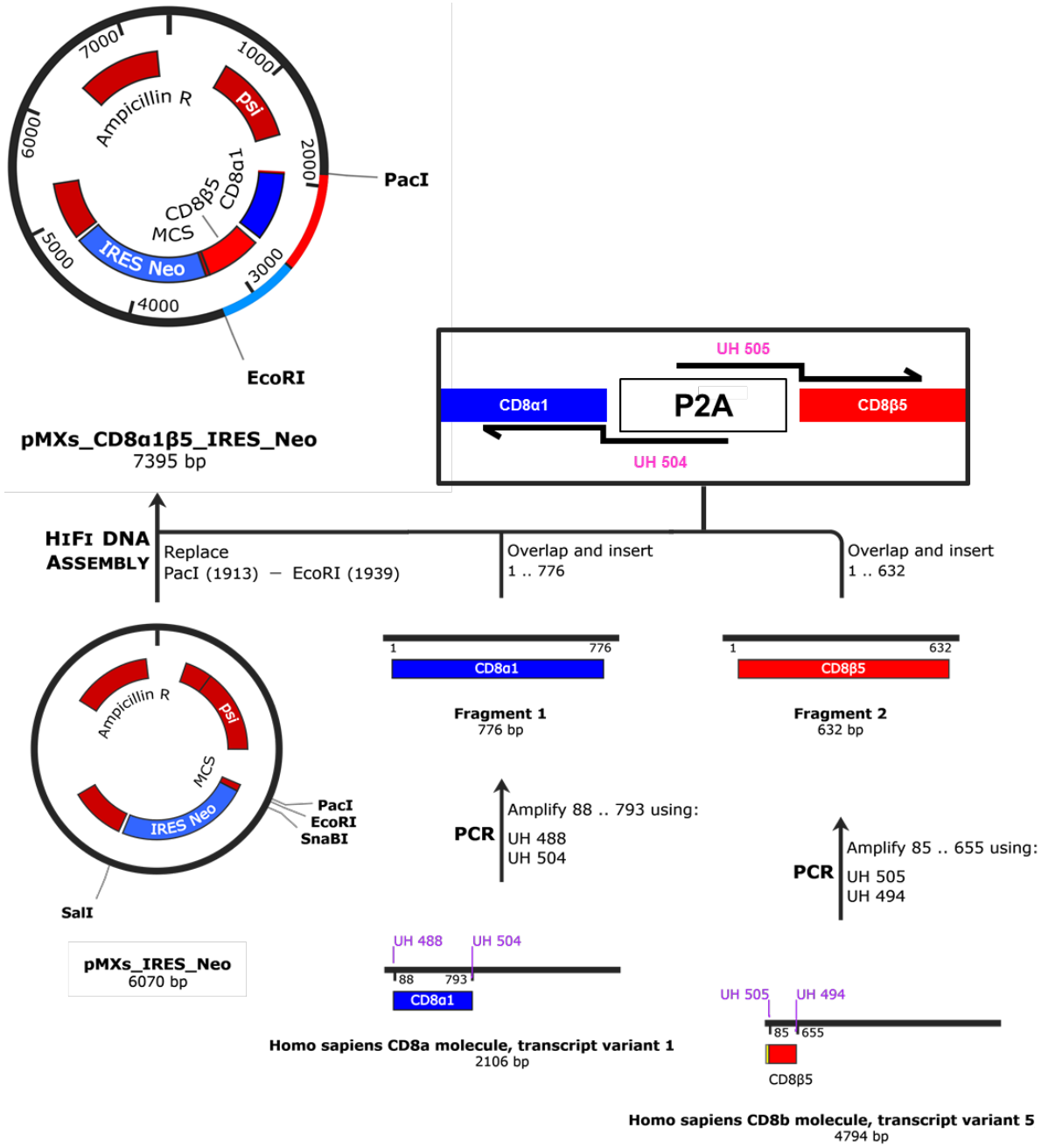

Figure 8.2.3 Cloning strategy for the generation of retroviral expression vectors encoding combinations of human CD8αβ complex isoforms. Exemplarily shown for the CD8α1β5-isoform, transcript variants of the CD8α- and β-chain were isolated from cDNA of cytotoxic T lymphocyte clones (CTL) 5B2 and 25F2, the TCRs 5B2 and 25F2 derived from, via PCR and integrated by NEBuilder® In-Fusion Cloning into the pMXs_IRES_Neo vector backbone for retroviral gene transfer into NK cells. The non-isoform-specific CD8α-chain reverse (UH 504) and CD8β-chain forward primer (UH 505) contained the P2A ribosomal skipping site sequence as a non-complimentary surplus linking the α- and β-chains via P2A during HiFi DNA assembly. Primers are labeled pink, restriction enzyme cutting sites are depicted in black.

As depicted in Fig. 8.2.3, cloning was conducted as In-Fusion cloning according to the manufacturer´s instructions of NEBuilder®. Thus, seamless ligation of the CD8α- and –β-chains linked via a P2A ribosomal skipping motif was enabled.

Firstly, PCR was performed in order to amplify the CD8α- and –β transcript variants expressed by CTLs 5B2 and 25F2. As a result, TV 1 and 2 of the α-chain as well as TV 1, 3 and 5 of the β-chain could be obtained.

Due to special primer design of the α-chain reverse (UH 504) and universal β-chain forward (UH 505) oligonucleotides, the CD8 sequences were elongated with parts of the DNA sequence of the ribosomal skipping site P2A (Fig. 8.2.3, box in the upper right), equipped with a “GSG-linker” at its 5´ end for enhanced “cutting” efficiency.

Secondly, the newly generated retroviral expression vector pMXs_IRES_Neo was linearized by incubation with the restriction digestion enzymes PacI and Eco RI. Successful processing of the pMXs_IRES_Neo backbone was confirmed by agarose gel electrophoresis.

Then NEBuilder HiFi-DNA-Assembly was performed according to manufacturer´s instructions resulting in seamless ligation of the CD8α-chain linked via the P2A self-cleaving peptide to downstream CD8β. The products of the DNA-assembly were transformed into Stbl3™ chemically competent E. coli bacteria and positive colonies were selected by colony PCR. Sanger sequencing was conducted from midipreps of positively tested colonies revealing the obtained CD8αβ isoform-combinations as depicted in Fig. 8.2.4.

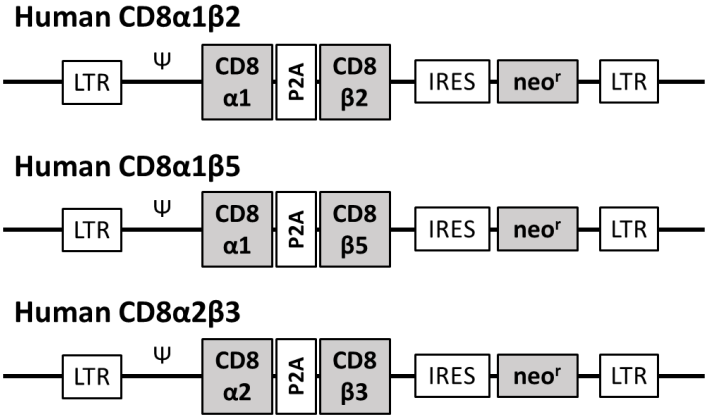

Figure 8.2.4 Retroviral expression vectors encoding different isoforms of the human CD8 complex. The combinations of the transcript variants 1 and 2 of the CD8 α chain and 2, 3, 5 of the CD8 β chain depicted, were linked via a P2A ribosomal skipping site and cloned into the pMXs_IRES_Neo vector backbone for retroviral gene transfer into NK cells. All vectors confer antibiotic resistances for ampicillin and neomycin (neo^r). LTR = retroviral long terminal repeat promoter; ψ = retroviral psi packaging element; IRES = internal ribosomal entry site

8.2.4 Sequencing analysis of CD8αβ transfer vectors.

The sequencing analysis of the resulting CD8αβ expression vectors was not only performed in order to identify the isolated transcript variants, but also to examine the integrity of the

amplified sequences. Therefore, the sequencing results of each transfer vector (Fig. 8.2.4) were aligned to the corresponding published DNA.

As depicted in Fig. 8.2.5, alignment analysis of the transcript variant 1 of CD8α, which is expressed by pMXs_CD8α1β2_IRES_Neo and pMXs_CD8α1β5_IRES_Neo, revealed a single base exchange at location 2487 bp (in both constructs) from thymine to cytosine (highlighted in red). This discrepancy from the original CD8α1 sequence resulted neither in an amino acid exchange nor in a stop codon and therefore represented a silent mutation which did not affect the integrity of the translated protein.

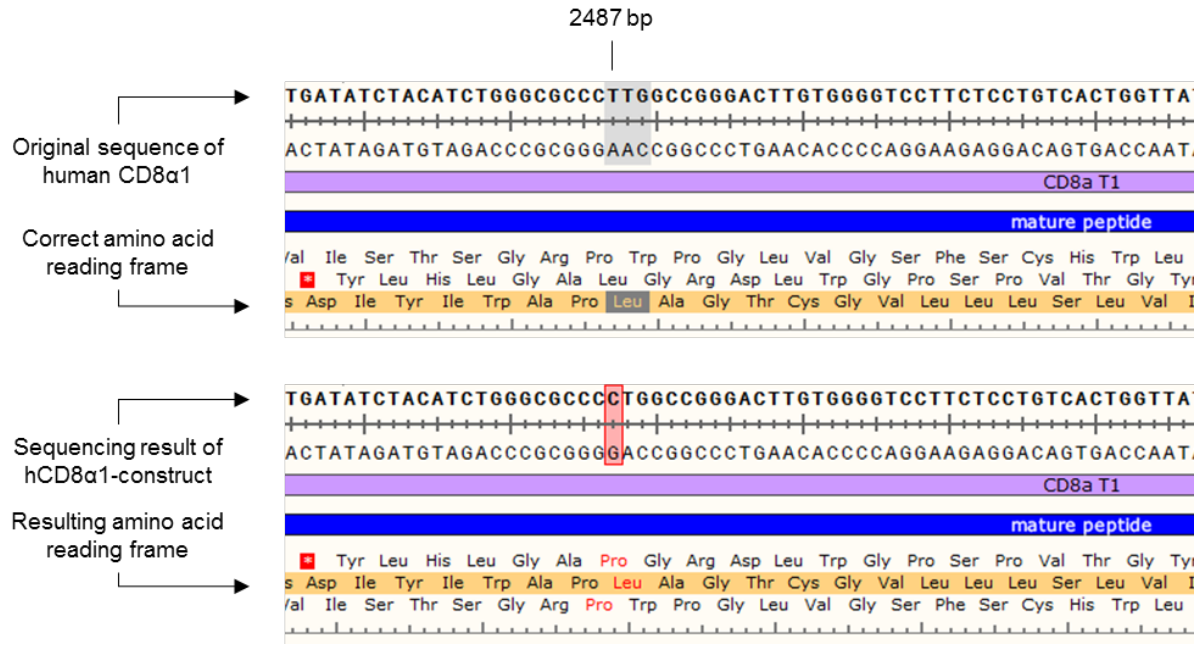

Figure 8.2.5 Sequencing result of CD8α transcript variant 1. Alignment of the original DNA-sequence of human CD8 α transcript variant 1 (top row) with the Sanger-sequencing result of the hCD8α1 insert (bottom row) contained in the pMXs_CD8α1β2_IRES_Neo and pMXs_CD8α1β5_IRES_Neo expression vectors. The discrepancy of the DNA-sequences is highlighted by a red box within the sequencing result. The translation reading frame encoding the human CD8 α-chain is marked in yellow. Amino acids affected by point mutations are dyed red in the depicted translation reading frames of the sequencing result DNA. The graphic was created with SnapGene®.

Furthermore, two mismatches could be detected between the original sequence of the CD8β transcript variant 2 and its counterpart contained in the pMXs_CD8α1β2_IRES_Neo (Fig. 8.2.6). Firstly, at location 3168 bp of the CD8α1β2 expression vector the nucleotide base guanine was changed to adenine (highlighted in red) resulting in a switch of amino acids from valine to isoleucine within the corresponding reading frame. Secondly, a single base exchange occurred at 3267 bp. There, the nucleotide base adenine of the original sequence was swapped to guanine leading to a change in amino acids from isoleucine to valine, coincidentally vice versa to the first point mutation.

Presumably, these reported changes in the amino acid sequence of the CD8β2 isoform expressed by the pMXs_CD8α1β2_IRES_Neo vector had little to no effect on the protein function as the amino acid substitutes were, consistent to the original, nonpolar. Therefore, no functional groups were additionally integrated into the CD8β2 protein that could have affected its tertiary or quaternary structure resulting in possible altered functional performance. Only the steric difference between valine and isoleucine could potentially have had an impact on protein function.

Sequencing analysis of TV 2 of the α-chain and TV 3 and 5 of the β-chain did not result in any discrepancies from the corresponding original sequences.

Figure 8.2.6 Sequencing result of CD8β transcript variant 2. Alignment of the original DNA-sequence of the human CD8 β transcript variant 2 (top row) with the Sanger-sequencing result of the hCD8β2 insert (bottom row) contained in the pMXs_CD8α1β2_IRES_Neo expression vector. Discrepancies of the DNA-sequences are highlighted by a red box within the sequencing result. The translation reading frame encoding the human CD8 β-chain is marked in yellow. Amino acids affected by point mutations are dyed red in the depicted translation reading frames of the sequencing result DNA. The graphic was created with SnapGene®.

8.3 Expression of tumor-reactive TCR-CD3 complexes together with the human CD8 coreceptor in NK92 cells.

8.3.1 Retroviral expression vectors for the formation of TCR-CD3 complexes in NK cells.

The polycistronic human CD3 complex expression vector (Fig. 8.3.1) was generated via Gateway® cloning by Dr. C. Wölfel based on the model published by Szymzcak, A. L. et al. in 2004. (176) Thereby, the DNA sequences of the γ-, δ-, ε- and ζ-chain of the human CD3 complex were connected by various 2A ribosomal skipping motives and inserted into the retroviral pMXs_IRES_Puro expression. NK92 cells already stably expressing the human CD3 complex upon retroviral transduction and puromycin enrichment were kindly obtained from Dr. C. Wölfel.

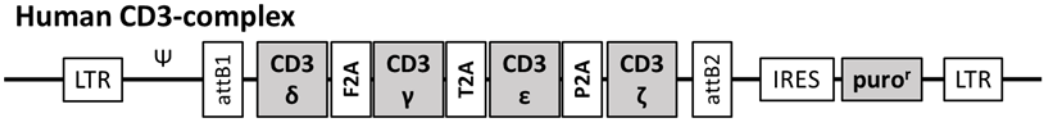

Figure 8.3.1 Retroviral expression vector encoding the human CD3 complex. DNA sequences of the γ-, δ-, ε- and ζ-chain of the human CD3 complex were linked by different 2A self-cleaving peptides and cloned into a pMXs_IRES_Puro vector backbone for retroviral gene transfer into NK cells. The vector confers antibiotic resistances for ampicillin and puromycin (puro^r). LTR = retroviral long terminal repeat promoter; ψ = retroviral psi packaging element; IRES = internal ribosomal entry site; attB1 = recombination site for Gateway® cloning

Likewise, In-house manufactured therapeutic T cell receptors (TCRs) were all cloned into retroviral pMXs expression vectors encoding resistances for puromycin (5H11-, 5B2- and 25F2-TCR) or neomycin (MDM2-TCR), illustrated in Fig. 8.3.2. While the MDM2-TCR was kindly provided by Dr. H. Echchannaoui and previously shown to recognize CD8 coreceptor-dependently the epitope$_{81\text{-}88}$ of the human mouse double minute homolog E3 ubiquitin-protein ligase (MDM2) in the context of HLA-A*02:01, the residual TCRs were established by Dr. J. Albrecht and Dr. A. Bhatti, both members of the Hartwig laboratory. Therefore, the TCRs 5H11 (Vβ8), 25F2 (Vβ8) and 5B2 (Vβ21.3) were isolated from AML-specific cytotoxic CD8$^+$ CTL clones by PCR cloning. Preliminary experiments revealed that the clones 5B2 and 25F2 recognized patient-derived AML blasts while CTL 5H11 exerted reactivity to both AML and EBV-transformed B cells (B-LCL) from the same patient but not to fibroblasts. These data suggested that the 5H11-TCR might recognize a hematopoiesis-specific minor-histocompatibility antigen whereas the TCRs 5B2 and 25F2 presumably recognize AML-associated or AML-specific antigens. HLA-restriction of the AML-reactive TCRs could be revealed by comparative analysis of targets recognized by each receptor. Thus, 5B2-TCR responds to an antigen presented in the context of HLA-Cw*07:01. The TCR 25F2 is restricted

to HLA-B*58:01 and 5H11-TCR recognizes antigens, when they are presented by either HLA-B*57:01 or HLA-Cw*06:02. The TCRs 5H11 and 5B2 are described in further detail by Distler et al. (160) The identification of the TCRs´ epitopes recognized is outsourced and to date still in progress.

Post sequence isolation, all TCRs underwent codon optimization and synthetic exchange of the TCRs` α- and β-chain human to murine constant regions, except for the MDM2-TCR as it already is of murine origin recognizing human $MDM2_{81-88}$ and HLA A2.01. Murinization of the TCRs was traditionally performed to avoid mispairing between transgenic and endogenous TCR in T lymphocyte based adoptive cellular therapy (ACT). Since NK cells do not possess an endogenous T cell receptor, TCR-mispairing is very unlikely and therefore does not need to be prevented by murinization. However, in order to ensure comparability of the generated NK92 effector cells to state-of-the-art ACT of T cells redirected with therapeutical TCRs, all common optimization processes were conducted even though they might not be absolutely necessary for the specific purpose of NK cell redirection.

In accordance with the CD3 and CD8 constructs, the α- and β-chain of the TCRs were linked by P2A self-cleaving peptides. The orientation of the two protein chains of the 5H11-TCR differed compared to the TCRs 5B2 and 25F2 as its β-chain is located upstream of α.

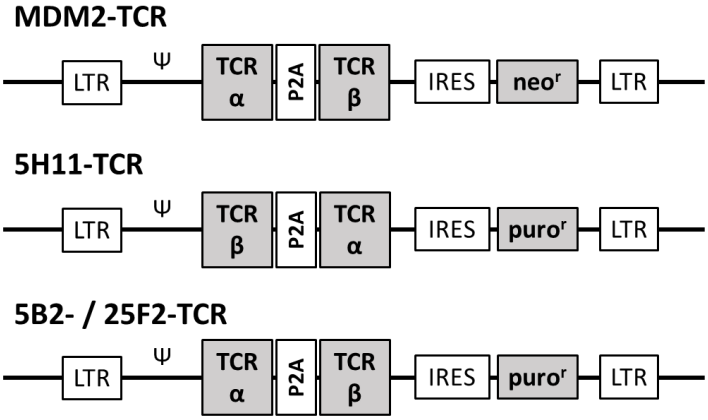

Figure 8.3.2 Retroviral expression vectors encoding therapeutic T cell receptors. Codon optimized and constant domain murinized TCR α- and β-chains were linked by the P2A ribosomal skipping site and cloned into pMXs_IRES_Puro (5H11-, 5B2- and 25F2-TCR) or pMXs_IRES_Neo (MDM2-TCR) vector backbones for genetic modification of NK cells. Besides resistances for puromycin ($puro^r$) or neomycin (neo^r) all vectors confer antibiotic resistance for ampicillin. LTR = retroviral long terminal repeat promoter; ψ = retroviral psi packaging element; IRES = internal ribosomal entry site

8.3.2 Three-step genetic engineering of NK92 cells to express TCR-CD3 complexes together with the CD8 coreceptor.

In order to establish an operable TCR complex on the surface of NK92, a polycistronic expression vector (Fig. 8.3.1) encoding the δ-, γ-, ε- and ζ-subunits of the human CD3 complex (hCD3) linked via 2A-self-cleaving motives was introduced into the Natural Killer cell line by retroviral transduction (NK92 CD3). Extracellular expression of hCD3, however, could not be detected by an anti-CD3ε-antibody (Fig. 8.3.3b) as translocation of hCD3 and TCR to the cell membrane only occurs codependently when the TCR-CD3 complex is formed. Subsequently, three AML-reactive TCRs that originally derived from the AML-specific $CD8^+$ CTL clones 5H11, 25F2 and 5B2 (Fig. 8.3.2), as well as a human leukocyte antigen (HLA)-A*02:01 dependent TCR recognizing the amino acids 81-88 of the human MDM2 protein were brought to expression resulting in NK92 TCR CD3 cells.

Upon successful isolation of the CD8α- and -β-chains expressed by the 5B2- and 25F2-TCR-donating CTLs and cloning of three different combinations of bicistronic αβ-CD8-heterodimer expression vectors (Fig. 8.2.5), NK92 TCR CD3 cells were superinfected resulting in NK92 TCR CD3 CD8. Both, NK92 TCR CD3 and NK92 TCR CD3 CD8, are referred to as NK92 TCR collectively. For every TCR, three different NK92 subsets were generated each expressing a different combination of CD8αβ-chains, namely CD8α1β2, CD8α1β5 and CD8α2β3.

All steps of gene transfer (Fig. 8.3.2) were performed by retroviral transduction of pMXs expression vectors. Enrichment of successfully genetically modified NK92 cells was achieved for CD3 by puromycin and CD8 by neomycin selection. The populations of NK cells expressing a TCR, however, were purified by MACS® for cells extracellularly expressing the human CD3 complex, as the antibiotic resistance conferred either by the CD3 (for 5H11-, 5B2- and 25F2-TCR) or CD8 expression vector (for MDM2-TCR) equaled the ones of the TCR transfer vectors. The indirect enrichment of TCR positive NK92 cells via anti-CD3 MACS® was only possible, because only in the presence of a TCR, CD3 is expressed on the cell surface.

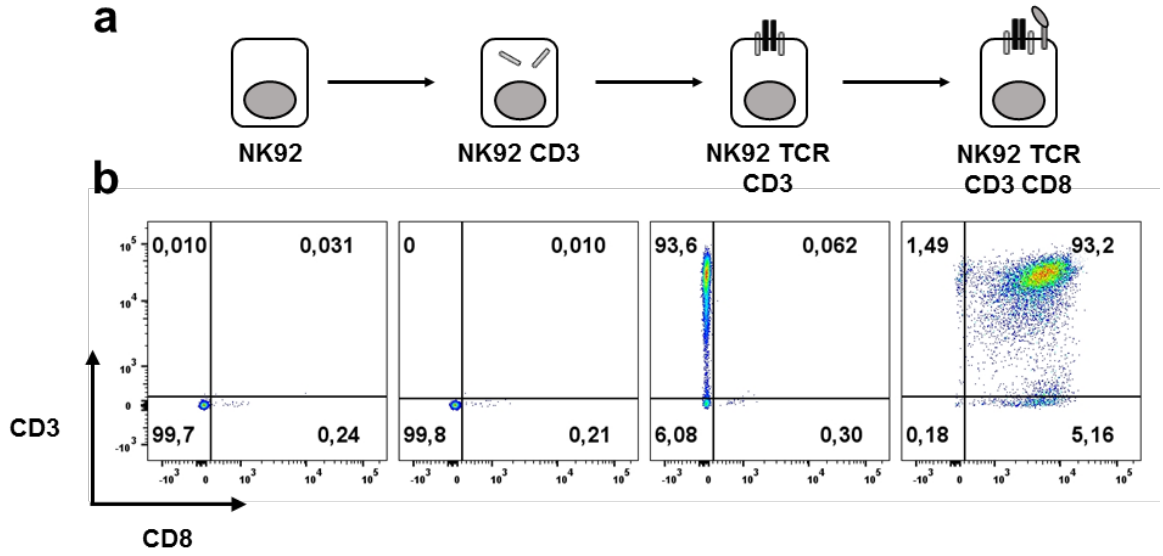

Figure 8.3.3 Generation of NK92 expressing a functional TCR-CD3 complex and human CD8. (**a**) Scheme of three-step genetic engineering process of wildtype NK92. Firstly, NK92 cells were transduced with the δ-, γ-, ε- and ζ-subunits of the human CD3 complex (hCD3). Following puromycin selection, NK92 CD3 were cotransfected with a therapeutic TCR and enriched via MACS® for extracellular CD3 expression. Finally NK92 TCR CD3 cells were superinfected with different isoforms of the human CD8 complex and enriched by neomycin selection. (**b**) Representative FACS-results of the generation process of NK92 5B2-TCR CD3 CD8α1β5. Presented dot plots were gated for living cell population on FSC/SSC. The frequencies depicted refer to said population. The human CD3 complex was not detectable by extracellular FACS-staining, when expressed solely, as translocation to the cell membrane only occurs as CD3-TCR complex in the context of TCR expression. Thus TCR expression correlates to extracellular CD3 detection. Therefore, depicting staining results for the TCR was waived due to clarity of display. For detailed TCR expression analysis see Fig. 8.3.4. Graphic generated with FlowJo®.

Upon antibiotic selection and MACS® sorting, TCR- and CD3-expression of NK92 TCR exceeded 85% for every transgenic TCR (Fig. 8.3.4). In addition, populations greater than 82% of TCR- and CD8-double positive NK92 TCR CD3 CD8 could be obtained for all TCRs as exemplified by CD8α1β2 transduced cells (Fig. 8.3.4) while the expression rates of the CD8α1β5-construct surpassed the ones depicted. Expression of the CD8α2β3-heterodimer, however, could not be determined, as all commercially available FACS-antibodies detecting CD8 recognize the CD8α1-isoform only. Therefore, for subsequent experiments it was hypothesized that a comparable expression rate of CD8α2β3 to the other transgenic coreceptor heterodimers was obtained, due to the fact that neomycin selection occurred analog for all CD8-isoform combinations and equaled between CD8α1β2 and –α1β5.

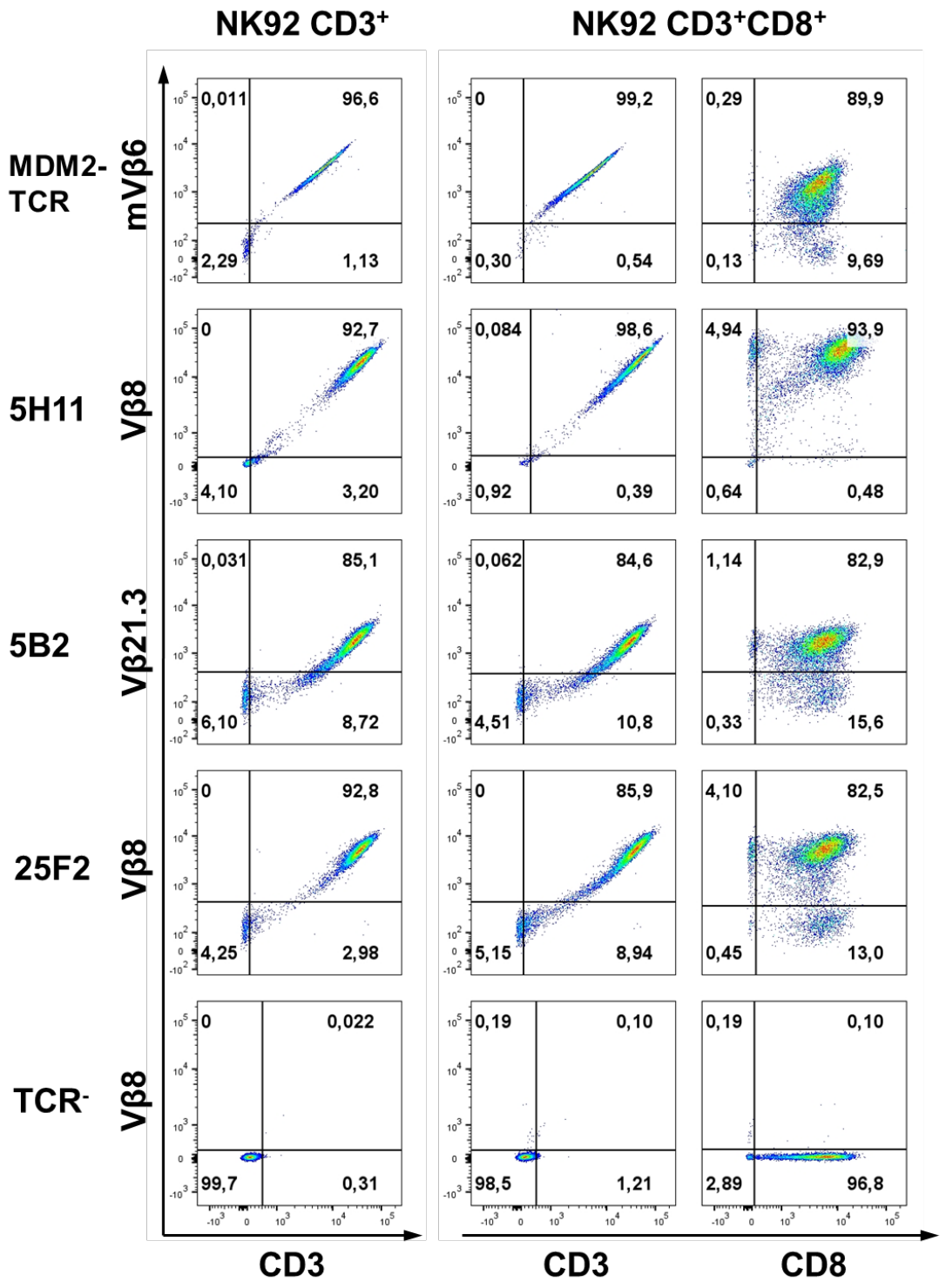

Figure 8.3.4 TCR complex and CD8 expression of genetically modified NK92 cells. Representative FACS-results of at least three independent experiments per cell line are depicted as dot-plots after FSC/SSC-gating for living cells. Extracellular expression of antigens was determined by flow cytometric analysis after staining with the following monoclonal antibodies (mAb): anti CD3-APC, anti CD8-PE or -Pacific Blue, anti TCR Vβ8-PE or -FITC, anti TCR Vβ21.3-FITC, anti-murine Vβ6-PE. The left column represents NK92 cells transduced with hCD3 and a therapeutic TCR, but without hCD8. TCR/CD3 double positive cells appear in the right upper quadrant. Columns in the middle and on the right illustrate FACS-results of NK92 expressing hCD3, a therapeutic TCR and hCD8. TCR/CD3 double positive cells of this population are depicted in the right upper quadrant of the middle and TCR/CD8 double positive cells in the right upper quadrant of the right column. As comparable frequencies of TCR/CD8 double positive cells could be obtained for the CD8α1β2 and CD8α1β5-isoforms, representative expression results of only one CD8αβ-isoform were illustrated for every NK92 TCR subset, due to clarity of display. The graphic was created with FlowJo®.

8.4 Genetically modified NK92 cells exert antitumoral activity.

Following the establishment of NK92 TCR cell lines different in vitro assays analyzing immune cell-effector functions, such as cytokine degranulation and cytotoxicity were performed to address the following questions: Do NK92 cells co-expressing a TCR-CD3 complex and CD8 mediate TCR-specific antitumoral effects? Does the superinfected human CD8-complex affect NK92 TCR effector functions?

8.4.1 Cytotoxicity and cytokine degranulation of AML-reactive TCR-redirected NK92 cells.

NK92 cells redirected with the AML-specific TCRs 5H11, 5B2 and 25F2, (see chapter 6.5.2.1), were comprehensively analyzed for cytokine release and cytolytic activity upon encounter with respective antigen expressing targets upon genetic modification.

8.4.1.1 5H11-TCR

NK92 5H11-TCR mediated killing was determined in a bioluminescence-based cytotoxicity assay. Therefore, the HLA-matched, EBV-immortalized B-LCL of patient MZ 580 (EBV-B 580) was transduced to stably express Firefly luciferase (FLuc) serving as an intracellular ATP-dependent reporter for cell death. In short, within vital cells, ATP is continuously generated and therefore present as a substrate for the reaction with transgenic Firefly luciferase resulting in bioluminescence upon addition of luciferin to cell culture. In the course of cell lysis, ATP-regeneration is abrogated leading to a reduction of FLuc mediated luminescence signal.

5H11-TCR-specific cytotoxicity of NK92 TCR was evaluated after 18 hours of coculture with EBV-B 580. Thereby, the effect of CD8-coexpression was examined comparing NK92 5H11-TCR CD3 CD8α1β5 with NK92 5H11-TCR CD3 (Fig. 8.4.1a). NK92 cells transduced with the 25F2-TCR and CD8α1β5 served as a specificity control. The implementation of a CD8-negative specificity control was not necessary as NK92 cell reactivity was never observed to be reduced due to CD8 expression. NK92 only expressing hCD3 were used as a control for inherent NK cell activity, which never exceeded 10% of target cell lysis. Therefore, cytotoxicity was calculated in relation to NK92 CD3-killing as (TCR)-specific lysis as described in chapter 7.2.2.10, in order to depict TCR-redirection related effects in greater detail.

As a result, NK92 5H11-TCR never exceeded 43% of TCR-specific killing in the absence of CD8α1β5-coexpression. However, upon superinfection with CD8, cytotoxicity of NK92 5H11-TCR CD3 CD8α1β5 was increased significantly and with a residual lysis of about 90% at an E:T of 0,625:1 remarkable robust to low effector to target ratios (Fig. 8.4.1a). NK92 25F2-TCR

did not elicit any noticeable cytotoxicity upon coculture with HLA-mismatched EBV-B 580 strongly suggesting that the observed killing of NK92 TCR was 5H11-TCR-specific.

In addition, IFN-γ release of NK92 5H11-TCR was determined upon 22 hours of coincubation with HLA-matched EBV-B 580 using an IFN-γ ELISpot assay. HLA-mismatched EBV-immortalized BLCL derived from patient MZ 667 (EBV-B 667) served as a specificity control. Effects of genetic modification on inherent NK cell-reactivity of NK92 TCR subsets were examined by coculture with K562.

As illustrated in Fig. 8.4.1b, appropriate IFN-γ-release upon incubation with HLA-matched EBV-B 580 could only be detected for NK92 5H11-TCR co-expressing CD8 (in this case CD8α1β5) while NK cells negative for the CD8 coreceptor secreted marginal cytokine amounts. Therefore, CD8-superinfection resulted in a significant increase in IFN-γ degranulation of 5H11-TCR redirected NK92 upon TCR-stimulation by the HLA-matched target cell line EBV-B 580. As virtually no reactivity of NK92 5H11-TCR against the HLA-mismatched specificity control EBV-B 667 could be observed, IFN-γ release towards EBV-B 580 was classified as 5H11-TCR-specific. Intriguingly, IFN-γ release mediated by inherent NK cell-reactivity was reduced significantly upon coculture with K562, when CD8 was expressed.

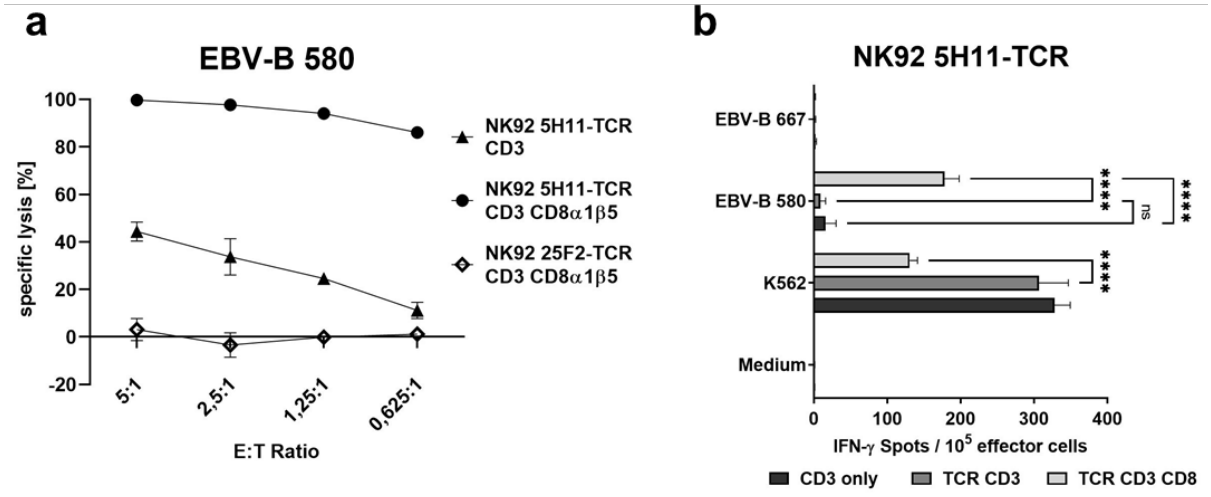

Figure 8.4.1 Antitumoral reactivity of NK92 5H11-TCR. (**a**) Representative result of a bioluminescence (BLI) – based cytotoxicity assay of 5H11-TCR redirected NK92 co-transfected with the human CD3-complex against HLA-matched and EBV-immortalized B cells (EBV-B 580) of patient MZ 580. NK92 5H11-TCR superinfected with the α1β5-isoform of the human CD8-complex were included, in order to examine the effect of additive CD8-expression on the lytic activity of TCR redirected NK92. NK92 25F2-TCR CD3 CD8α1β5 served as specificity control. NK92 CD3 served as control for NK-mediated cytotoxicity and never exceeded 10% of general lysis. Therefore, specific lysis was calculated in relation to NK92 CD3 as described in chapter 7.2.2.10 and is depicted. Error bars represent SD. n = 3. (**b**) IFN-γ release of NK92 5H11-TCR subsets was analyzed following overnight stimulation (22h) with HLA-matched EBV-B 580 via IFN-γ ELISpot assay. EBV-immortalized, HLA-mismatched B cells of patient MZ 667 (EBV-B 667) served as specificity control. Effects of genetic modification on NK-mediated IFN-γ release were analyzed by coculture with K562. Medium resembled effector cells without target cells. CD8 represents the isoform CD8α1β2. n = 2. Columns and error bars depict mean and standard deviation (SD). Statistical analysis was performed as Two-way-ANOVA with Tukey´s multiple comparisons test. (ns = not significant; **** = $p < 0.0001$)

8.4.1.2 5B2- and 25F2-TCR

As the 5B2- and 25F2-TCR both only recognize original AML blasts, they were not available for the BLI-based cytotoxicity assay, due to the fact that AML blasts could not be genetically modified to stably express the FLuc-reporter enzyme. Hence, analysis of effector functions mediated by NK92 5B2-/25F2-TCR was limited to the determination of cytokine release.

Therefore, IFN-γ ELISpot assays were conducted under the same conditions as described for the NK92 5H11-TCR subset (Fig. 8.4.2). In analogy, HLA-matched AML samples from patient MZ 653 (AML653; for 5B2-TCR) and MZ 921 (AML921; for 25F2-TCR) served as target cells. Moreover, HLA-mismatched AML samples from patient MZ 667 (AML667) were utilized as a specificity control in both assays. Again, the NK92 TCR cell lines were cocultured with K562 cells, in order to evaluate the effect of TCR- and CD8-expression on endogenous NK cell-reactivity.

As a result, expression of the 5B2-TCR in NK92 CD3 significantly increased the amount of IFN-γ released when compared to TCR-negative NK cells co-incubated with HLA-matched AML blasts from patient MZ 653 (Fig. 8.4.2a). Co-expression of the CD8 construct, however, did not result in a significant rise of IFN-γ degranulation towards NK92 5B2-TCR cells lacking CD8-coreceptor expression while still exerting superior reactivity compared to NK92 CD3. Furthermore, incubation with K562 resulted in significantly less IFN-γ spots of NK92 genetically modified to express the 5B2-TCR than of NK92 CD3. In contrast to the K562 reactivity-profile of NK92 5H11-TCR, no significant difference in IFN-γ release could be observed between CD8-expressing and coreceptor negative NK92 5B2-TCR cells.

The IFN-γ ELISpot assay depicted in Fig. 8.4.2b, revealed significant increase in IFN-γ release upon 25F2-TCR- and further CD8-coexpression when cocultured with HLA-matched AML921. In analogy to NK92 5H11-TCR, the amount of IFN-γ spots generated by CD8-expressing NK92 25F2-TCR was significantly lower than of NK92 25F2-TCR CD3 upon stimulation with K562. In contrast, IFN-γ secretion mediated by inherent NK cell-reactivity upon recognition of K562 cells used as control, was comparable between NK92 CD3 and NK92 25F2-TCR CD3.

As in both assays for all NK92 subsets only basal IFN-γ release upon stimulation with HLA-mismatched AML blasts of patient MZ 667 (AML667) could be detected, reactivity towards HLA-matched target cells was considered to be TCR-specific.

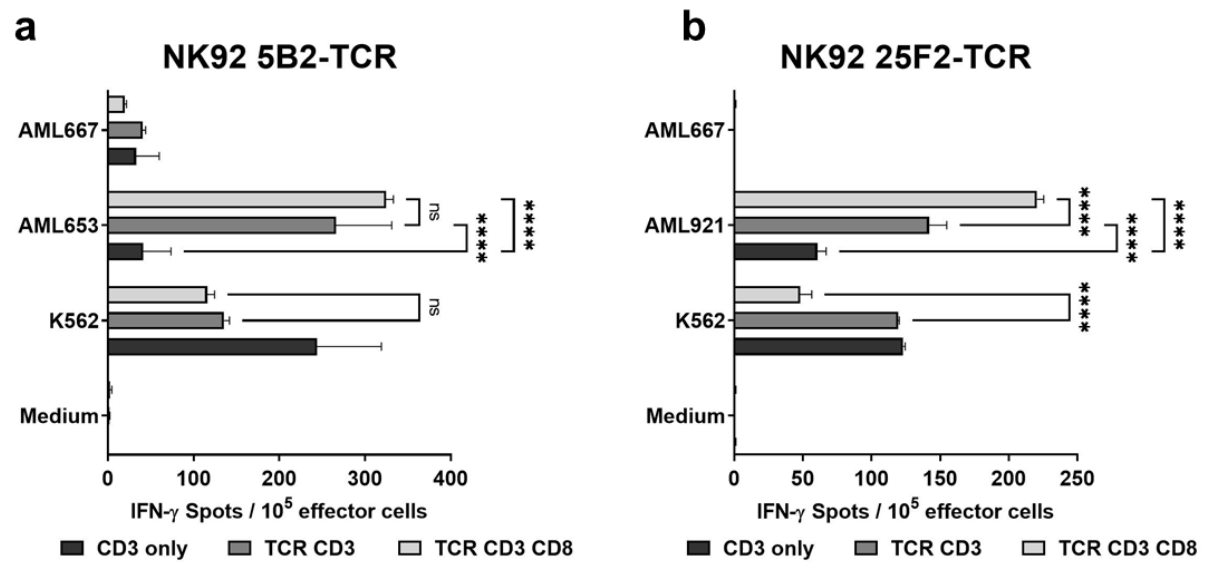

Figure 8.4.2 TCR-specific cytokine degranulation of NK92 TCR upon coculture with primary AML blasts. IFN-γ release was determined in a 22h IFN-γ ELISpot assay. NK92 cells expressing the human CD3 complex (NK92 CD3) were redirected with AML-reactive TCRs 5B2 and 25F2 and superinfected with the CD8α1β2-isoform (±CD8 subsets are both referred to as NK92 5B2/25F2-TCR). NK92 CD3 served as effector- and K562 as target-control for NK-mediated IFN-γ degranulation. "Medium" represented effector cells without target cells. (**a**) NK92 5B2-TCR were cocultured with HLA-matched primary AML blasts of patient MZ 653 (AML653). (**b**) NK92 25F2-TCR were incubated with HLA-matched primary AML-blasts of patient MZ 921 (AML 921). AML 667 served in both assays as HLA-mismatched TCR-specificity control. Both assays were run in duplicates. Columns and error bars represent mean and SD. Statistical analysis was performed as Two-way-ANOVA with Tukey´s multiple comparisons test. (ns = not significant; **** = $p < 0.0001$)

8.4.2 Co-expression of different CD8αβ coreceptor combinations influences cytolytic activity of TCR redirected NK92 CD3$^+$ cells.

In order to determine the efficacy in enhancing TCR-signaling of the different CD8 heterodimers generated, a comparative cytotoxicity assay was performed under the same conditions as described for Fig. 8.4.1a. After the three different subsets of 5H11-TCR redirected NK92 expressing either CD8α1β2, CD8α1β5 or CD8α2β3 were established, the amount of TCR- and CD8-double positive cells was aligned to 70% prior to 18h of coculture with HLA-matched target cells EBV-B 580. (NK92 5H11-TCR CD3 CD8α1β5 used for the assay of Fig. 8.4.1a were 85% double positive for TCR and CD8 expression)

Comparing the different CD8 subsets, 5H11-TCR-specific cytotoxicity was enhanced most efficiently by CD8α1β5 with a lysis rate >70% at E:T 5:1 (Fig. 8.4.3a). The construct CD8α1β2 also supported killing of NK92 TCR, although less effective than CD8α1β5. Interestingly, the combination of 5H11-TCR with the CD8 coreceptor encoding the transcript variant 2 of the α-chain along with the β3-isoform did not result in any noteworthy lysis of target cells. These data suggested that the effector function of CD8-dependent TCR-NK92 might dependent on a particular CD8 / TCR combination to allow for effective signaling upon pMHC binding.

In line with the results described above, IFN-γ degranulation of NK92 5B2-TCR superinfected with the three different CD8αβ-isoforms was determined after 22h of coculture with HLA-matched AML653 (from patient MZ 653) by an IFN-γ ELISpot assay (Fig. 8.4.3b). Interestingly and in contrast to cytotoxicity of NK92 5H11-TCR, IFN-γ release of NK92 5B2-TCR did not vary significantly between the different CD8αβ-heterodimers expressed, when cocultured with HLA-matched AML653 target cells. Furthermore, no noticeable difference in IFN-γ release mediated by inherent NK cell reactivity against K562 target cells could be observed. AML 667 (from patient MZ 667) served as specificity control and confirmed by resulting in almost no IFN-γ spots 5B2-TCR-specific IFN-γ release against the HLA-matched target AML653.

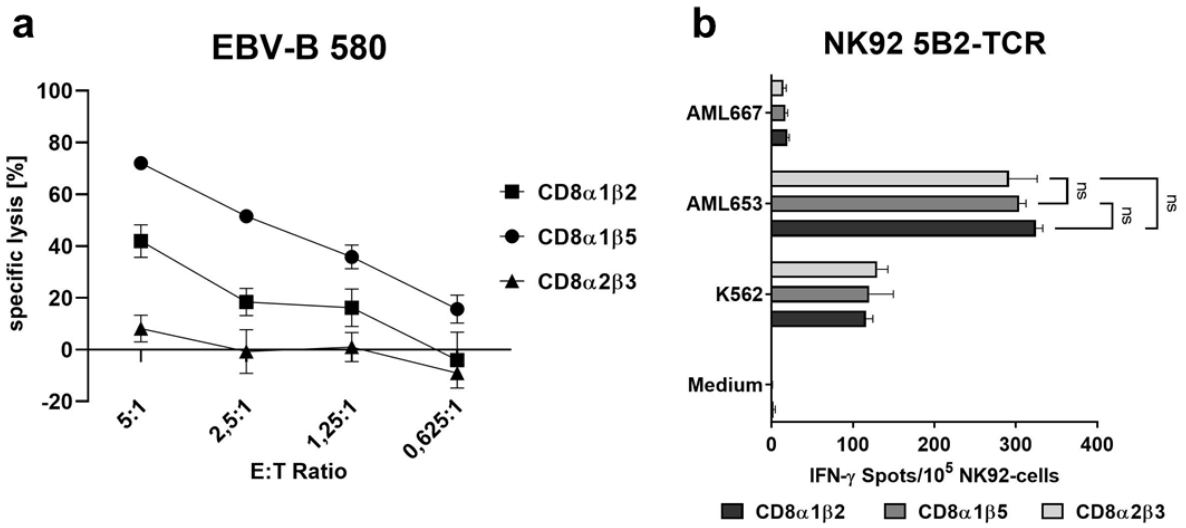

Figure 8.4.3 Functional comparison of different CD8-isoforms. (**a**) Cytotoxicity of 5H11-TCR redirected NK92 CD3, superinfected with different CD8αβ-isoforms, was analyzed upon 18h coculture with HLA-matched, EBV-immortalized B cells from patient MZ 580 (EBV-B 580) at varying effector to target (E:T) ratios via bioluminescence (BLI) – based cytotoxicity assay. Specific lysis was calculated in relation to NK92 CD3 as described in chapter 7.2.2.10. n = 3. Error bars represent SD. (**b**) IFN-γ release of NK92 5B2-TCR expressing different CD8αβ-isoforms following overnight stimulation (22h) with HLA-matched AML 653 (from patient MZ 653) measured by an IFN-γ ELISpot assay. AML 667 (from patient MZ 667) served as specificity control. Effects of genetic modification of NK92 on NK-mediated IFN-γ release were evaluated via K562. Medium corresponds to effector cells without targets. n = 2. Error bars represent SD. Statistical analysis was performed as Two-way-ANOVA with Tukey´s multiple comparisons test. (ns = not significant; * = $p < 0.05$)

8.4.3 MDM-2$^{81-88}$ -specific TCR redirected NK92 cells demonstrate potent antumor reactivity.

As TCR-specific antitumoral effects of NK92 TCR cells could be observed upon transduction of AML-reactive TCRs, the well characterized and highly efficient therapeutic TCR recognizing epitope$_{81-88}$ (amino acids 81-88) of the human homolog of the mouse double minute 2 oncoprotein (MDM2) restricted by HLA-A*02:01 was introduced into NK92 cells, in order to validate prior observations and broaden the spectrum of tumor entities addressed by NK92 TCR-ACT.

In contrast to the 5H11-TCR, not only one but multiple continuously growing target cell lines recognized by the MDM2-TCR were available and thus accessible for stable transgenic FLuc-expression. Therefore, BLI-based cytotoxicity assays were performed under the same conditions as described previously. First, lysis mediated by NK92 MDM2-TCR cells was determined after 18 hours of coculture with FLuc-expressing IM-9 cells (Fig. 8.4.4a). IM-9 resembles a B-lymphoblastoid cell line (B-LCL) established from a patient with Multiple Myeloma which expresses endogenously the human MDM2, an E3 ubiquitin-protein ligase serving as an important negative regulator of the p53 tumor suppressor. NK92 CD3 were used as a reference for NK cell-reactivity. NK92 25F2-TCR CD3 CD8α1β5 served as specificity control. As killing of NK92 CD3 surpassed 10% at an E:T-ratio of 5:1, endogenous NK cell killing played a considerable role and thus cytotoxicity was depicted as general lysis, calculated in reference to luminescence of target cells without effectors as described in chapter 7.2.2.10.

As illustrated in Fig. 8.2.4a, maximum killing of HLA-matched IM-9 target cells occurred, when NK92 MDM2-TCR were superinfected with CD8 (CD8α1β5 for the data depicted). Cytotoxicity of NK92 expressing the MDM2-TCR-CD3-complex alone, was comparable to the NK92 CD3 control and in both cases significantly lower than lysis mediated by the CD8-positive NK92 MDM2-TCR subset. The CD8-dependent killing by NK92 redirected with the MDM2-TCR, observed in this assay, was therefore in line with previous experiments on redirected T cells postulating CD8 coreceptor-dependency of the MDM2-TCR. (169) Moreover, coincubation of NK92 25F2-TCR CD3 CD8 with IM-9 cells resulted in the lowest killing rates detected, suggesting an MDM2-TCR-specific enhancement of target cell lysis. Since the 25F2-TCR transduced NK92 cells, as a specificity control, were, due to an HLA-mismatch, designated not to recognize the IM-9 target cells TCR-specifically, the cytotoxicity detected was attributed to inherent NK cell-reactivity. The fact that general lysis of NK92 25F2-TCR CD3 CD8 undercut cytotoxicity of NK92 CD3, serving as a reference for endogenous NK cell-killing, was in accordance with prior observations of reduced IFN-γ release upon K562-stimulation of NK92 25F2-TCR CD3 CD8 compared to NK92 CD3 (Fig. 8.4.2b). Therefore, the previously revealed reduction of inherent NK cell-reactivity, monitored by IFN-γ degranulation, in the course of 25F2-TCR and CD8 expression could be confirmed at the level of cytotoxicity.

Characterization of the cytotoxicity profile of NK92 MDM2-TCR cells was extended by analysis of lytic activity towards peptide loaded K562 A2 target cells (Fig. 8.4.4b). Thereby, K562 A2 refers to K562 cells genetically modified to express human HLA-A*02:01 for subsequent peptide loading. Prior to coculture, K562 A2 were pulsed with 0,1 µg (equals 0,113 µmol) of MDM2-oligopeptide$_{81\text{-}88}$ or Melan A, as irrelevant peptide, per 1 ml of serum-free medium. The mean of general lysis after 18 hours of incubation at an effector to target ratio of 5:1 was

depicted as columns with error bars representing SD. NK92 expressing the 5H11-TCR served as specificity control, NK92 CD3 as control for endogenous NK cell-lysis.

As a result, both NK92 MDM2-TCR cell lines conveyed highly efficient cytotoxicity of greater than 80% after 18h of coculture against K562 A2 pulsed with the $MDM2_{81-88}$-oligopeptide, independent of CD8-coexpression. Moreover, killing mediated by NK92 MDM2-TCR subsets of target cells loaded with an irrelevant peptide, Melan A, not recognized by the given TCRs was significantly lower when compared to MDM2-triggered lysis. Therefore, the increase of lytic activity from Melan A- to MDM2-pulsed target cells was considered to be MDM2-TCR-specific. In turn, killing of K562 A2 loaded with the Melan A-peptide mediated by the two NK92 MDM2-TCR subsets, was attributed to residual inherent NK cell-reactivity. Cytotoxicity of NK92 CD3 towards K562 A2 was unattached to peptide-loading and with about 50% of general lysis for both targets comparable high. However, this observation was expected as wildtype K562 are prone to NK cell killing, due to the absence of MHC class I-expression. This effect, is partially reversed within the K562 A2 subpopulation as transgenic expression of HLA-A*02:01 reduces the activating stimulus on NK cells originating from the absence of MHC class I. Nevertheless, K562 A2 still remain target cells highly susceptible to NK cell lysis, regardless of HLA-A*02:01 expression, resulting in high inherent NK-cell reactivity.

Just like previously elaborated for the NK92 TCR subsets transduced with the AML-reactive TCRs, inherent NK-reactivity of NK92 cells expressing the MDM2-TCR was reduced as compared to NK92 CD3 as endogenous NK cell-activity of the NK92 MDM2-TCR subsets was represented by their lysis of K562 A2 pulsed with the irrelevant peptide, Melan A. Moreover, NK92 5H11-TCR CD3 CD8 did not exert any noticeable cytotoxicity towards K562 A2, regardless of any peptide loaded, and therefore underlined the MDM2-TCR-specific enhancement of MDM2-pulsed target cell-killing.

To complete the characterization of NK92 MDM2-TCR´s effector functions, TCR-mediated IFN-γ degranulation of the genetically modified NK92 cells was analyzed via an IFN-γ ELISpot assay following 22h of stimulation with peptide-pulsed K562 A2. In analogy to the cytotoxicity-assay (Fig. 8.4.4b), Melan A, representing an irrelevant peptide not recognized by the MDM2-TCR, served as specificity control. TCR-related IFN-γ release was determined by coculture of NK92 effector cell subsets with K562 A2 previously loaded with $MDM2_{81-88}$-oligopeptide. NK92 CD3 indicated cytokine degranulation in the course of inherent NK cell reactivity.

As depicted in Fig. 8.4.4c, stimulation with MDM2-peptide-pulsed K562 A2 target cells resulted in significantly more IFN-γ-spots upon expression of the MDM2-TCR on NK92 cells than compared to TCR-negative NK92 CD3. In addition, NK92 MDM2-TCR effector cells superinfected with the CD8 coreceptor released more IFN-γ than TCR-redirected NK cells lacking coreceptor-expression on a level of significance of $p < 0,05$ thus indicating an

enhancing effect of CD8 on TCR-induced cytokine degranulation. IFN-γ release of all NK92 subsets towards K562 A2 loaded with an irrelevant peptide (Melan A) was merely noticeable and therefore IFN-γ degranulation of NK92 MDM2-TCR induced by the presence of MDM2-peptide was considered as MDM2-TCR-specific. In analogy to the TCRs 5H11 and 25F2, cytokine release upon stimulation with wild type K562 (K562), representing endogenous NK cell reactivity, was significantly reduced for NK92 MDM2-TCR CD3 CD8 compared to CD8-negative NK92 MDM2-TCR effector cells that roughly equaled the reactivity of reference NK92 CD3. Moreover, changes in IFN-γ release of NK92 CD3 attributed to HLA-A*02:01 expression on K562 target could be studied by quantifying IFN-spots by these effector cells upon stimulation with wild type K562 and peptide-pulsed K562 A2. As a result, cytokine degranulation was significantly lower when K562 cells expressed HLA-A*02:01. Expectedly, no noteworthy difference between the peptides loaded could be detected for the K562 A2 subpopulations thus suggesting independence of the observed effect to the peptides presented. Therefore, the reduction of IFN-γ release mediated by NK92 CD3 upon K562 A2-stimulation can be most likely attributed to the inhibiting stimulus of MHC class I on inherent NK cell-reactivity.

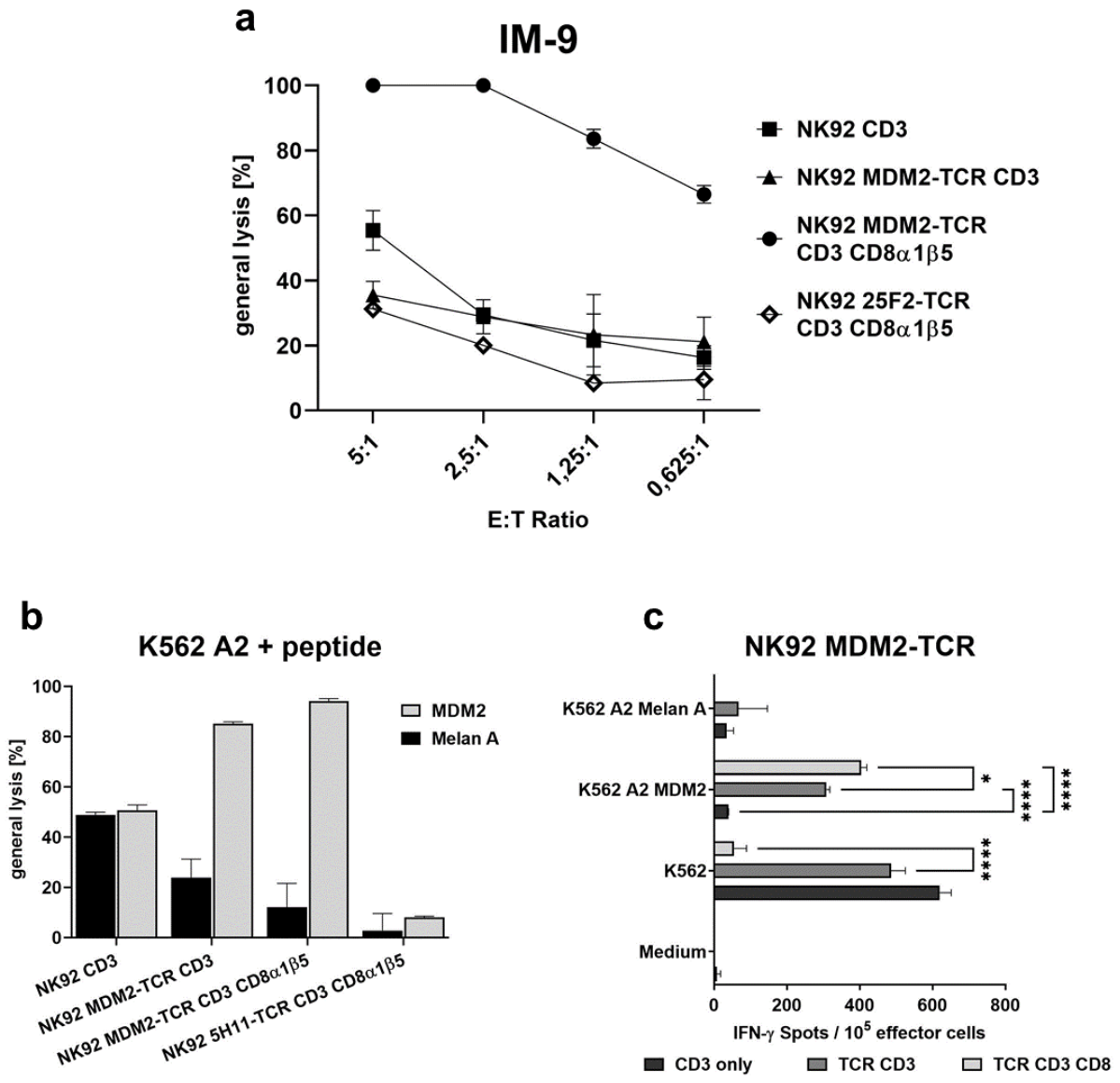

Figure 8.4.4 Antitumoral reactivity of NK92 MDM2-TCR. Cytotoxicity of MDM2-TCR redirected NK92 was analyzed in a BLI-based cytotoxicity assay after 18h of coculture with peptide-loaded, HLA A2 positive K562 and endogenously MDM2-expressing B-LCL IM-9. IFN-γ release was determined after 22h with an ELISpot assay of NK92 MDM2-TCR against peptide loaded K562 A2. (**a**) Representative result of an 18h BLI-based cytotoxicity assay of NK92 expressing the human CD3 complex cotransfected with a therapeutic TCR recognizing the epitope$_{81-88}$ (amino acid 81-88) of the human MDM2 peptide in the context of HLA-A*02:01. To study the effect of CD8-coexpression, NK92 MDM2-TCR were superinfected with the α1β5-isoform of the human CD8 complex. NK92 25F2-TCR CD3 CD8α1β5 served as specificity control. NK92 CD3 were used to study NK-mediated cytotoxicity. (**b**) In analogy to (a) general lysis of peptide loaded K562 A2 was determined after 18h of coculture with NK92 MDM2-TCR at an effector to target ratio of 5:1. Melan A served as a specificity control as it is not recognized by the MDM2-TCR. Therefore, lysis against Melan A loaded K562 A2 can be attributed to inherent natural killer cell cytotoxicity. NK92 5H11-TCR CD3 CD8α1β5 served as effector control. For both assays (a,b) general lysis was calculated as described in 7.2.2.10 with mean of triplicates depicted as graph or columns and error bars representing SD. (**c**) Representative result of NK92 MDM2-TCR mediated IFN-γ release following 22h of coculture with MDM2-peptide loaded K562 stably expressing HLA-A*02:01. CD8 represents the isoform CD8α1β5. Wild type K562 served as control for NK-mediated, TCR-independent, IFN-γ release. K562 A2 loaded with Melan A peptide were used as specificity control. “Medium” represents effector cells without target cells. n = 2. Columns and error bars represent mean and SD. For (b,c) peptide loading was performed with 0,1µg peptide per ml of serum-free medium (5µg in 500µl) and statistical analysis was conducted as Two-way-ANOVA with Tukey´s multiple comparisons test. (ns = not significant; * = $p < 0.05$; **** = $p < 0.0001$)

Due to the fact that cytotoxicity of NK92 MDM2-TCR effector cells towards IM-9 cells was strictly dependent on CD8-coexpression (Fig. 8.4.4a), whereas killing of K562 A2 loaded with MDM2-peptide seemed to be equal between both NK92 MDM2-TCR subsets irrespective of the presence of CD8, it was hypothesized that this observation was related to the abundance of artificial peptide-MHC-complexes (pMHC) present on K562 A2 compared to endogenously expressed MDM2-MHC-complexes on IM-9. Therefore, a BLI-based cytotoxicity assay was conducted determining general lysis of K562 A2 pulsed with MDM2 at various peptide-concentrations mediated by NK92 MDM2-TCR CD3 ±CD8 assuming, that the amount of artificial MDM2-MHC-complexes being present on K562 A2 target cells would be reduced in the course of MDM2-peptide dilution, respectively. Luminescence was measured at several time points throughout coincubation and representative data were depicted in Fig. 8.4.5 referring to an E:T ratio of 5:1 and analysis after 4h of coculture.

As a result, significant reduction of target cell lysis could be detected within the NK92 MDM2-TCR CD3 effector cell subset for 1,25µg and 0,625µg of MDM2-peptide used for loading of K562 A2 compared to the fraction pulsed with 5µg. In contrast, NK92 cells superinfected with the CD8 coreceptor did not show any deterioration in lytic activity. Therefore, the previous hypothesis seemed to be confirmed, so that the MDM2-TCR appeared to be dependent on CD8-coexpression in a physiological antigen-presenting environment for sufficient effector function.

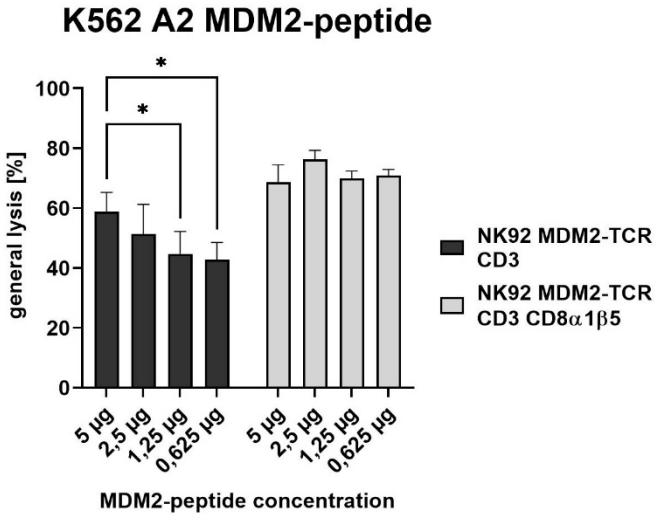

Figure 8.4.5 MDM2-peptide titration. General lysis of NK92 MDM2-TCR ± CD8α1β5 vs. MDM2-peptide loaded K562 A2 determined at various peptide concentrations after 4h of coculture at an E:T-ratio of 5:1 with BLI-based cytotoxicity assay. General lysis was calculated as described in chapter 7.2.2.10. Mean and SD of triplicates are depicted as columns with error bars. Statistical analysis was performed with Two-way-ANOVA and Tukey´s multiple comparisons test. (* = $p < 0.05$)

8.4.4 Comparing the antitumoral efficacy of TCR-redirected NK92 with original CTLs.

Following detailed analysis of effector functions elicited by TCR-redirected and CD8-coexpressing NK92 cells, comparative analyses were conducted, in order to evaluate whether NK92 TCR were able to match the current standard of TCR-based adoptive cellular therapy (ACT) relying on T lymphocytes as effector cells. Therefore, BLI-based cytotoxicity assays were performed under the same conditions as described previously. EBV-B 580 served as target cells for NK92 5H11-TCR CD3 CD8α1β5 and $CD8^+$ T cell clone 5H11 (CTL 5H11), from which the eponymous TCR was originally isolated from at day 58 of specific stimulation. Moreover, IM-9 cells were utilized to compare the killing-capacity of NK92 MDM2-TCR CD3 CD8α1β5 with peripheral blood-derived mononuclear cells (PBMCs) genetically modified to express the MDM2-TCR at day 41 of antigen-specific T cell-stimulation (CTL MDM2-TCR). Since CTL MDM2-TCR resembled, in contrast to CTL 5H11, an inhomogenous cell population, the percentage of cytotoxic T lymphocytes expressing the MDM2-TCR was determined, prior testing, by flow cytometry as previously CD3-positive- and FSC/SSC-gated living cells doublepositive for murine Vβ6 (specific staining of the transgenic TCR) and CD8. As depicted in Fig. 8.4.6c, 69,2% of the CTL MDM2-TCR population resembled cytotoxic T lymphocytes successfully redirected with the therapeutic TCR (illustrated in the upper right quadrant). In comparison, 89,9% of the NK92 MDM2-TCR CD3 CD8α1β5 effector cell population expressed the MDM2-TCR together with CD8 (Fig. 8.3.4). In both cytotoxicity assays NK92 CD3 and CTL 25F2 served as controls for the determination of specific lysis as described in chapter 7.2.2.10. As background luminescence varies between different cell types and media, NK92 TCR were normalized to NK92 CD3 and given CTLs to the $CD8^+$ T cell clone 25F2, neither recognizing EBV-B 580 nor IM-9. Both controls, NK92 CD3 and CTL 25F2, never exceeded 10% of target cell lysis. Therefore, cytotoxicity could be depicted as specific lysis for both assays.

As depicted in Fig. 8.4.6a, the number of EBV-B 580 target cells killed after 18h of incubation was overall comparable between NK92 expressing the 5H11-TCR-CD3-complex together with the CD8 coreceptor and CTL 5H11. In more detail, however, NK92 TCR effector cells were more resilient to low effector to target ratios as their EBV-B 580 cell lysis surpassed T cell killing from E:T 1,25:1 to 0,625:1, increasingly. In addition, specific lysis mediated by NK92 MDM2-TCR was significantly higher than IM-9 killing of CTL MDM2-TCR (Fig. 8.4.6b). Thereby, comparability of cytotoxicity was limited, though, as the NK cell population comprised additional 20% of functional effector cells towards the CTL MDM2-TCR population.

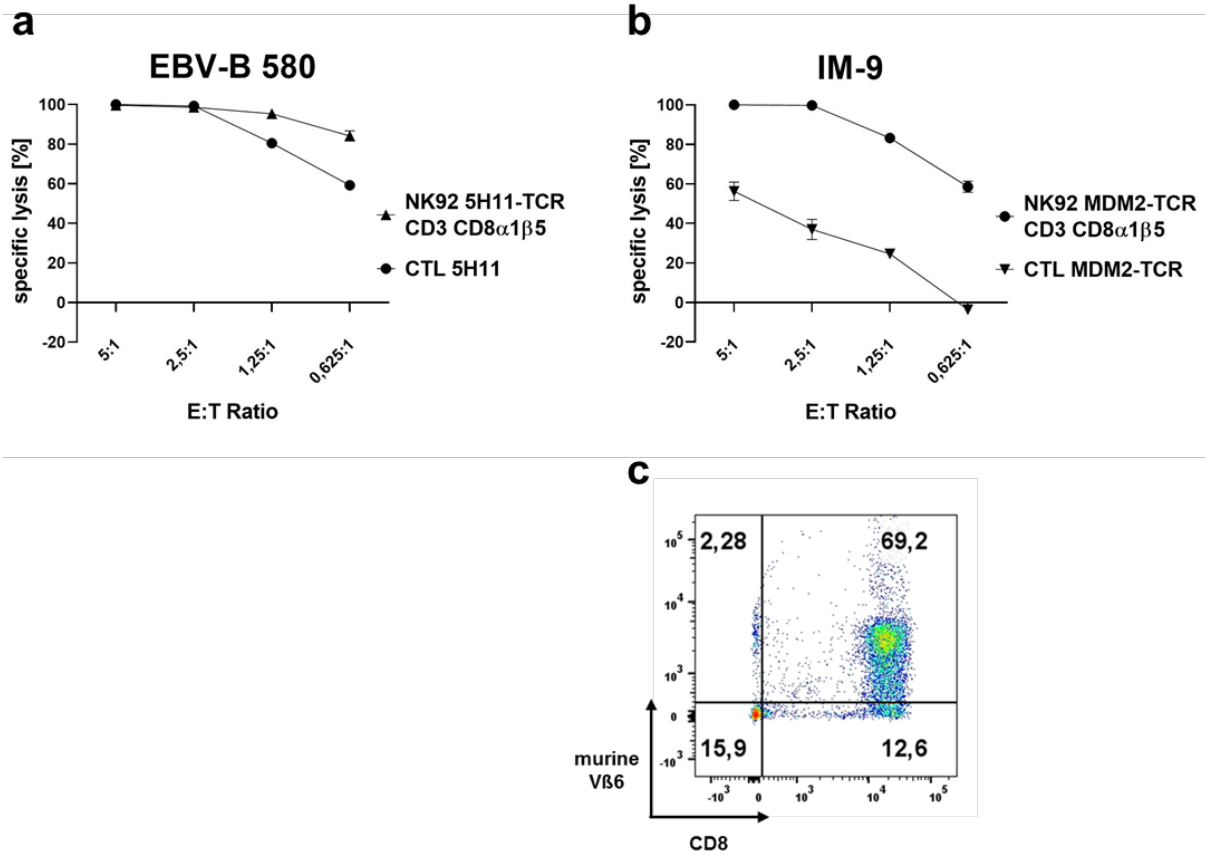

Figure 8.4.6 Comparison of tumor cell lysis between NK92 TCR and corresponding cytotoxic T lymphocytes (CTL). (**a**,**b**) Cytotoxicity of CD8α1β5-isoform expressing NK92 5H11-/MDM2-TCR and corresponding CTLs 5H11/MDM2-TCR against Firefly-Luciferase transduced B-LCLs EBV-B 580 and IM-9 was determined after 18h of coculture in a BLI-based cytotoxicity assay. Specific lysis was calculated as described in chapter 7.2.2.10. Therefore, NK92 CD3 served as reference for NK92 TCRs whereas CTL 25F2 did for effector CTLs, respectively. General lysis of NK92 CD3 and CTL 25F2 never exceeded 10%. Both assays were performed in triplicates and depicted as mean ± SD. "CTL 5H11" represents a clonal population of cytotoxic T cells, the TCR 5H11 was isolated from, at day 58 of stimulation. "CTL MDM2-TCR" were PBMCs transduced with the MDM2-TCR and antigen-specific stimulated at day 41 of culture. (**c**) The percentage of MDM2-TCR expressing cytotoxic T lymphocytes was determined by flow cytometric analysis after staining the CTL MDM2-TCR population with PE-labeled mAb for murine Vβ6 (specific for MDM2-TCR) and APC-labeled mAb for human CD8 at the day of the cytotoxicity assay. Cells positive for the MDM2-TCR and human CD8 appear in the upper right quadrant. The frequencies depicted relate to the totality of living cells of the CTL MDM2-TCR population. Graphic generated with FlowJo®.

8.5 Phenotypic analysis of genetically modified NK92 cells.

During the characterization of NK92 TCR´s effector function, changes of the inherent NK cell-reactivity were observed varying in their extent between different levels of genetic modification and also between the different therapeutic TCRs. Therefore, detailed phenotypical analysis of transgenic NK92 cells regarding relevant NK cell- and potentially expressed immune checkpoint-receptors was conducted following representative analysis of endogenous NK cell-cytotoxicity against wild type K562 cells.

8.5.1 Genetically modified NK cells display changes in their phenotype.

In addition to wild type K562-induced IFN-γ release analyses of NK92 TCR already conducted during effector function evaluation, inherent NK cell-reactivity-mediated lysis of K562 by genetically modified NK92 was determined via a BLI-based cytotoxicity assay under the same conditions as described above. In contrast to previous killing assays, residual luminescence of FLuc-expressing K562 target cells was measured hourly for 5h upon start of coculture enabling analysis of differences within the kinetic of NK92 TCR´s cytolytic activity. Final determination of remaining target cells was performed after 24h. Since differences in the genetic modification-associated change of the IFN-γ degranulation-profile upon K562-stimulation, especially between the CD8-positive effector cells, were observed previously, NK92 TCR cell lines expressing the 5B2- or 5H11-TCRs were chosen as representatives for NK92 cells redirected with both, a CD8-dependent and a coreceptor-independent TCR. Cytotoxicity was depicted as general lysis, due to the fact that killing of wild type K562 could not be attributed to one specific effector cell property, but was mediated by endogenous NK cell-reactivity. Transgenic-TCRs were unable to operate, because of missing MHC class I on target cells.

As depicted in 8.5.1a, all NK92 effector cells were able to kill 100% of K562 target cells within 24 hours of coculture, regardless of prior genetic modification. However, focusing on the 5h killing kinetic, differences in lytic efficiency became apparent. General lysis of NK92 cells redirected with the 5B2-TCR was lower when compared to NK92 CD3, irrespective of CD8-coexpression of the effector cells. Conversely, only NK92 5H11-TCR cells superinfected with the CD8-coreceptor resulted in lower killing-rates whereas CD8-negative NK92 5H11-TCR CD3 and NK92 CD3 mediated comparable high cytotoxicity towards K562. These differences in cytolytic efficiency were in line with the previous observations of TCR-specific changes within the cytokine degranulation profile upon genetic modification.

In order to gain an understanding of the underlying mechanisms responsible for the reduction of inherent NK cell-reactivity upon genetic modification of NK92 cells, expression of activating and inhibiting receptors on NK92 5B2- and 5H11-TCR subsets was determined by flow cytometry and depicted as histograms in relation to corresponding isotype controls in Fig. 8.5.1b. Wild type (wt) NK92 served as a reference for the physiological NK92 phenotype. NK92 expressing a chimeric antigen receptor (CAR) redirected against CD19 (antiCD19-CAR) were included in this study to evaluate differences in expression profile in the course of TCR-transduction and CAR-expression. For detailed information on the antibodies being used see chapter 7.1.13 and the figure description.

As illustrated in Fig. 8.5.1b, no expression of activating NKG2C and CD96 as well as of inhibiting receptors TIM-3, CTLA-4 and PD1 could be detected on wild type NK92 cells and

genetic modification did not result in their upregulation. In contrast, NKG2A, a common antigen presented by NK cells that results in inhibitory signaling upon binding of its ligand HLA-E, was highly expressed by all NK92 cell lines examined. Detailed comparative analyses based on the mean fluorescence intensity (MFI) of the NKG2A-PE-signal detected, which correlates to the amount of antigen expressed on single cell level, revealed no relevant difference in NKG2A being present on most of the NK92 lineages tested. Only for NK92 redirected with the anti-CD19-CAR, discreet upregulation of NKG2A could be observed. TIGIT, another receptor resulting in NK cell inhibition by binding to its ligand CD155, was slightly upregulated within both NK92 5H11-TCR subsets whereas minimal to no expression was detected on the residual NK92 cell subtypes.

MFI-based analysis of activating receptors present on NK92 revealed that solely NKp44, a member of the natural cytotoxicity receptors (NCRs) exclusively expressed on the surface of activated NK cells, was upregulated upon genetic modification. Therefore, TCR-redirection of both TCRs tested resulted in a subtle rise of NKp44 expression independently to CD8-superinfection. However, this effect appeared negligible when compared with the tenfold increase of NKp44 presented on anti-CD19-CAR-transduced NK92 in contrast to the parental wild type cell line. Moreover, comparing the MFI of the NKG2D-APC-signal detected for each lineage revealed, that in wild type NK92 highly expressed NKG2D was downregulated within all genetically modified NK cells. Thus, lowest expression of the activating receptor NKG2D recognizing malignant transformed induced-self proteins of the MIC-family, was observed for the NK92 5B2-TCR CD3 cell line. However, all NK92 cell lines remained considerably positive for NKG2D despite gene transfer-associated downregulation.

As reactivity of NK cells towards K562 is described to be predominantly driven by another member of the NCR family, the activating receptor NKp30 recognizing the B7H6-antigen on tumor cells, relative NKp30-expression was determined for each NK92-TCR subset (Fig. 8.5.1c). Relative expression was calculated by the MFI ratio of genetically modified NK92 cells to wild type NK92 after normalization with isotype controls. Therefore, relative expression (re) of 1,0 represented the amount of NKp30 being present on the surface of NK92 wt. As a result, NKp30-re of NK92 5H11-TCR was only reduced upon superinfection of the CD8-coreceptor. On the contrary, expression of NKp30 was reduced for both subsets of NK92 redirected with the 5B2-TCR, regardless of CD8-coexpression. Interestingly, when NKp30-downregulation occurred, relative expression amounted about 0,5 in each case. These findings were in line with previous observations of changes in NK cell-reactivity towards K562.

In order to examine the impact of the checkpoint molecules tested for NK92 TCR´s effector functions, expression of the corresponding ligands of the regulating receptors was determined on target cells by flow cytometry. FACS-results were depicted as histograms in relation to

appropriate isotype controls. For detailed information of the antibodies used see chapter 7.1.13.

As a result, HLA-E, the ligand to NKG2A and NKG2C, was highly expressed on EBV-B 580, AML653 and AML921 target cells. Low HLA-E-expression could be detected on AML667, whereas AML580 was negative. Moreover, all cell populations screened were negative for CD155 resembling the ligand of the inhibitory receptor TIGIT. CD80 and CD86 both representing the counterpart to CTLA-4 were only expressed by the EBV-B 580 cell line. CD274, also known as PDL-1, could not be detected on any specimen tested.

Taken together, the results of receptors expressed on the effector and their corresponding ligands on target cells, simultaneous presence of a receptor-ligand-couple was only observed for NKG2A and HLA-E.

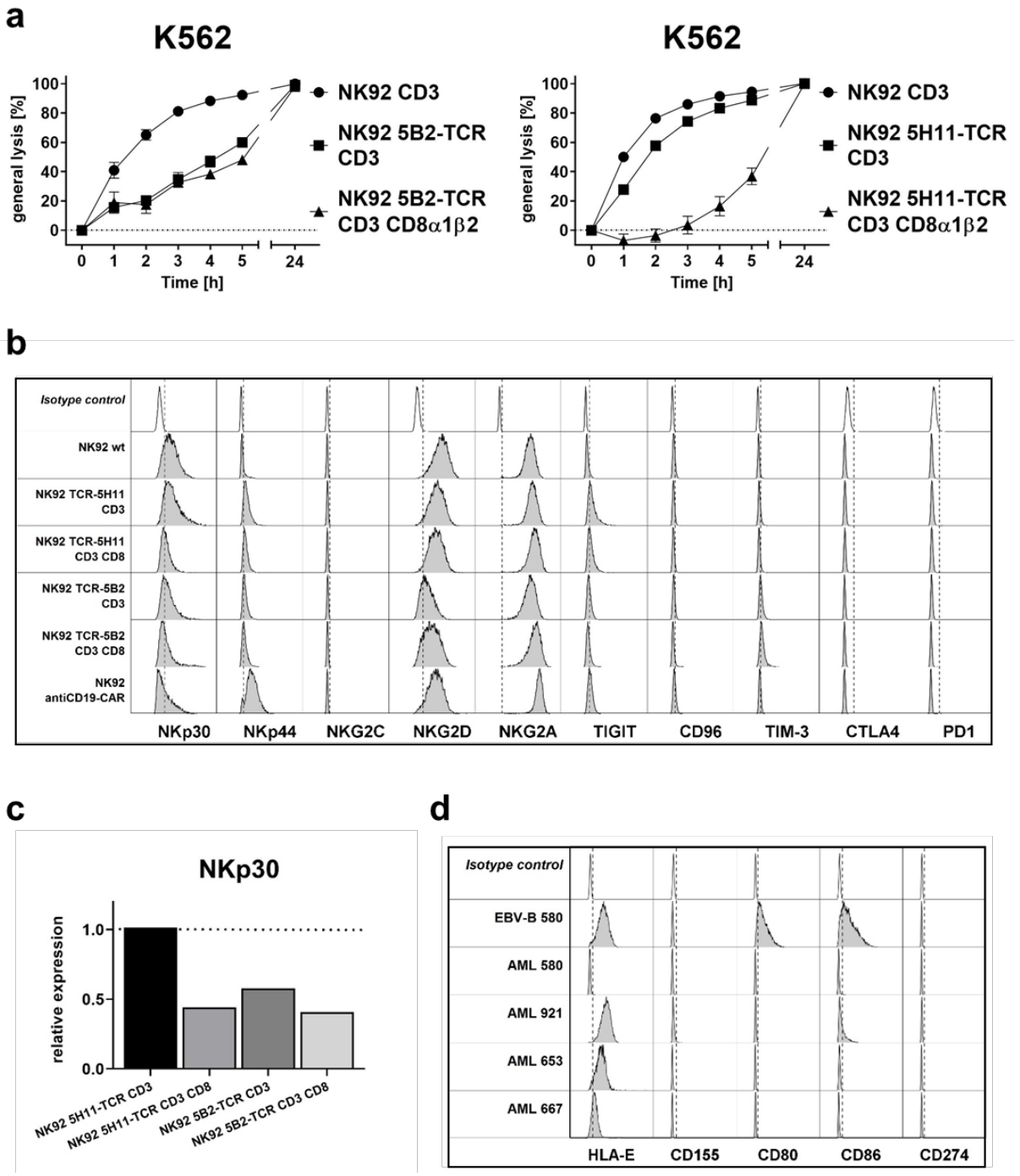

Figure 8.5.1 Effects of genetic modification on NK cell phenotype of NK92 cells. (**a**) Killing kinetic of 5B2- and 5H11-TCR redirected NK92 ± CD8α1β2 against Firefly-Luciferase expressing K562 determined by BLI-based cytotoxicity assay at an E:T ratio of 10:1. Luminescence was measured hourly for 5 hours upon start of coculture and after 24h of incubation. NK92 CD3 served as reference for NK-mediated cytotoxicity. General lysis was calculated as described in chapter 7.2.2.10. Both assays were performed as triplicates and depicted as mean ± SD. (**b**) Histograms of representative FACS-analyses of different NK92 TCR subsets after FSC/SSC-gating for living cells. NK92 cells were stained for various activating and inhibiting receptors in order to examine differences within the endogenous receptor repertoire of NK92 derivatives. The following mAb-conjugates were used to detect expression by flow cytometry: anti NKp30-APC, anti NKp44-PE, anti NKG2C-PE, anti NKG2D-APC, anti NKG2A-PE, anti TIGIT-PE, anti CD96-PE, anti TIM3-PE, anti CTLA-4-APC, anti PD1-APC. Wild type NK92 (NK92 wt) served as reference, NK92 transduced with antiCD19-CAR were analyzed to compare differences in the expression profile between therapeutic redirection agents (TCR vs. CAR). Corresponding isotype controls for every mAB used were performed for every sample and exemplarily shown for NK92 wt. (**c**) Relative NKp30-expression of NK92 5B2/5H11-TCR ± CD8 in relation to NK92 wt. Relative expression was calculated by the MFI ratio of genetically modified NK92 cells to wild type NK92 after normalization with isotype controls. (**d**) Representative flow cytometric expression analysis of a selection of corresponding ligands to the receptors tested in (b) of AML and B-LCL target cells. Histograms represent FSC/SSC gated living cells positive for the antigen labeled. FACS-analysis was

conducted with the following mAbs: anti HLA-E-APC, anti CD155-APC, anti CD80-PE, anti CD86-APC, anti CD274-FITC. Corresponding isotype controls were performed for every sample and exemplarily shown for AML 921. Both graphics (a and c) were generated with FlowJo®.

8.5.2 Impact of checkpoint inhibition on cytokine release of genetically modified NK92 cells.

As expression profiling of NK92 TCR and target cells revealed the concurrent expression of the inhibitory receptor NKG2A on all TCR-redirected NK cells and its corresponding ligand HLA-E on the majority of target cells (EBV-B 580, AML653, AML921), potential supplementary effects of checkpoint inhibition on NK92 TCR effector functions were examined. Therefore, IFN-γ degranulation of 25F2-TCR-redirected and CD8-superinfected NK92 cells was determined via IFN-γ ELISpot following incubation with AML921 target cells previously shown to highly express HLA-E, which were treated with an antibody blocking the HLA-E antigen prior coculture. Untreated AML blasts of patient MZ 921 (AML921) served as a reference for IFN-γ release of unblocked checkpoint interaction. Effects of inhibited NKG2A-HLA-E-interaction on inherent NK cell-reactivity were examined by cytokine degranulation of the NK92 CD3 cell line.

Preventing inhibition of NK92 25F2-TCR CD3 CD8 by blocking NKG2A-HLA-E-interaction did not result in a significant increase in TCR-specific IFN-γ release upon stimulation with AML921 target cells preincubated with blocking-Ab. In addition, no significant effect of checkpoint inhibition on endogenous NK cell-reactivity could be observed.

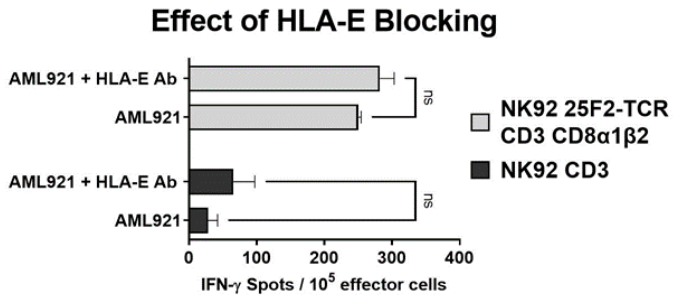

Figure 8.5.2 Effects on IFN-γ release by NK92 TCR upon blocking of inhibitory HLA-E antigen on tumor cells. IFN-γ release of NK92 25F2-TCR CD3 CD8α1β2 was determined via ELISpot assay after 18h of coculture with HLA-matched AML blasts of patient MZ 921 (AML 921). When indicated, AML 921 blasts were incubated with blocking HLA-E mAB at a final concentration of 10µg/ml prior testing. NK92 CD3 served as control for NK-mediated IFN-γ degranulation. n = 2. Columns and error bars represent mean and SD. Statistical analysis was performed with Two-way-ANOVA and Šídák's multiple comparisons test. (ns = not significant)

9 Discussion

With a current 5-year survival rate lower than 30%, AML patients face poor prognosis, despite continuous efforts of improvement. (38, 44) As within the last decades major breakthroughs in cancer-treatment could be achieved due to advances in immunotherapy, especially CAR-T cell-therapy, ACT appears to be a promising approach for more effective AML-treatment. (1, 5, 6) However, due to its characteristically low immunogenicity, the majority of antigens highly expressed on the surface of AML blasts is simultaneously present on healthy stem cells and myeloid progenitors which leads to challenges in designing leukemia-specific CARs not causing severe adverse events, like neutropenia, due to on-target/off-leukemia reactivity. (9) Therefore, TCRs bearing the potential to recognize the AML-mutagenome represent an efficient tool for redirection addressing the LAA-scarcity in AML. (10, 86) Due to the great risk of GvHD, current T cell therapy is mainly limited to autologous transfer, still resulting in significant toxicities throughout treatment. (13, 14, 109-111) Contrarily, ACT-suitability of NK cells for allogeneic transfer with a more favorable side effect-profile has been abundantly proven while exerting comparable effector functions to T cells. Moreover, NK92, the highly tumor-responsive NK cell line, has been approved by the FDA and represents an indefinite source for allogeneic adoptive immunotherapy across HLA-barriers. Thus using NK cell as a cellular source could contribute significantly to reduce costs and eliminate inter-donor variability which both are current limitations for the broad application of CAR-T cell-therapy. (10, 15, 21)

Focusing on the special demands on AML-immunotherapy, the clinical benefits of NK cell therapy and economic efficiency of NK92 combined with the exclusive antigen-recognition-capacity of TCRs represents a promising approach to efficiently combat AML-propagation and improve the poor prognosis of AML-patients. (10, 21) Firstly described by Mensali et al. in 2019, since then, the cell line NK92 has been successfully redirected with TCRs reactive to melanoma and colorectal carcinoma, in the context of transgenic CD3 co-expression, resulting in efficient antitumoral responses *in vivo* and *in vitro*. (10, 21) However, as NK cells and also NK92 do not endogenously express the TCR-coreceptors CD4 or CD8, the TCR-mediated reactivity of the effector cells observed in these studies was coreceptor-independent. In fact, the TCRs applied in this new approach in ACT were specifically chosen by their CD4/CD8-independent properties representing a limitation in applicability of this newly established cellular platform for new therapeutic TCRs.

Intending to generate efficient ACT against AML, in line with the studies mentioned previously, we genetically modified the NK92 cell line to express the γ-, δ-, ε-, ζ-subunits of the human CD3 complex. Next, we redirected the newly established NK92 CD3 cell line with three lab-manufactured TCRs (for more information see chapter 9.5.2) deriving from CTL clones 25F2,

5B2 and 5H11 previously shown to target primary AML blasts with high efficacy. (160) Furthermore, we studied function of a well characterized and CD8-coreceptor dependent TCR, reactive against the oncoprotein MDM2 shown to be expressed by multiple tumor entities covering hematological to solid malignancies. (164, 169) Finally, we generated CD8 expression vectors from cDNA of the original AML-reactive CTL clones and successfully superinfected the established NK92 TCR cell lines. (Fig. 8.3.4) Determining the TCR-specific effector functions *in vitro* of the different NK92 subsets generated, we were able to examine the effects of CD8-coreceptor expression in TCR-redirected NK92 and to evaluate the suitability of our lab-manufactured, AML-reactive TCRs as a potential redirecting agent for ACT against AML.

9.1 Genetically engineered NK92 cells obtain TCR-specific reactivity against AML.

Upon retroviral transfer, NK92 cell lines were obtained which stably expressed high levels of the human CD3 complex and one of the three different AML-reactive TCRs, described in detail in chapter 9.5.2. Illustrated in Fig. 8.3.4, genetic modification of the NK92 cells resulted in similar CD3, CD8 and TCR expression rates for all TCRs used in this study enabling comparative analysis of the transgenic constructs´ effects on NK92 effector functions between the different cell lines generated.

As previously reported by two independent studies, NK92 cells supplied with the CD3 complex and a therapeutic TCR were capable of eliciting antigen-specific effector functions. (10, 21) In support of these data we observed, that the polycistronic CD3-construct and the AML-reactive TCR 5B2 used in our study also resulted in significant and TCR-specific IFN-γ degranulation upon coculture with HLA-matched primary AML blasts from patient MZ 653 (AML653). (depicted in Fig. 8.4.2a) Moreover, NK92 CD3 cells redirected with the TCR 25F2 also exerted significant and TCR-dependent IFN-γ release, when stimulated with HLA-matched target cells, AML921. (Fig. 8.4.2b). Therefore, these results strongly suggest that our transgenic TCR-CD3 complex is functional and can thus be considered as a proof of concept for the functionality of TCR-redireczed NK cells. (10, 21) Contrarily, no increase in IFN-γ secretion of effector cells expressing TCR 5H11 and CD3 could be observed upon coculture with their corresponding target cell line EBV-B 580. Furthermore, cytotoxicity assays revealed only marginal lytic activity of NK92 5H11-TCR CD3 at low effector to target ratios against HLA-matched EBV-B580, as depicted in Fig. 8.4.1b. However, as the feasibility of NK92´s TCR-redirection and the functional integrity of our CD3 construct were already confirmed by the TCR 5B2 and 25F2 based approaches, we hypothesized that the missing reactivity of TCR 5H11, deriving from a

CD8 positive CTL clone, might be due to the lack of TCR-coreceptor expression in NK cells. Therefore, we superinfected the existing cell lines with an expression vector encoding the human CD8αβ-heterodimer to examine the effects of the CD8-coreceptor on the TCR-mediated antitumoral reactivity of our NK92 lineages. Prior to our study the TCRs used to redirect NK92 cells in the context of CD3 comprised: i) a TCRα/β specific for the HLA-A2-restricted tyrosinase-derived "YMDGTMSQV" melanoma epitope (Tyr368-377) (21) ii) a TCRα/β specific for HLA-A2-restricted MART-1/Melan-A overexpressed in melanoma and iii) a TCR α/β against a TGF-βRII frameshift mutation peptide specific for colorectal cancer. (10) Thus, our data suggest that redirecting NK cells with AML-reactive TCRs could transfer this new approach to the treatment of AML and other hematological malignancies. When analyzed in detail, it became apparent that the previous studies relied on TCRs with coreceptor-independent reactivity. Therefore, facing antigen-scarcity as a great challenge in immunotherapy against AML, the implementation of TCR-coreceptor expression to this specific NK92 effector cell design does not only serve as an experimental model to study the effects of CD8 in NK92 TCR cell lines, but also bears the potential to broaden the spectrum of therapeutic TCR-candidates (such as TCR 5H11) suitable for NK92 TCR therapy targeting AML.

9.1.1 Additional expression of the CD8-coreceptor alters TCR-specific reactivity of redirected NK cells significantly.

As elaborated in chapter 6.5.3, the TCR-coreceptors enhance TCR-signaling via recruitment of intracellular signaling molecules, namely Lck, and the stabilization of the TCR-pMHC-interaction. (173) Intending to exploit these beneficial effects on TCR-reactivity for increased antitumoral efficiency of TCR-redirected NK92 cells, we successfully generated three CD8αβ-expression vectors encoding different isoforms of both chains, namely α 1; 2 and β 2; 3; 5, expressed by the original AML-reactive CTL clones where the TCRs used in this study derived from (see Fig. 8.2.3 for an overview of the cloning process). Upon retroviral superinfection of the already established NK92 clones expressing CD3 in combination with an AML-reactive TCR, following neomycin selection, high expression rates of CD8 could be detected by flow cytometry for the constructs CD8α1β2 and CD8α1β5, as illustrated in Fig. 8.3.4. However, FACS analysis of NK cells transduced with the CD8α2β3 isoform did not result in any positive staining of human CD8 on the surface of any NK92 transfectant (data not shown). Initially, we attributed this observation to the fact that, according to the manufacturer´s specifications, all commercially available antibodies binding to CD8 were recognizing an antigen of the CD8α isoform 1 only. Based on the assumption that detection was just not possible due to the lack of an appropriate antibody, we decided to include CD8α2β3 in our functional analyses

(illustrated in Fig. 8.4.3). Despite missing expression data, the CD8α2β3-transfectants successfully passed the CD8-specific selection process just as well as the NK92 TCR cells co-expressing CD8α1β2 or CD8α1β5.

Comparative analysis of cytotoxicity mediated by 5H11-TCR redirected NK92 cells expressing the three different CD8αβ-constructs against HLA-matched EBV-B 580 target cells revealed significant discrepancies between the different CD8αβ-heterodimers in their potential to enhance TCR-specific lytic activity of the NK92 subsets. As depicted in Fig. 8.4.3 a, NK92 cells co-expressing the CD8α1β5-isoform exerted superior cytotoxicity. Interestingly, no noteworthy TCR-mediated lytic activity could be detected for the CD8α2β3-transfectant. Initiated by this observation, detailed “RefSeq”-based analysis of the CD8α-isoforms, illustrated in Fig. 8.2.2, resulted in the finding, that the isoforms 1 and 2 differ in one exon present in α1 but missing in α2. Interestingly, this exon is considered to encode for the transmembrane region of the CD8 α-chain. (RefSeq) Therefore, it appears likely that the isoform 2, lacking the original transmembrane domain, cannot stably integrate into the cellular membrane. Consequently, the CD8α2β3-construct would not result in expression of a functional TCR-coreceptor explaining the missing enhancement of NK92 TCR cytotoxicity observed. In order to examine this hypothesis, further investigations, for example Western Blot detection of the CD8 α2- and β3-chains, are warranted.

In addition to the TCR 5H11-model, we also investigated the differences in stimulatory capacity of the three CD8-constructs on TCR 5B2-specific NK92 effector functions, illustrated in Fig. 8.4.3 b. As the luciferase-based cytotoxicity assay relied on continuously growing target cells and the TCR 5B2 recognizes AML blasts only, the comparative analysis between the CD8 expression vectors had to be performed via IFN-γ-ELISpot, respectively. In contrast to the previous experiment with TCR 5H11-redirected NK92 cells, no significant difference between the CD8-constructs could be observed for the TCR 5B2. However, this discrepancy was explained as differences in the CD8-coreceptor dependency of the two TCRs compared became apparent, depicted in Fig. 8.4.1 b and 8.4.2 a. While NK92 cells expressing the 5H11 TCR secreted significant amounts of IFN-γ only in the presence of the CD8-coreceptor, TCR 5B2-specific IFN-γ-release could already be detected without the expression of CD8 and was not significantly increased by the presence of CD8. Therefore, the coreceptor-independent TCR 5B2-model did not convey any information on the potential to enhance effector functions of every CD8 construct, but revealed that the additional expression of the TCR-coreceptor does not negatively affect effector functions of NK92 cells mediated by a coreceptor-independent TCR.

As the CD8α1β5-construct resulted in the greatest enhancement of NK92 5H11-TCR´s reactivity, all following experiments were performed with this isoform-combination, referred to

as “CD8”. As illustrated in Fig. 8.4.1, co-expression of CD8 greatly increased both cytotoxicity and IFN-γ degranulation of 5H11 TCR-redirected NK cells towards HLA-matched EBV-B 580 target cells. While the TCR-specific IFN-γ-secretion observed (Fig. 8.4.1b) could be considered as strictly coreceptor-dependent, cytotoxicity assays revealed basal TCR 5H11-mediated responses in the absence of CD8. (Fig. 8.4.1a) Therefore, the 5H11 TCR´s reactivity might not be categorized as completely CD8-dependent, but is greatly enhanced upon coreceptor expression. Effector functions of NK92 cells redirected with the 25F2 TCR were also altered significantly upon CD8-co-expression. In accordance to TCR 5B2, NK92 25F2 TCR´s cytotoxicity could not be tested as they only recognize AML blasts which are not suitable for the luciferase based killing assay. However, in contrast to the 5H11 TCR-model, TCR 25F2-specific IFN-γ degranulation of CD8-negative NK92 cells was higher, when compared to the same 5H11 TCR-subpopulation. Thus, TCR 25F2 reactivity improved significantly but less than the 5H11 TCR from CD8-coexpression, depicted in Fig. 8.4.2b. As already elaborated previously, IFN-γ release of NK92 cells expressing the 5B2 TCR was not affected by the presence or absence of the CD8 coreceptor. Therefore, the 5B2 TCR´s reactivity was considered as CD8-independent.

In conclusion, we were able to show that our CD8 coreceptor construct generated could significantly enhance TCR-specific effector functions in the context of NK cell redirection. Thereby, the CD8-construct´s effect of alteration appeared to be proportional to the extent of coreceptor-dependency of the TCR used for redirection. Moreover, CD8 co-expression in the context of a coreceptor-independent TCR did not affect effector functions negatively.

To assess further molecules contributing to the beneficial effect of coreceptor-expression in TCR-redirected NK cells, our study could be expanded to CD4, as CD4 and CD8 differ significantly in their binding-affinity to the corresponding MHC-complex. While the CD4/MHC class II interaction is among the weakest measured, CD8 contributes significantly to the interaction between the effector cell and the pMHC-complex. (174, 178) As in this study we only focused on the effect of CD8-coexpression, the attributional effect of coreceptor expression cannot be traced back to one of the two factors mentioned previously, increased binding affinity or additional recruitment of Lck. This, however, could be further evaluated by expressing CD4 in NK92 cells. As already mentioned, CD4 does not notably contribute to the effector cell´s binding affinity to pMHC-complexes. Thus, the supportive effect of CD4 on TCR-signaling is based on Lck-recruitment alone. As a consequence, successful enhancement of TCR-mediated responses by CD4 would reveal Lck-recruitment, as the essential benefit of coreceptor expression. However, if CD4-coexpression would not result in increased effector functions, stabilization of the TCR/pMHC-interaction would appear as the effective mechanism of reactivity-alteration.

9.2 NK92 MDM2-TCR – an universal anti-tumor cellular therapeutic.

Since the nature of antigens recognized by the AML-reactive TCRs (5B2, 25F2 and 5H11) has not yet been resolved, we included a well-defined and strictly CD8-dependent therapeutic TCR recognizing the epitope$_{81-88}$ of the MDM2 oncoprotein (for further information see chapter 6.5.2.2) in our studies to confirm our observations, especially on the beneficial effect of CD8-coexpression in the context of a coreceptor-dependent TCR. (164, 169)

Following the generation of NK92 cells stably expressing the MDM2-TCR, CD3 and the CD8α1β5-construct (Fig. 8.3.4), MDM2-peptide specific cytotoxicity and IFN-γ-release of MDM2-TCR redirected NK92 could be observed against HLA A*02:01 positive K562 (Fig. 8.4.4 b and c). However, in contrast to previous reports, K562 A2 killing data did not show any beneficial effect of CD8 co-expression on MDM2-TCR-mediated reactivity. Nevertheless, the results of the IFN-γ-ELISpot (Fig. 8.4.4 c) indicated an increase of reactivity attributed to the CD8-expression at low significance. Moreover, strictly CD8-dependent TCR-performance could be observed in the context of the B-LCL line IM-9, originally isolated from a multiple myeloma patient, and shown to express the MDM2-peptide endogenously. (Fig. 8.4.4 a) Therefore, we concluded that most likely the abundance of pMHC-complexes generated by pulsing K562 A*02:01 cells with the MDM2$_{81-88}$ oligopeptide, was responsible for the coreceptor-independent reactivity of the MDM2-TCR transduced NK92 cells. As depicted in Fig. 8.4.5, we examined this hypothesis by diluting the concentration of peptide loaded onto K562 cells. This resulted in a significant reduction of NK92 MDM2-TCR CD3 cytotoxicity, whereas killing of CD8-expressing NK92 TCR cells remained unaffected. Therefore, CD8-independent cytotoxicity was most likely caused by the unphysiological high presence of MDM2$_{81-88}$-HLA-complexes within the experimental setting.

In conclusion, we were able to confirm our previous observations that co-expression of the CD8α1β5 construct in the context of coreceptor dependent TCRs clearly improves TCR-mediated antitumor efficacy in NK92 ACT. In addition, these results indicate the broad spectrum of therapeutic applicability of this specific TCR/CD3 (and CD8) complex expressing NK92 cell line, redirected to a variety of tumor entities comprising leukemia, lymphoma, gliomas, neuroblastoma, sarcomas, testicular germ cell tumors, breast and urothelial cancer. (165-167)

9.3 Expression of a functional TCR-complex is accompanied by a reduction of inherent NK cell reactivity.

As described in chapter 6.5.1, NK cells possess a variety of receptors regulating their innate antitumoral reactivity. Therefore, the NK92 TCR approach, bears the potential to combine the highly specific targeting property of a therapeutic TCR with the inherent antitumoral reactivity of NK cells. Consequently, additional NK cell-mediated pathways of tumor cell recognition could prevent common immune escape mechanisms to occur during NK92 TCR-treatment. (107) Frequently observed HLA-allele loss of cancer cells, for example, would impair TCR-mediated stimulation of the effector cell´s antitumoral responses. (179) However, the inherent NK cell reactivity would simultaneously be highly activated based on NK cell´s potential of missing-self recognition. While HLA-dependence represents an indisputable limitation to all TCR-based approaches in immunotherapy, it does not apply to TCR-redirected NK cells, due to their dual (TCR and NK cell reactivity) mode of activation. (21)

In order to examine the extent of inherent NK cell reactivity conserved in the course of genetic modification, we analyzed our NK92 cell line´s effector functions towards K562. As this specific cell line does not express FACS-detectable levels of HLA-I or -II, the cytotoxicity and IFN-γ-release of the genetically modified NK92 cells detected can be attributed to endogenous NK cell activity exclusively.

As illustrated in Figs. 8.4.1/2/4, IFN-γ-degranulation upon stimulation with K562 was significantly reduced compared to NK92 CD3 cells, serving as reference for the original NK reactivity, for all NK92 subsets co-expressing the CD8-construct. Interestingly, NK92 cells expressing the seemingly coreceptor-independent TCR 5B2 did already release significantly less IFN-γ even without the presence of CD8, compared to NK92 CD3, as depicted in Fig. 8.4.2 a. Since previous experiments indicated that 5B2 was the only coreceptor-independent TCR in our experimental setup, we assumed that the divergent reduction of innate NK cell activity observed might be related to the extent of coreceptor dependency of the given TCR. Therefore, to confirm this assumption, we performed a cytotoxicity assay comparing the K562 killing kinetic of NK92 subsets expressing either the coreceptor-independent TCR 5B2 or the CD8-dependent TCR 5H11. (Fig. 8.5.1 a) Again, cytotoxicity of NK92 5B2-TCR against K562 was reduced in both, CD8-dependent and independent, situations while, in the case of TCR 5H11, only the CD8 positive population presented with lower lytic activity. Therefore, inherent NK cell-reactivity appeared to be only reduced, when a potentially functional TCR-complex,

including CD8 for coreceptor-dependent TCRs, was present on the membrane surface of transgenic NK92 cells.

In order to find possible explanations for this characteristic change of the NK92 cells´ functional phenotype upon genetic modification, we performed a FACS-based expression analysis of common activating and inhibiting receptors responsible for the inherent NK cell reactivity, illustrated in Fig. 8.5.1 b. Interestingly, while the expression of most receptors did not vary characteristically, for TCRs 5B2 and 5H11 we were able to detect a specific pattern of NKp30-downregulation associated with TCR-expression and correlating to the effector functions against K562. (Fig. 8.5.1 c) Therefore, it was likely that the observed reduction of reactivity against K562 was due to TCR- and CD8-associated downregulation of NKp30. However, as this finding is mainly based on the analysis of two different TCRs expressed in NK92 with and without CD8 co-expression, comparing our results with previous studies, they are in line with the observation of Mensali et al. who reported that NK92 obtain a T cell-like phenotype upon TCR-expression. (10) In contrast, Parlar et al. observed in their studies that TCR-NK cells could retain their capacity to recognize and eliminate targets on the basis of missing-self recognition. (21) The conservation of NK activity in TCR-NK cells is supported by the observation that they retain their original ability to respond to K562 targets potentially through engagement of NK cell activating receptors such as NKp30, NKp44, and DNAM-1. (21). Thus, further studies are needed to examine the role of the TCR´s coreceptor-dependency in this context in more detail.

9.4 Appropriate effector cell supply for TCR-redirection of NK cells.

Recently, Morton et al. were the first to transfer the NK92 TCR-approach to a NK cell source other than the continuously expanding NK92 cell line. Utilizing primary NK cells from peripheral blood of healthy donors they were able to express a therapeutic TCR (HLA- B*07:02 restricted, BOB1- specifc TCR) together with the human CD3- and CD8-complex. In line with the previous, NK92-based, observations, efficient TCR-specific antitumoral reactivity mediated by the genetically modified NK cells could be observed *in vivo* and *in vitro*. Proving the applicability of TCR-redirection to NK cell sources other than NK92, these findings raise the question whether primary and in vitro expanded NK cells or established NK cell lines would be the preferred cellular source for TCR-NK mediated ACT. (107)

While the NK92 cell line represents a homogenous, well-defined cell population, that is easy to genetically manipulate, and is highly suitable for an indefinite off-the-shelf cellular therapy

with low logistic and financial expenses, a variety of limitations must be considered when utilized as a cellular platform for ACT. (10, 103) Being a continuously growing cell line, it is mandatory for NK92 cells to be irradiated prior infusion to prevent potential graft-tumorigenisis. (180) This, however, reduces therapeutic persistence and efficacy making repetitive dose-application necessary. (180) In addition, NK92 cells, despite expressing numerous activating receptors, lack expression of CD16, and of most inhibitory KIRs. (21, 181) Consequently, while missing the potential to exert antibody-dependent cellular cytotoxicity (due to the lack of CD16), NK92 cells are less prone to be activated by HLA-loss, compared to other NK cell subsets. Therefore, the previously described (chapter 13.3) dual mode of NK cell activation leading to persistence of antitumoral reactivity despite HLA-downregulation of tumor cells is less present in NK92, as compared to other NK cell subpopulations.

Primary NK cells generated from peripheral blood (PB) express a diverse array of members of the KIR-family which is conserved during genetic modification. Thus, absence of HLA-class I on cancer cells likely results in efficient activation of PB-derived NK TCR effector cells. Moreover, TCR-redirected, primary NK cells express high levels of CD16 enabling access to ADCC-based combinational treatment approaches. (107) Nevertheless, PB-derived NK cells are considered to be difficult to genetically engineer. (182) Additionally, since cryopreservation has been shown to affect the cytotoxic potential of primary NK cell preparations negatively, upscaling of manufacturing protocols to guarantee treatment availability appears to be both cost- and time-consuming. (183) In contrast to NK92 cells, PB-derived NK cells do not need to be irradiated prior application. Consequently, ACT based on primary NK cells possesses the great advantage of long-term *in vivo* persistence and expansion. However, current findings suggest limited proliferation capacity of peripheral blood-derived NK cells compared to other primary NK cells, for example isolated from cord blood. (184)

Taken together the advantages and disadvantages of both NK cell sources, NK92 and PB-derived NK cells, utilized for TCR-redirection, one must conclude, that despite highly efficient antitumoral reactivity, both approaches face specific limitations which will impact clinical success of NK TCR-therapy. Therefore, NK cells derived from induced pluripotent stem cells (iPSCs) appear as an attractive, alternative cellular platform to use as they represent the combination of the benefits of both established NK sources. Like NK92, iPSC NK cells represent a quickly available, standardized cell population for genetic engineering with high cytolytic potential, while, comparable to primary NK cells, they do not need to be irradiated prior infusion to patients resulting in long-term persistence. (102, 185) As iPSC NK cells were the most recent to join the NK cell-ACT armamentarium, clinical experience is just being built on gene edited (CAR-redirected) iPSC NK cells in several trials. Therefore, it has to be awaited whether previously raised concerns about genomic instability of this particular cellular source

will prove true in clinical application. (186) If this won´t be the case, for further improvement of the NK-TCR-approach, TCR-redirection should be transferred to NK cells induced from pluripotent stem cells.

10 Summary

Background: Adoptive cellular therapy (ACT) with redirected T cells expressing a chimeric antigen receptor (CAR) or transgenic T-cell-receptor (tTCR) has revolutionized cellular immunotherapy to hematological neoplasia, in particular to acute lymphoid leukemia, and also shows great promise as therapy for solid tumors. While CARs can only detect fully cell surface expressed target structures, TCR-mediated recognition is not limited to surface antigens, but covers processed tumor neoantigens derived from the whole proteome. However, mispairing of transgenic and endogenous TCRs and restriction to patient-derived, autologous T lymphocytes with variable “fitness” and T cell subsets due to individual health conditions and age of the patient exemplify the current limitations encountered in TCR-redirected ACT. The natural killer (NK) cell line NK92 elicits lytic activity comparable to T cells, has been approved by the FDA for ACT and shown not to cause graft-vs-host disease. Since NK cell redirection is currently limited to CARs, NK92 cells engineered to express a CD3/TCR or CD3/CD8/TCR complex might evolve as an attractive, standardized cellular source for off-the-shelf TCR-based ACT.

Aims: Thus, the goal of this study was to explore NK92-CD3+ and NK92-CD3+CD8+ variants redirected to acute myeloid leukemia (AML) and mdm-2 expressing tumor targets by expression of different reactive TCRs for antitumoral immunity in vitro.

Methods: NK92CD3+cells (provided by Dr. C. Wölfel, III. Dept. of Med.) were further engineered to express human CD8. Upon viral gene transfer of optimized TCRs recognizing primary AML-blasts or EBV-BLCL from patient MZ580 (TCRs from CTL 5H11, 25F2 and 5B2) and the mdm-2 peptide (anti-mdm2 TCR) NK92 CD3+ and NK92CD3+CD8+ were expanded and enriched for >90% TCR expression (referred to as NK92TCR+). Additional expression profiling of checkpoint molecules (e.g. CD80/86, PD1/PDL1, NKG2A, TIM3, TIGIT) and NCRs was performed by FACS. IFN-γ release and cytolytic activity was tested by ELISpot and bioluminescence-based assays, respectively.

Results: Upon coculture with MZ580 BLCL or mdm-2 expressing IM9 (myeloma) and mdm-2 peptide loaded HLA-A*02:01^{+} K562 targets NK92TCR^{+} cells elicited strong TCR-dependent IFN–γ release and cytotoxicity. This reactivity was greatly enhanced upon CD8 coexpression for TCR 5H11 and indispensable for the mdm-2 TCR clearly demonstrating CD8 coreceptor

dependency for both TCRs. Cytolytic activity of 5H11 T cells and 5H11TCR$^+$NK92 was comparable. Intriguingly, NK92TCR$^+$ cells shifted to a more T cell-like phenotype and showed reduced NKp30-mediated killing of K562. First adoptive transfer studies of NK92TCR$^+$ cells into a NSG-AML PDX model are in progress.

Summary/Conclusion: These studies demonstrate that the established and FDA approved NK92 cell line can be redirected to elicit TCR-mediated antitumoral immunity to AML. NK92TCR$^+$ cells might thus represent a promising universal tool for an ‘off-the-shelf’ ACT product.

TCR-redirected NK92CD3$^+$CD8$^+$ cells elicit antitumoral immunity comparable to original cytotoxic T cell clones. Co-expression of CD8 broadens the spectrum of therapeutic TCRs applicable to adoptive NK92TCR$^+$ cell therapy. Thus, TCR-redirected NK92 cells might represent a promising new tool for an ‘off-the-shelf’ ACT with limited off-target effects.

11 Zusammenfassung

Im vergangenen Jahrzehnt hat die adoptive zelluläre Therapie (ACT) unter Verwendung von T-Zell-Rezeptor- oder CAR-exprimierender T-Zellen die zelluläre Immuntherapie zur Behandlung hämatologischer Neoplasien, insbesondere der akuten lymphatischen Leukämie (ALL) sowie des diffus großzelligen B-Zell Lymphoms (DLBCL), revolutioniert und weist bereits vielversprechende Resultate in der Behandlung solider Tumoren auf. Während chimäre Antigenrezeptoren (CARs) in Ihrer klassischen Form lediglich an der Zelloberfläche exprimierte Strukturen detektieren können, reicht das Spektrum durch TZR erkannter Antigene weit darüber hinaus. Aufgrund des Mechanismus der Antigenpräsentation, vermittelt über Peptid-MHC-Komplexe, können TZRs an prozessierte Oligopeptide aus dem Inneren der Zelle und damit auch an Tumor-Neoantigene binden und erreichen damit, gegenüber CARs, ein ungleich höheres Maß an Spezifität der induzierten antitumoralen Reaktivität. Die TZR-basierte ACT ist zum aktuellen Zeitpunkt in der klinischen Anwendung auf autologe T-Lymphozyten beschränkt, da der allogene T-Zell-Transfer regelmäßig zu einer ausgeprägten „graft versus host disease“ (GvHD) führt. Im Laufe der Jahre kamen diverse Limitationen bei der Verwendung autologer T-Zellen im Kontext der TZR-basierten ACT zu Tage. Insbesondere die Gefahr von TZR-Mispaarungen zwischen dem trans- und endogenen Rezeptor sowie die schwankende Viabilität des autologen Zellproduktes, z.B. aufgrund der Morbidität oder des Alters der PatientInnen, stellen die vordergründigen Probleme dieses Therapieansatzes dar. Im Unterschied zu T-Lymphozyten, konnte für Natürliche Killerzellen in zahlreichen klinischen Studien die Unbedenklichkeit des allogenen Transfers nachgewiesen werden. NK92, eine Natürliche Killerzelllinie, erhielt seitens der amerikanischen FDA eine Zulassung für den universalen adoptiven Transfer und weist eine mit T-Zellen vergleichbares Effektorpotential auf. Während in klinischen Studien die NK92-basierte ACT aktuell noch auf die Verwendung von CARs beschränkt ist, gibt es bereits erste experimentelle Daten, die auf ein großes Potential TZR-CD3-Komplex- oder TZR-CD3-CD8-exprimierender NK92 Zellen als eine attraktive, standardisierte und schnell verfügbare adoptive zelluläre Therapie hinweisen.

Aus diesem Grund war das Ziel dieser Studie die antitumorale Effektivität von NK92-CD3+ und NK92-CD3+CD8+ Zellen, transduziert mit einem TZR gegen AML-Blasten oder MDM2-exprimierende Tumorzellen, in vitro zu untersuchen.

Hierfür wurden freundlicherweise von Dr. C. Wölfel (aus der hiesigen Klinik) zur Verfügung gestellte NK92-CD3+ Zellen mittels retroviralen Transfers optimierter AML-reaktiver TZRs oder eines MDM2-reaktiven TZR sowie dem humanen CD8-Korezeptor gentechnisch modifiziert. Nach abgeschlossener Expansion und Selektion konnten für alle TZRs vergleichbar hohe Expressionsraten (> 80%) erzielt werden. Im weiteren Verlauf wurde eine detaillierte Durchflusszytometrie-basierte Analyse des Expressionsprofils aktivierender und

inhibierender Oberflächenmolekülen (z.B. NKG2A, TIGIT, NKp30, NKp44) der generierten Zellprodukte durchgeführt. Die antitumorale Reaktivität wurde mittels IFN-γ-ELISpot und einem Biolumineszenz-basierten Zytotoxizitäts-Assay ermittelt.

Für alle TZR, die in diese Studie eingeschlossen wurden, konnte eine ausgeprägte TZR-spezifische Tumorzelllyse und Interferon-γ-Ausschüttung festgestellt werden. Darüber hinaus wurde – im Falle der TZRs 25F2, 5H11 und MDM2 – diese Reaktivität signifikant durch die Koexpression des CD8-Konstruktes gesteigert. Dagegen blieben die Effektorfunktionen TZR-5B2-transduzierter NK92-Zellen von der CD8-Expression unbeeinflusst. Die phänotypische Charakterisierung der verschiedenen NK-Zelllinien ergab überdies eine am ehesten NKp30-assoziierte Reduktion der inherenten NK-Zellaktivität bei Expression eines funktionellen TZR-Komplexes.

Zusammenfassend geben die Ergebnisse dieser Studie Hinweis auf das große Potential TZR-transduzierter NK92 im Zusammenhang der adoptiven zellulären Therapie, insbesondere gegen AML. Dabei ermöglicht die Koexpression des CD8-Konstruktes den Einsatz Korezeptor-abhängiger TZRs und erweitert damit das Spektrum zugänglicher TZRs für diesen Therapieansatz. Derart gentechnisch veränderte NK92 stellen somit eine attraktive und allzeit verfügbare Behandlungsmethode mit geringem Nebenwirkungsspektrum dar.

12 Appendix

12.1 CD8 α- and β-chain sequences

12.1.1 CD8 α

12.1.1.1 CD8 α Transcript variant 1

5´GCCACCATGGCCTTACCAGTGACCGCCTTGCTCCTGCCGCTGGCCTTGCTGCTCCAC
GCCGCCAGGCCGAGCCAGTTCCGGGTGTCGCCGCTGGATCGGACCTGGAACCTGGGC
GAGACAGTGGAGCTGAAGTGCCAGGTGCTGCTGTCCAACCCGACGTCGGGCTGCTCG
TGGCTCTTCCAGCCGCGCGGCGCCGCCGCCAGTCCCACCTTCCTCCTATACCTCTCCC
AAAACAAGCCCAAGGCGGCCGAGGGGCTGGACACCCAGCGGTTCTCGGGCAAGAGGT
TGGGGGACACCTTCGTCCTCACCCTGAGCGACTTCCGCCGAGAGAACGAGGGCTACTA
TTTCTGCTCGGCCCTGAGCAACTCCATCATGTACTTCAGCCACTTCGTGCCGGTCTTCC
TGCCAGCGAAGCCCACCACGACGCCAGCGCCGCGACCACCAACACCGGCGCCCACCA
TCGCGTCGCAGCCCCTGTCCCTGCGCCCAGAGGCGTGCCGGCCAGCGGCGGGGGGC
GCAGTGCACACGAGGGGGCTGGACTTCGCCTGTGATATCTACATCTGGGCGCCCCTGG
CCGGGACTTGTGGGGTCCTTCTCCTGTCACTGGTTATCACCCTTTACTGCAACCACAGG
AACCGAAGACGTGTTTGCAAATGTCCCCGGCCTGTGGTCAAATCGGGAGACAAGCCCA
GCCTTTCGGCGAGATACGTC-3´

12.1.1.2 CD8 α Transcript variant 2

5´GCCACCATGGCCTTACCAGTGACCGCCTTGCTCCTGCCGCTGGCCTTGCTGCTCCAC
GCCGCCAGGCCGAGCCAGTTCCGGGTGTCGCCGCTGGATCGGACCTGGAACCTGGGC
GAGACAGTGGAGCTGAAGTGCCAGGTGCTGCTGTCCAACCCGACGTCGGGCTGCTCG
TGGCTCTTCCAGCCGCGCGGCGCCGCCGCCAGTCCCACCTTCCTCCTATACCTCTCCC
AAAACAAGCCCAAGGCGGCCGAGGGGCTGGACACCCAGCGGTTCTCGGGCAAGAGGT
TGGGGGACACCTTCGTCCTCACCCTGAGCGACTTCCGCCGAGAGAACGAGGGCTACTA
TTTCTGCTCGGCCCTGAGCAACTCCATCATGTACTTCAGCCACTTCGTGCCGGTCTTCC
TGCCAGCGAAGCCCACCACGACGCCAGCGCCGCGACCACCAACACCGGCGCCCACCA
TCGCGTCGCAGCCCCTGTCCCTGCGCCCAGAGGCGTGCCGGCCAGCGGCGGGGGGC
GCAGGGAACCGAAGACGTGTTTGCAAATGTCCCCGGCCTGTGGTCAAATCGGGAGACA
AGCCCAGCCTTTCGGCGAGATACGTC-3´

12.1.2 CD8 β

12.1.2.1 CD8 β Transcript variant 2

5´CTCCAGCAGACCCCTGCATACATAAAGGTGCAAACCAACAAGATGGTGATGCTGTCCT
GCGAGGCTAAAATCTCCCTCAGTAACATGCGCATCTACTGGCTGAGACAGCGCCAGGC
ACCGAGCAGTGACAGTCACCACGAGTTCCTGGCCCTCTGGGATTCCGCAAAAGGGACT
ATCCACGGTGAAGAGGTGGAACAGGAGAAGATAGCTGTGTTTCGGGATGCAAGCCGGT
TCATTCTCAATCTCACAAGCGTGAAGCCGGAAGACAGTGGCATCTACTTCTGCATGATC
GTCGGGAGCCCCGAGCTGACCTTCGGGAAGGGAACTCAGCTGAGTGTGGTTGATTTCC
TTCCCACCACTGCCCAGCCCACCAAGAAGTCCACCCTCAAGAAGAGAGTGTGCCGGTT
ACCCAGGCCAGAGACCCAGAAGGGCCCACTTTGTAGCCCCATCACCCTTGGCCTGCTG
GTGGCTGGCATCCTGGTTCTGCTGGTTTCCCTGGGAGTGGCCATCCACCTGTGCTGCC
GGCGGAGGAGAGCCCGGCTTCGTTTCATGAAACAGCCTCAAGGGGAAGGTGTATCAGG
AACCTTTGTCCCCCAATGCCTGCATGGATACTACAGCAATACTACAACCTCACAGAAGC
TGCTTAACCCATGGATCCTGAAAACATAG-3´

12.1.2.2 CD8 β Transcript variant 3

5´CTCCAGCAGACCCCTGCATACATAAAGGTGCAAACCAACAAGATGGTGATGCTGTCCT
GCGAGGCTAAAATCTCCCTCAGTAACATGCGCATCTACTGGCTGAGACAGCGCCAGGC
ACCGAGCAGTGACAGTCACCACGAGTTCCTGGCCCTCTGGGATTCCGCAAAAGGGACT
ATCCACGGTGAAGAGGTGGAACAGGAGAAGATAGCTGTGTTTCGGGATGCAAGCCGGT
TCATTCTCAATCTCACAAGCGTGAAGCCGGAAGACAGTGGCATCTACTTCTGCATGATC
GTCGGGAGCCCCGAGCTGACCTTCGGGAAGGGAACTCAGCTGAGTGTGGTTGATTTCC
TTCCCACCACTGCCCAGCCCACCAAGAAGTCCACCCTCAAGAAGAGAGTGTGCCGGTT
ACCCAGGCCAGAGACCCAGAAGGGCCCACTTTGTAGCCCCATCACCCTTGGCCTGCTG
GTGGCTGGCGTCCTGGTTCTGCTGGTTTCCCTGGGAGTGGCCATCCACCTGTGCTGCC
GGCGGAGGAGAGCCCGGCTTCGTTTCATGAAACAACTAAGATTACATCCACTGGAGAAA
TGTTCCAGAATGGACTACTGA-3´

12.1.2.3 CD8 β Transcript variant 5

5´CTCCAGCAGACCCCTGCATACATAAAGGTGCAAACCAACAAGATGGTGATGCTGTCCT
GCGAGGCTAAAATCTCCCTCAGTAACATGCGCATCTACTGGCTGAGACAGCGCCAGGC
ACCGAGCAGTGACAGTCACCACGAGTTCCTGGCCCTCTGGGATTCCGCAAAAGGGACT
ATCCACGGTGAAGAGGTGGAACAGGAGAAGATAGCTGTGTTTCGGGATGCAAGCCGGT
TCATTCTCAATCTCACAAGCGTGAAGCCGGAAGACAGTGGCATCTACTTCTGCATGATC
GTCGGGAGCCCCGAGCTGACCTTCGGGAAGGGAACTCAGCTGAGTGTGGTTGATTTCC

TTCCCACCACTGCCCAGCCCACCAAGAAGTCCACCCTCAAGAAGAGAGTGTGCCGGTT
ACCCAGGCCAGAGACCCAGAAGGGCCCACTTTGTAGCCCCATCACCCTTGGCCTGCTG
GTGGCTGGCGTCCTGGTTCTGCTGGTTTCCCTGGGAGTGGCCATCCACCTGTGCTGCC
GGCGGAGGAGAGCCCGGCTTCGTTTCATGAAACAATTTTACAAATGA-3´

13 References

1. Allison M, Mathews J, Gilliland T, Mathew SO. Natural Killer Cell-Mediated Immunotherapy for Leukemia. Cancers (Basel). 2022;14(3).
2. Hao T, Li-Talley M, Buck A, Chen W. An emerging trend of rapid increase of leukemia but not all cancers in the aging population in the United States. Sci Rep. 2019;9(1):12070.
3. Shah A, Andersson TM-L, Rachet B, Björkholm M, Lambert PC. Survival and cure of acute myeloid leukaemia in England, 1971-2006: a population–based study. British Journal of Haematology. 2013;162(4):509-16.
4. Thein MS, Ershler WB, Jemal A, Yates JW, Baer MR. Outcome of older patients with acute myeloid leukemia. Cancer. 2013;119(15):2720-7.
5. Maude SL, Laetsch TW, Buechner J, Rives S, Boyer M, Bittencourt H, et al. Tisagenlecleucel in Children and Young Adults with B-Cell Lymphoblastic Leukemia. N Engl J Med. 2018;378(5):439-48.
6. Brown CE, Mackall CL. CAR T cell therapy: inroads to response and resistance. Nat Rev Immunol. 2019;19(2):73-4.
7. Curran EK, Godfrey J, Kline J. Mechanisms of Immune Tolerance in Leukemia and Lymphoma. Trends in immunology. 2017;38(7):513-25.
8. Martincorena I, Campbell PJ. Somatic mutation in cancer and normal cells. Science (New York, NY). 2015;349(6255):1483-9.
9. Anguille S, Van Tendeloo VF, Berneman ZN. Leukemia-associated antigens and their relevance to the immunotherapy of acute myeloid leukemia. Leukemia. 2012;26(10):2186-96.
10. Mensali N, Dillard P, Hebeisen M, Lorenz S, Theodossiou T, Myhre MR, et al. NK cells specifically TCR-dressed to kill cancer cells. EBioMedicine. 2019.
11. Heemskerk MH, Hagedoorn RS, van der Hoorn MA, van der Veken LT, Hoogeboom M, Kester MG, et al. Efficiency of T-cell receptor expression in dual-specific T cells is controlled by the intrinsic qualities of the TCR chains within the TCR-CD3 complex. Blood. 2007;109(1):235-43.
12. Schumacher TN. T-cell-receptor gene therapy. Nat Rev Immunol. 2002;2(7):512-9.
13. Rosenberg SA, Restifo NP. Adoptive cell transfer as personalized immunotherapy for human cancer. Science (New York, NY). 2015;348(6230):62-8.
14. Rosenberg SA, Restifo NP, Yang JC, Morgan RA, Dudley ME. Adoptive cell transfer: a clinical path to effective cancer immunotherapy. Nat Rev Cancer. 2008;8(4):299-308.
15. Daher M, Rezvani K. Next generation natural killer cells for cancer immunotherapy: the promise of genetic engineering. Curr Opin Immunol. 2018;51:146-53.
16. Carlsten M, Järås M. Natural Killer Cells in Myeloid Malignancies: Immune Surveillance, NK Cell Dysfunction, and Pharmacological Opportunities to Bolster the Endogenous NK Cells. Front Immunol. 2019;10:2357.
17. Arruga F, Gyau BB, Iannello A, Vitale N, Vaisitti T, Deaglio S. Immune Response Dysfunction in Chronic Lymphocytic Leukemia: Dissecting Molecular Mechanisms and Microenvironmental Conditions. International journal of molecular sciences. 2020;21(5).
18. Ruggeri L, Mancusi A, Capanni M, Urbani E, Carotti A, Aloisi T, et al. Donor natural killer cell allorecognition of missing self in haploidentical hematopoietic transplantation for acute myeloid leukemia: challenging its predictive value. Blood. 2007;110(1):433-40.
19. Marofi F, Al-Awad AS, Sulaiman Rahman H, Markov A, Abdelbasset WK, Ivanovna Enina Y, et al. CAR-NK Cell: A New Paradigm in Tumor Immunotherapy. Front Oncol. 2021;11:673276.
20. Curti A, Ruggeri L, D'Addio A, Bontadini A, Dan E, Motta MR, et al. Successful transfer of alloreactive haploidentical KIR ligand-mismatched natural killer cells after infusion in elderly high risk acute myeloid leukemia patients. Blood. 2011;118(12):3273-9.
21. Parlar A, Sayitoglu EC, Ozkazanc D, Georgoudaki A-M, Pamukcu C, Aras M, et al. Engineering antigen-specific NK cell lines against the melanoma-associated antigen tyrosinase via TCR gene transfer. European journal of immunology. 2019;49(8):1278-90.
22. Herold G, editor. Innere Medizin : eine vorlesungsorientierte Darstellung; 2016; unter Berücksichtigung des Gegenstandskataloges für die Ärztliche Prüfung; mit ICD 10-Schlüssel im Text und Stichwortverzeichnis. Köln: Herold, Gerd; 2016.
23. Juliusson G, Hough R. Leukemia. Prog Tumor Res. 2016;43:87-100.
24. Cazzola M. Introduction to a review series: the 2016 revision of the WHO classification of tumors of hematopoietic and lymphoid tissues. Blood. 2016;127(20):2361-4.
25. Kato M, Manabe A. Treatment and biology of pediatric acute lymphoblastic leukemia. Pediatr Int. 2018;60(1):4-12.
26. Marinescu C, Vlădăreanu AM, Mihai F. Acute Lymphocytic Leukemia in Adults. Pathologic Features and Prognosis. Rom J Intern Med. 2015;53(1):31-6.
27. Marcotte EL, Spector LG, Mendes-de-Almeida DP, Nelson HH. The Prenatal Origin of Childhood Leukemia: Potential Applications for Epidemiology and Newborn Screening. Front Pediatr. 2021;9:639479.
28. Jain MD, Davila ML. Concise Review: Emerging Principles from the Clinical Application of Chimeric Antigen Receptor T Cell Therapies for B Cell Malignancies. Stem Cells. 2018;36(1):36-44.
29. Kipps TJ, Stevenson FK, Wu CJ, Croce CM, Packham G, Wierda WG, et al. Chronic lymphocytic leukaemia. Nat Rev Dis Primers. 2017;3:16096.
30. Parikh SA. Chronic lymphocytic leukemia treatment algorithm 2018. Blood Cancer J. 2018;8(10):93.

31. Calvo T, Reina-Ortiz C, Giraldos D, Gascón M, Woods D, Asenjo J, et al. Expanded and activated allogeneic NK cells are cytotoxic against B-chronic lymphocytic leukemia (B-CLL) cells with sporadic cases of resistance. Sci Rep. 2020;10(1):19398.
32. Hofland T, Eldering E, Kater AP, Tonino SH. Engaging Cytotoxic T and NK Cells for Immunotherapy in Chronic Lymphocytic Leukemia. International journal of molecular sciences. 2019;20(17).
33. Radivoyevitch T, Jankovic GM, Tiu RV, Saunthararajah Y, Jackson RC, Hlatky LR, et al. Sex differences in the incidence of chronic myeloid leukemia. Radiat Environ Biophys. 2014;53(1):55-63.
34. Röllig C. [Diagnosis and treatment of acute myeloid leukemia : The updated 2018 Onkopedia Guideline]. Internist (Berl). 2019;60(3):257-72.
35. Southam CM, Craver LF, Dargeon HW, Burchenal JH. A study of the natural history of acute leukemia with special reference to the duration of the disease and the occurrence of remissions. Cancer. 1951;4(1):39-59.
36. Crowther D, Bateman CJ, Vartan CP, Whitehouse JM, Malpas JS, Fairley GH, et al. Combination chemotherapy using L-asparaginase, daunorubicin, and cytosine arabinoside in adults with acute myelogenous leukaemia. Br Med J. 1970;4(5734):513-7.
37. Greiner J, Götz M, Wais V. Increasing Role of Targeted Immunotherapies in the Treatment of AML. International journal of molecular sciences. 2022;23(6).
38. Andreozzi F, Massaro F, Wittnebel S, Spilleboudt C, Lewalle P, Salaroli A. New Perspectives in Treating Acute Myeloid Leukemia: Driving towards a Patient-Tailored Strategy. International journal of molecular sciences. 2022;23(7).
39. Juliusson G, Lazarevic V, Hörstedt AS, Hagberg O, Höglund M. Acute myeloid leukemia in the real world: why population-based registries are needed. Blood. 2012;119(17):3890-9.
40. Papaemmanuil E, Gerstung M, Bullinger L, Gaidzik VI, Paschka P, Roberts ND, et al. Genomic Classification and Prognosis in Acute Myeloid Leukemia. New England Journal of Medicine. 2016;374(23):2209-21.
41. Fircanis S, Merriam P, Khan N, Castillo JJ. The relation between cigarette smoking and risk of acute myeloid leukemia: An updated meta-analysis of epidemiological studies. American Journal of Hematology. 2014;89(8):E125-E32.
42. Kayser S, Döhner K, Krauter J, Köhne C-H, Horst HA, Held G, et al. The impact of therapy-related acute myeloid leukemia (AML) on outcome in 2853 adult patients with newly diagnosed AML. Blood. 2011;117(7):2137-45.
43. Ishii H, Yano S. New Therapeutic Strategies for Adult Acute Myeloid Leukemia. Cancers (Basel). 2022;14(11).
44. Ferrara F, Lessi F, Vitagliano O, Birkenghi E, Rossi G. Current Therapeutic Results and Treatment Options for Older Patients with Relapsed Acute Myeloid Leukemia. Cancers (Basel). 2019;11(2).
45. Kantarjian H, O'Brien S, Cortes J, Giles F, Faderl S, Jabbour E, et al. Results of intensive chemotherapy in 998 patients age 65 years or older with acute myeloid leukemia or high-risk myelodysplastic syndrome. Cancer. 2006;106(5):1090-8.
46. Ossenkoppele G, Löwenberg B. How I treat the older patient with acute myeloid leukemia. Blood. 2015;125(5):767-74.
47. Antar AI, Otrock ZK, Abou Dalle I, El-Cheikh J, Bazarbachi A. Pharmacologic Therapies to Prevent Relapse of Acute Myeloid Leukemia After Allogeneic Hematopoietic Stem Cell Transplantation. Front Oncol. 2020;10:596134.
48. Levin M, Stark M, Ofran Y, Assaraf YG. Deciphering molecular mechanisms underlying chemoresistance in relapsed AML patients: towards precision medicine overcoming drug resistance. Cancer Cell Int. 2021;21(1):53.
49. Oshima K, Zhao J, Pérez-Durán P, Brown JA, Patiño-Galindo JA, Chu T, et al. Mutational and functional genetics mapping of chemotherapy resistance mechanisms in relapsed acute lymphoblastic leukemia. Nat Cancer. 2020;1(11):1113-27.
50. DiNardo CD, Stein EM, de Botton S, Roboz GJ, Altman JK, Mims AS, et al. Durable Remissions with Ivosidenib in IDH1-Mutated Relapsed or Refractory AML. N Engl J Med. 2018;378(25):2386-98.
51. Stein EM, DiNardo CD, Pollyea DA, Fathi AT, Roboz GJ, Altman JK, et al. Enasidenib in mutant IDH2 relapsed or refractory acute myeloid leukemia. Blood. 2017;130(6):722-31.
52. DiNardo CD, Rausch CR, Benton C, Kadia T, Jain N, Pemmaraju N, et al. Clinical experience with the BCL2-inhibitor venetoclax in combination therapy for relapsed and refractory acute myeloid leukemia and related myeloid malignancies. Am J Hematol. 2018;93(3):401-7.
53. Nguyen R, Wu H, Pounds S, Inaba H, Ribeiro RC, Cullins D, et al. A phase II clinical trial of adoptive transfer of haploidentical natural killer cells for consolidation therapy of pediatric acute myeloid leukemia. J Immunother Cancer. 2019;7(1):81.
54. Xu J, Niu T. Natural killer cell-based immunotherapy for acute myeloid leukemia. J Hematol Oncol. 2020;13(1):167.
55. Rubnitz JE, Inaba H, Kang G, Gan K, Hartford C, Triplett BM, et al. Natural killer cell therapy in children with relapsed leukemia. Pediatr Blood Cancer. 2015;62(8):1468-72.
56. Godal R, Bachanova V, Gleason M, McCullar V, Yun GH, Cooley S, et al. Natural killer cell killing of acute myelogenous leukemia and acute lymphoblastic leukemia blasts by killer cell immunoglobulin-like receptor-negative natural killer cells after NKG2A and LIR-1 blockade. Biology of blood and marrow transplantation : journal of the American Society for Blood and Marrow Transplantation. 2010;16(5):612-21.
57. Ciurea SO, Kongtim P, Soebbing D, Trikha P, Behbehani G, Rondon G, et al. Decrease post-transplant relapse using donor-derived expanded NK-cells. Leukemia. 2022;36(1):155-64.

58. Chen X, Han J, Chu J, Zhang L, Zhang J, Chen C, et al. A combinational therapy of EGFR-CAR NK cells and oncolytic herpes simplex virus 1 for breast cancer brain metastases. Oncotarget. 2016;7(19):27764-77.
59. Genßler S, Burger MC, Zhang C, Oelsner S, Mildenberger I, Wagner M, et al. Dual targeting of glioblastoma with chimeric antigen receptor-engineered natural killer cells overcomes heterogeneity of target antigen expression and enhances antitumor activity and survival. Oncoimmunology. 2016;5(4):e1119354.
60. Murakami T, Nakazawa T, Natsume A, Nishimura F, Nakamura M, Matsuda R, et al. Novel Human NK Cell Line Carrying CAR Targeting EGFRvIII Induces Antitumor Effects in Glioblastoma Cells. Anticancer Res. 2018;38(9):5049-56.
61. Hanahan D, Weinberg RA. Hallmarks of cancer: the next generation. Cell. 2011;144(5):646-74.
62. Gonzalez H, Hagerling C, Werb Z. Roles of the immune system in cancer: from tumor initiation to metastatic progression. Genes Dev. 2018;32(19-20):1267-84.
63. Wu T, Dai Y. Tumor microenvironment and therapeutic response. Cancer Lett. 2017;387:61-8.
64. Wetzler M, McElwain BK, Stewart CC, Blumenson L, Mortazavi A, Ford LA, et al. HLA-DR antigen-negative acute myeloid leukemia. Leukemia. 2003;17(4):707-15.
65. MacFarlane AWt, Jillab M, Smith MR, Alpaugh RK, Cole ME, Litwin S, et al. NK cell dysfunction in chronic lymphocytic leukemia is associated with loss of the mature cells expressing inhibitory killer cell Ig-like receptors. Oncoimmunology. 2017;6(7):e1330235.
66. Duault C, Kumar A, Taghi Khani A, Lee SJ, Yang L, Huang M, et al. Activated natural killer cells predict poor clinical prognosis in high-risk B- and T-cell acute lymphoblastic leukemia. Blood. 2021;138(16):1465-80.
67. Chen CI, Koschmieder S, Kerstiens L, Schemionek M, Altvater B, Pscherer S, et al. NK cells are dysfunctional in human chronic myelogenous leukemia before and on imatinib treatment and in BCR-ABL-positive mice. Leukemia. 2012;26(3):465-74.
68. Mundy-Bosse BL, Scoville SD, Chen L, McConnell K, Mao HC, Ahmed EH, et al. MicroRNA-29b mediates altered innate immune development in acute leukemia. J Clin Invest. 2016;126(12):4404-16.
69. Leone P, Shin EC, Perosa F, Vacca A, Dammacco F, Racanelli V. MHC class I antigen processing and presenting machinery: organization, function, and defects in tumor cells. J Natl Cancer Inst. 2013;105(16):1172-87.
70. Groh V, Wu J, Yee C, Spies T. Tumour-derived soluble MIC ligands impair expression of NKG2D and T-cell activation. Nature. 2002;419(6908):734-8.
71. Raneros AB, Minguela A, Rodriguez RM, Colado E, Bernal T, Anguita E, et al. Increasing TIMP3 expression by hypomethylating agents diminishes soluble MICA, MICB and ULBP2 shedding in acute myeloid leukemia, facilitating NK cell-mediated immune recognition. Oncotarget. 2017;8(19):31959-76.
72. Buller CW, Mathew PA, Mathew SO. Roles of NK Cell Receptors 2B4 (CD244), CS1 (CD319), and LLT1 (CLEC2D) in Cancer. Cancers (Basel). 2020;12(7).
73. Müller R, Misund K, Holien T, Bachke S, Gilljam KM, Våtsveen TK, et al. Targeting proliferating cell nuclear antigen and its protein interactions induces apoptosis in multiple myeloma cells. PLoS One. 2013;8(7):e70430.
74. Horton NC, Mathew SO, Mathew PA. Novel interaction between proliferating cell nuclear antigen and HLA I on the surface of tumor cells inhibits NK cell function through NKp44. PLoS One. 2013;8(3):e59552.
75. Pardoll DM. The blockade of immune checkpoints in cancer immunotherapy. Nat Rev Cancer. 2012;12(4):252-64.
76. Pickup M, Novitskiy S, Moses HL. The roles of TGFβ in the tumour microenvironment. Nat Rev Cancer. 2013;13(11):788-99.
77. Rossi GR, Trindade ES, Souza-Fonseca-Guimaraes F. Tumor Microenvironment-Associated Extracellular Matrix Components Regulate NK Cell Function. Front Immunol. 2020;11:73.
78. Schreiber RD, Old LJ, Smyth MJ. Cancer immunoediting: integrating immunity's roles in cancer suppression and promotion. Science (New York, NY). 2011;331(6024):1565-70.
79. Boissel L, Betancur-Boissel M, Lu W, Krause DS, Van Etten RA, Wels WS, et al. Retargeting NK-92 cells by means of CD19- and CD20-specific chimeric antigen receptors compares favorably with antibody-dependent cellular cytotoxicity. Oncoimmunology. 2013;2(10):e26527.
80. Dudley ME, Wunderlich JR, Robbins PF, Yang JC, Hwu P, Schwartzentruber DJ, et al. Cancer regression and autoimmunity in patients after clonal repopulation with antitumor lymphocytes. Science (New York, NY). 2002;298(5594):850-4.
81. Spear TT, Nagato K, Nishimura MI. Strategies to genetically engineer T cells for cancer immunotherapy. Cancer Immunol Immunother. 2016;65(6):631-49.
82. Neelapu SS, Tummala S, Kebriaei P, Wierda W, Gutierrez C, Locke FL, et al. Chimeric antigen receptor T-cell therapy - assessment and management of toxicities. Nat Rev Clin Oncol. 2018;15(1):47-62.
83. Robbins PF, Morgan RA, Feldman SA, Yang JC, Sherry RM, Dudley ME, et al. Tumor regression in patients with metastatic synovial cell sarcoma and melanoma using genetically engineered lymphocytes reactive with NY-ESO-1. J Clin Oncol. 2011;29(7):917-24.
84. Rapoport AP, Stadtmauer EA, Binder-Scholl GK, Goloubeva O, Vogl DT, Lacey SF, et al. NY-ESO-1-specific TCR-engineered T cells mediate sustained antigen-specific antitumor effects in myeloma. Nat Med. 2015;21(8):914-21.
85. Morgan RA, Dudley ME, Wunderlich JR, Hughes MS, Yang JC, Sherry RM, et al. Cancer regression in patients after transfer of genetically engineered lymphocytes. Science (New York, NY). 2006;314(5796):126-9.
86. Stauss HJ, Morris EC, Abken H. Cancer gene therapy with T cell receptors and chimeric antigen receptors. Curr Opin Pharmacol. 2015;24:113-8.

87. Offner S, Hofmeister R, Romaniuk A, Kufer P, Baeuerle PA. Induction of regular cytolytic T cell synapses by bispecific single-chain antibody constructs on MHC class I-negative tumor cells. Mol Immunol. 2006;43(6):763-71.
88. Amir AL, van der Steen DM, van Loenen MM, Hagedoorn RS, de Boer R, Kester MD, et al. PRAME-specific Allo-HLA-restricted T cells with potent antitumor reactivity useful for therapeutic T-cell receptor gene transfer. Clin Cancer Res. 2011;17(17):5615-25.
89. Jahn L, van der Steen DM, Hagedoorn RS, Hombrink P, Kester MG, Schoonakker MP, et al. Generation of CD20-specific TCRs for TCR gene therapy of CD20low B-cell malignancies insusceptible to CD20-targeting antibodies. Oncotarget. 2016;7(47):77021-37.
90. van der Lee DI, Reijmers RM, Honders MW, Hagedoorn RS, de Jong RC, Kester MG, et al. Mutated nucleophosmin 1 as immunotherapy target in acute myeloid leukemia. J Clin Invest. 2019;129(2):774-85.
91. Jahn L, Hombrink P, Hagedoorn RS, Kester MG, van der Steen DM, Rodriguez T, et al. TCR-based therapy for multiple myeloma and other B-cell malignancies targeting intracellular transcription factor BOB1. Blood. 2017;129(10):1284-95.
92. Miller JS, Soignier Y, Panoskaltsis-Mortari A, McNearney SA, Yun GH, Fautsch SK, et al. Successful adoptive transfer and in vivo expansion of human haploidentical NK cells in patients with cancer. Blood. 2005;105(8):3051-7.
93. Bachanova V, Cooley S, Defor TE, Verneris MR, Zhang B, McKenna DH, et al. Clearance of acute myeloid leukemia by haploidentical natural killer cells is improved using IL-2 diphtheria toxin fusion protein. Blood. 2014;123(25):3855-63.
94. Guillerey C, Huntington ND, Smyth MJ. Targeting natural killer cells in cancer immunotherapy. Nature immunology. 2016;17(9):1025-36.
95. Shah N, Li L, McCarty J, Kaur I, Yvon E, Shaim H, et al. Phase I study of cord blood-derived natural killer cells combined with autologous stem cell transplantation in multiple myeloma. Br J Haematol. 2017;177(3):457-66.
96. Iliopoulou EG, Kountourakis P, Karamouzis MV, Doufexis D, Ardavanis A, Baxevanis CN, et al. A phase I trial of adoptive transfer of allogeneic natural killer cells in patients with advanced non-small cell lung cancer. Cancer Immunol Immunother. 2010;59(12):1781-9.
97. Oberschmidt O, Kloess S, Koehl U. Redirected Primary Human Chimeric Antigen Receptor Natural Killer Cells As an "Off-the-Shelf Immunotherapy" for Improvement in Cancer Treatment. Front Immunol. 2017;8:654.
98. Levin AM, Bates DL, Ring AM, Krieg C, Lin JT, Su L, et al. Exploiting a natural conformational switch to engineer an interleukin-2 'superkine'. Nature. 2012;484(7395):529-33.
99. Liu E, Tong Y, Dotti G, Shaim H, Savoldo B, Mukherjee M, et al. Cord blood NK cells engineered to express IL-15 and a CD19-targeted CAR show long-term persistence and potent antitumor activity. Leukemia. 2018;32(2):520-31.
100. Liu E, Marin D, Banerjee P, Macapinlac HA, Thompson P, Basar R, et al. Use of CAR-Transduced Natural Killer Cells in CD19-Positive Lymphoid Tumors. N Engl J Med. 2020;382(6):545-53.
101. Imai C, Iwamoto S, Campana D. Genetic modification of primary natural killer cells overcomes inhibitory signals and induces specific killing of leukemic cells. Blood. 2005;106(1):376-83.
102. Li Y, Hermanson DL, Moriarity BS, Kaufman DS. Human iPSC-Derived Natural Killer Cells Engineered with Chimeric Antigen Receptors Enhance Anti-tumor Activity. Cell Stem Cell. 2018;23(2):181-92.e5.
103. Uherek C, Tonn T, Uherek B, Becker S, Schnierle B, Klingemann HG, et al. Retargeting of natural killer-cell cytolytic activity to ErbB2-expressing cancer cells results in efficient and selective tumor cell destruction. Blood. 2002;100(4):1265-73.
104. Zhang C, Oberoi P, Oelsner S, Waldmann A, Lindner A, Tonn T, et al. Chimeric Antigen Receptor-Engineered NK-92 Cells: An Off-the-Shelf Cellular Therapeutic for Targeted Elimination of Cancer Cells and Induction of Protective Antitumor Immunity. Frontiers in immunology. 2017;8:533-.
105. Tang X, Yang L, Li Z, Nalin AP, Dai H, Xu T, et al. First-in-man clinical trial of CAR NK-92 cells: safety test of CD33-CAR NK-92 cells in patients with relapsed and refractory acute myeloid leukemia. Am J Cancer Res. 2018;8(6):1083-9.
106. Ngoenkam J, Schamel WW, Pongcharoen S. Selected signalling proteins recruited to the T-cell receptor-CD3 complex. Immunology. 2018;153(1):42-50.
107. Morton LT, Wachsmann TLA, Meeuwsen MH, Wouters AK, Remst DFG, van Loenen MM, et al. T cell receptor engineering of primary NK cells to therapeutically target tumors and tumor immune evasion. J Immunother Cancer. 2022;10(3).
108. Rahmani S, Yazdanpanah N, Rezaei N. Natural killer cells and acute myeloid leukemia: promises and challenges. Cancer Immunol Immunother. 2022.
109. Liu P, Liu M, Lyu C, Lu W, Cui R, Wang J, et al. Acute Graft-Versus-Host Disease After Humanized Anti-CD19-CAR T Therapy in Relapsed B-ALL Patients After Allogeneic Hematopoietic Stem Cell Transplant. Front Oncol. 2020;10:573822.
110. Cummins KD, Frey N, Nelson AM, Schmidt A, Luger S, Isaacs RE, et al. Treating Relapsed / Refractory (RR) AML with Biodegradable Anti-CD123 CAR Modified T Cells. Blood. 2017;130:1359.
111. Wang QS, Wang Y, Lv HY, Han QW, Fan H, Guo B, et al. Treatment of CD33-directed chimeric antigen receptor-modified T cells in one patient with relapsed and refractory acute myeloid leukemia. Mol Ther. 2015;23(1):184-91.
112. Tasian SK, Kenderian SS, Shen F, Ruella M, Shestova O, Kozlowski M, et al. Optimized depletion of chimeric antigen receptor T cells in murine xenograft models of human acute myeloid leukemia. Blood. 2017;129(17):2395-407.

113. Ferrara J, Reddy P, Paczesny S. Immunotherapy through T-cell receptor gene transfer induces severe graft-versus-host disease. Immunotherapy. 2010;2(6):791-4.
114. Legut M, Dolton G, Mian AA, Ottmann OG, Sewell AK. CRISPR-mediated TCR replacement generates superior anticancer transgenic T cells. Blood. 2018;131(3):311-22.
115. Restifo NP, Marincola FM, Kawakami Y, Taubenberger J, Yannelli JR, Rosenberg SA. Loss of functional beta 2-microglobulin in metastatic melanomas from five patients receiving immunotherapy. J Natl Cancer Inst. 1996;88(2):100-8.
116. Ljunggren HG, Kärre K. In search of the 'missing self': MHC molecules and NK cell recognition. Immunol Today. 1990;11(7):237-44.
117. Tonn T, Becker S, Esser R, Schwabe D, Seifried E. Cellular immunotherapy of malignancies using the clonal natural killer cell line NK-92. Journal of hematotherapy & stem cell research. 2001;10(4):535-44.
118. Tonn T, Schwabe D, Klingemann HG, Becker S, Esser R, Koehl U, et al. Treatment of patients with advanced cancer with the natural killer cell line NK-92. Cytotherapy. 2013;15(12):1563-70.
119. Arai S, Meagher R, Swearingen M, Myint H, Rich E, Martinson J, et al. Infusion of the allogeneic cell line NK-92 in patients with advanced renal cell cancer or melanoma: a phase I trial. Cytotherapy. 2008;10(6):625-32.
120. Campillo-Davo D, Flumens D, Lion E. The Quest for the Best: How TCR Affinity, Avidity, and Functional Avidity Affect TCR-Engineered T-Cell Antitumor Responses. Cells. 2020;9(7).
121. Abel AM, Yang C, Thakar MS, Malarkannan S. Natural Killer Cells: Development, Maturation, and Clinical Utilization. Front Immunol. 2018;9:1869.
122. Poli A, Michel T, Thérésine M, Andrès E, Hentges F, Zimmer J. CD56bright natural killer (NK) cells: an important NK cell subset. Immunology. 2009;126(4):458-65.
123. Moretta L, Bottino C, Pende D, Mingari MC, Biassoni R, Moretta A. Human natural killer cells: their origin, receptors and function. European journal of immunology. 2002;32(5):1205-11.
124. Chan A, Hong DL, Atzberger A, Kollnberger S, Filer AD, Buckley CD, et al. CD56bright human NK cells differentiate into CD56dim cells: role of contact with peripheral fibroblasts. Journal of immunology (Baltimore, Md : 1950). 2007;179(1):89-94.
125. Cooper MA. Natural killer cells might adapt their inhibitory receptors for memory. Proceedings of the National Academy of Sciences of the United States of America. 2018;115(45):11357-9.
126. Fauriat C, Long EO, Ljunggren HG, Bryceson YT. Regulation of human NK-cell cytokine and chemokine production by target cell recognition. Blood. 2010;115(11):2167-76.
127. Chan CJ, Smyth MJ, Martinet L. Molecular mechanisms of natural killer cell activation in response to cellular stress. Cell Death Differ. 2014;21(1):5-14.
128. Biassoni R. Natural killer cell receptors. Adv Exp Med Biol. 2008;640:35-52.
129. Vivier E, Tomasello E, Baratin M, Walzer T, Ugolini S. Functions of natural killer cells. Nature immunology. 2008;9(5):503-10.
130. Sungur CM, Murphy WJ. Positive and negative regulation by NK cells in cancer. Crit Rev Oncog. 2014;19(1-2):57-66.
131. Carrillo-Bustamante P, Keşmir C, de Boer RJ. The evolution of natural killer cell receptors. Immunogenetics. 2016;68(1):3-18.
132. Brodin P, Lakshmikanth T, Johansson S, Kärre K, Höglund P. The strength of inhibitory input during education quantitatively tunes the functional responsiveness of individual natural killer cells. Blood. 2009;113(11):2434-41.
133. Romee R, Foley B, Lenvik T, Wang Y, Zhang B, Ankarlo D, et al. NK cell CD16 surface expression and function is regulated by a disintegrin and metalloprotease-17 (ADAM17). Blood. 2013;121(18):3599-608.
134. Schmiedel D, Mandelboim O. NKG2D Ligands-Critical Targets for Cancer Immune Escape and Therapy. Front Immunol. 2018;9:2040.
135. Cao Y, Wang X, Jin T, Tian Y, Dai C, Widarma C, et al. Immune checkpoint molecules in natural killer cells as potential targets for cancer immunotherapy. Signal Transduct Target Ther. 2020;5(1):250.
136. Pazina T, Shemesh A, Brusilovsky M, Porgador A, Campbell KS. Regulation of the Functions of Natural Cytotoxicity Receptors by Interactions with Diverse Ligands and Alterations in Splice Variant Expression. Front Immunol. 2017;8:369.
137. Rosental B, Brusilovsky M, Hadad U, Oz D, Appel MY, Afergan F, et al. Proliferating cell nuclear antigen is a novel inhibitory ligand for the natural cytotoxicity receptor NKp44. Journal of immunology (Baltimore, Md : 1950). 2011;187(11):5693-702.
138. Pende D, Falco M, Vitale M, Cantoni C, Vitale C, Munari E, et al. Killer Ig-Like Receptors (KIRs): Their Role in NK Cell Modulation and Developments Leading to Their Clinical Exploitation. Front Immunol. 2019;10:1179.
139. Konjević G, Vuletić A, Mirjačić Martinović K. Natural killer cell receptors: alterations and therapeutic targeting in malignancies. Immunol Res. 2016;64(1):25-35.
140. Zingoni A, Ardolino M, Santoni A, Cerboni C. NKG2D and DNAM-1 activating receptors and their ligands in NK-T cell interactions: role in the NK cell-mediated negative regulation of T cell responses. Front Immunol. 2012;3:408.
141. Chauvin JM, Zarour HM. TIGIT in cancer immunotherapy. J Immunother Cancer. 2020;8(2).
142. Dong W, Wu X, Ma S, Wang Y, Nalin AP, Zhu Z, et al. The Mechanism of Anti-PD-L1 Antibody Efficacy against PD-L1-Negative Tumors Identifies NK Cells Expressing PD-L1 as a Cytolytic Effector. Cancer Discov. 2019;9(10):1422-37.
143. Zhu X, Lang J. Soluble PD-1 and PD-L1: predictive and prognostic significance in cancer. Oncotarget. 2017;8(57):97671-82.

144. Del Zotto G, Marcenaro E, Vacca P, Sivori S, Pende D, Della Chiesa M, et al. Markers and function of human NK cells in normal and pathological conditions. Cytometry B Clin Cytom. 2017;92(2):100-14.
145. Wu Y, Tian Z, Wei H. Developmental and Functional Control of Natural Killer Cells by Cytokines. Front Immunol. 2017;8:930.
146. Li L, Chen H, Marin D, Xi Y, Miao Q, Lv J, et al. A novel immature natural killer cell subpopulation predicts relapse after cord blood transplantation. Blood Adv. 2019;3(23):4117-30.
147. Quintarelli C, Sivori S, Caruso S, Carlomagno S, Falco M, Boffa I, et al. Efficacy of third-party chimeric antigen receptor modified peripheral blood natural killer cells for adoptive cell therapy of B-cell precursor acute lymphoblastic leukemia. Leukemia. 2020;34(4):1102-15.
148. Rezvani K. Adoptive cell therapy using engineered natural killer cells. Bone Marrow Transplant. 2019;54(Suppl 2):785-8.
149. Gong JH, Maki G, Klingemann HG. Characterization of a human cell line (NK-92) with phenotypical and functional characteristics of activated natural killer cells. Leukemia. 1994;8(4):652-8.
150. Suck G, Odendahl M, Nowakowska P, Seidl C, Wels WS, Klingemann HG, et al. NK-92: an 'off-the-shelf therapeutic' for adoptive natural killer cell-based cancer immunotherapy. Cancer Immunol Immunother. 2016;65(4):485-92.
151. Klingemann H, Boissel L, Toneguzzo F. Natural Killer Cells for Immunotherapy - Advantages of the NK-92 Cell Line over Blood NK Cells. Front Immunol. 2016;7:91.
152. Schmidt P, Raftery MJ, Pecher G. Engineering NK Cells for CAR Therapy-Recent Advances in Gene Transfer Methodology. Front Immunol. 2020;11:611163.
153. Boyiadzis M, Agha M, Redner RL, Sehgal A, Im A, Hou JZ, et al. Phase 1 clinical trial of adoptive immunotherapy using "off-the-shelf" activated natural killer cells in patients with refractory and relapsed acute myeloid leukemia. Cytotherapy. 2017;19(10):1225-32.
154. Williams BA, Law AD, Routy B, denHollander N, Gupta V, Wang XH, et al. A phase I trial of NK-92 cells for refractory hematological malignancies relapsing after autologous hematopoietic cell transplantation shows safety and evidence of efficacy. Oncotarget. 2017;8(51):89256-68.
155. Fabian KP, Hodge JW. The emerging role of off-the-shelf engineered natural killer cells in targeted cancer immunotherapy. Mol Ther Oncolytics. 2021;23:266-76.
156. Bergman H, Sissala N, HÄgerstrand H, Lindqvist C. Human NK-92 Cells Function as Target Cells for Human NK Cells - Implications for CAR NK-92 Therapies. Anticancer Res. 2020;40(10):5355-9.
157. Suck G, Linn YC, Tonn T. Natural Killer Cells for Therapy of Leukemia. Transfus Med Hemother. 2016;43(2):89-95.
158. Duan L, Mukherjee E. Janeway's Immunobiology, Ninth Edition: Yale J Biol Med. 2016 Sep 30;89(3):424-5. eCollection 2016 Sep.
159. Birkholz K, Hofmann C, Hoyer S, Schulz B, Harrer T, Kämpgen E, et al. A fast and robust method to clone and functionally validate T-cell receptors. J Immunol Methods. 2009;346(1-2):45-54.
160. Distler E, Albrecht J, Brunk A, Khan S, Schnurer E, Frey M, et al. Patient-individualized CD8(+) cytolytic T-cell therapy effectively combats minimal residual leukemia in immunodeficient mice. International journal of cancer. 2016;138(5):1256-68.
161. Theobald M, Biggs J, Dittmer D, Levine AJ, Sherman LA. Targeting p53 as a general tumor antigen. Proceedings of the National Academy of Sciences of the United States of America. 1995;92(26):11993-7.
162. Vonderheide RH, Hahn WC, Schultze JL, Nadler LM. The telomerase catalytic subunit is a widely expressed tumor-associated antigen recognized by cytotoxic T lymphocytes. Immunity. 1999;10(6):673-9.
163. Minev B, Hipp J, Firat H, Schmidt JD, Langlade-Demoyen P, Zanetti M. Cytotoxic T cell immunity against telomerase reverse transcriptase in humans. Proceedings of the National Academy of Sciences of the United States of America. 2000;97(9):4796-801.
164. Stanislawski T, Voss RH, Lotz C, Sadovnikova E, Willemsen RA, Kuball J, et al. Circumventing tolerance to a human MDM2-derived tumor antigen by TCR gene transfer. Nature immunology. 2001;2(10):962-70.
165. Roth J, Dobbelstein M, Freedman DA, Shenk T, Levine AJ. Nucleo-cytoplasmic shuttling of the hdm2 oncoprotein regulates the levels of the p53 protein via a pathway used by the human immunodeficiency virus rev protein. Embo j. 1998;17(2):554-64.
166. Freedman DA, Levine AJ. Regulation of the p53 protein by the MDM2 oncoprotein--thirty-eighth G.H.A. Clowes Memorial Award Lecture. Cancer Res. 1999;59(1):1-7.
167. Oliner JD, Kinzler KW, Meltzer PS, George DL, Vogelstein B. Amplification of a gene encoding a p53-associated protein in human sarcomas. Nature. 1992;358(6381):80-3.
168. Qin JJ, Li X, Hunt C, Wang W, Wang H, Zhang R. Natural products targeting the p53-MDM2 pathway and mutant p53: Recent advances and implications in cancer medicine. Genes Dis. 2018;5(3):204-19.
169. Voss RH, Kuball J, Engel R, Guillaume P, Romero P, Huber C, et al. Redirection of T cells by delivering a transgenic mouse-derived MDM2 tumor antigen-specific TCR and its humanized derivative is governed by the CD8 coreceptor and affects natural human TCR expression. Immunol Res. 2006;34(1):67-87.
170. Gangadharan D, Cheroutre H. The CD8 isoform CD8alphaalpha is not a functional homologue of the TCR co-receptor CD8alphabeta. Curr Opin Immunol. 2004;16(3):264-70.
171. Turner JM, Brodsky MH, Irving BA, Levin SD, Perlmutter RM, Littman DR. Interaction of the unique N-terminal region of tyrosine kinase p56lck with cytoplasmic domains of CD4 and CD8 is mediated by cysteine motifs. Cell. 1990;60(5):755-65.
172. Bosselut R, Kubo S, Guinter T, Kopacz JL, Altman JD, Feigenbaum L, et al. Role of CD8β Domains in CD8 Coreceptor Function: Importance for MHC I Binding, Signaling, and Positive Selection of CD8+ T Cells in the Thymus. Immunity. 2000;12(4):409-18.

173. Artyomov MN, Lis M, Devadas S, Davis MM, Chakraborty AK. CD4 and CD8 binding to MHC molecules primarily acts to enhance Lck delivery. Proceedings of the National Academy of Sciences of the United States of America. 2010;107(39):16916-21.
174. Mørch AM, Bálint Š, Santos AM, Davis SJ, Dustin ML. Coreceptors and TCR Signaling - the Strong and the Weak of It. Front Cell Dev Biol. 2020;8:597627.
175. Parham P. The immune system: Second edition. New York, NY : Garland Science, [2005] ©2005; 2005.
176. Szymczak AL, Workman CJ, Wang Y, Vignali KM, Dilioglou S, Vanin EF, et al. Correction of multi-gene deficiency in vivo using a single 'self-cleaving' 2A peptide–based retroviral vector. Nature Biotechnology. 2004;22:589.
177. Thakral D, Dobbins J, Devine L, Kavathas PB. Differential expression of the human CD8beta splice variants and regulation of the M-2 isoform by ubiquitination. Journal of immunology (Baltimore, Md : 1950). 2008;180(11):7431-42.
178. Jönsson P, Southcombe JH, Santos AM, Huo J, Fernandes RA, McColl J, et al. Remarkably low affinity of CD4/peptide-major histocompatibility complex class II protein interactions. Proceedings of the National Academy of Sciences of the United States of America. 2016;113(20):5682-7.
179. Kärre K, Ljunggren HG, Piontek G, Kiessling R. Selective rejection of H-2-deficient lymphoma variants suggests alternative immune defence strategy. Nature. 1986;319(6055):675-8.
180. Zhang C, Oberoi P, Oelsner S, Waldmann A, Lindner A, Tonn T, et al. Chimeric Antigen Receptor-Engineered NK-92 Cells: An Off-the-Shelf Cellular Therapeutic for Targeted Elimination of Cancer Cells and Induction of Protective Antitumor Immunity. Front Immunol. 2017;8:533.
181. Maki G, Klingemann HG, Martinson JA, Tam YK. Factors regulating the cytotoxic activity of the human natural killer cell line, NK-92. Journal of hematotherapy & stem cell research. 2001;10(3):369-83.
182. Smith SL, Kennedy PR, Stacey KB, Worboys JD, Yarwood A, Seo S, et al. Diversity of peripheral blood human NK cells identified by single-cell RNA sequencing. Blood Adv. 2020;4(7):1388-406.
183. Heipertz EL, Zynda ER, Stav-Noraas TE, Hungler AD, Boucher SE, Kaur N, et al. Current Perspectives on "Off-The-Shelf" Allogeneic NK and CAR-NK Cell Therapies. Front Immunol. 2021;12:732135.
184. Herrera L, Santos S, Vesga MA, Anguita J, Martin-Ruiz I, Carrascosa T, et al. Adult peripheral blood and umbilical cord blood NK cells are good sources for effective CAR therapy against CD19 positive leukemic cells. Sci Rep. 2019;9(1):18729.
185. Goldenson BH, Zhu H, Wang YM, Heragu N, Bernareggi D, Ruiz-Cisneros A, et al. Umbilical Cord Blood and iPSC-Derived Natural Killer Cells Demonstrate Key Differences in Cytotoxic Activity and KIR Profiles. Front Immunol. 2020;11:561553.
186. Yoshihara M, Hayashizaki Y, Murakawa Y. Genomic Instability of iPSCs: Challenges Towards Their Clinical Applications. Stem Cell Reviews and Reports. 2017;13(1):7-16.

14 Acknowledgement

I would like to express my sincere gratitude to everyone who supported me during this formative endeavor.

First an foremost, I would like to thank my supervisor [redacted] not only for entrusting me with this well chosen project, but also for true and great mentorship over more than 5 years of cooperation. Under your guidance, I was able to make my first steps in medical research and gain a deeper understanding in the processes of basic research. Thank you for continuously firing my fascination and motivation.

In addition, I would like to thank the reviewers of this thesis for dedicating their precious time surveying this research project.

Moreover, I would like to emphasize my gratitude to Shamsul Khan for his tremendous support and true friendship!

Over the years, many colleagues accompanied me with professional and emotional support during the work on this project. [redacted] – You helped me to get through tough periods and made this project even more enjoyable – Thank you!

Last but not least, I would like to express my gratitude to my family and girlfriend, [redacted] – without your tremendous support, I would have never been able to come to this point. It is your selfless dedication, which allows me to flourish – I will never forget that.

15 Curriculum vitae

Jan Wernersbach

[redacted]

Geburtsdatum: 08.03.1996

Geburtsort: Worms

Familienstand: Ledig

Ausbildung:

Seit 10/2022 Arzt in Weiterbildung
Zum Facharzt Herzchirurgie in der Klinik und Poliklinik für Herz- und Gefäßchirurgie der Universitätsmedizin der Johannes Gutenberg-Universität Mainz

2022-06-20 Approbation als Arzt
Erteilt durch das Landesamt für Soziales, Jugend und Versorgung Rheinland Pfalz

2015-2022 – Medizinstudium
Universitätsmedizin der Johannes Gutenberg-Universität Mainz
2022 Abschluss der Ärztlichen Prüfung mit der Gesamtnote sehr gut (1,33)

2002-2015 – Schulische Ausbildung
Bischöfliches Willigis Gymnasium Mainz; Allgemeine Hochschulreife (Abitur)
2015: Endnote 1,0

Praktische Erfahrung:

Klinische Tätigkeit
Assistenzarzt in der Klinik und Poliklinik für Herz- und Gefäßchirurgie der Universitätsmedizin der Johannes Gutenberg-Universität Mainz (seit 01.10.2022)

PJ-Tertiale
Radiologie, Universitätsmedizin Mainz (05.-08.2021)
Chirurgie, Universitätsmedizin Mainz (09.-12.2021)
Innere Medizin, Universitätsmedizin Mainz (01.-04.2021)

Famulaturen:
Internistische Notaufnahme, Klinikum Worms (2018);
Plastische und Rekonstruktive Chirurgie, Greenslopes Private Hospital, Brisbane,
Australien (2019);
Anästhesiologie, Klinikum Worms (2020);
Allgemein-medizinische Gemeinschafts-praxis Medici, Wiesbaden (2020)

Stipendien:
2018-2022 Stipendium der Studienstiftung des Deutschen Volkes
2018-2019 Mildred Scheel Doktorandenstipendium der Deutschen Krebshilfe

Engagement:
Seit 2018 Unterstützung des universitären Projektes zur Förderung der Ausbildung Medizinstudierender in der Ultraschalldiagnostik „sonoforklinik“ als Tutor und Autor
Seit 2018 Jugendwart und Vereinstrainer des TC Dalheim e.V.

Mainz, den 29.01.2023